"PARAMETRIC ANALYSIS OF LASER TREPAN DRILLING ON MONEL K-500"

By

BITAB BISWAS

B.Tech. (Mechanical Engineering)

Kalyani Govt. Engineering College (KGEC)

EXAMINATION ROLL NO. – M4PRD19005

THESIS

SUBMITED IN PARTIAL FULFILMENT OF THE REQUIREMENTS FOR THE AWARD OF THE DEGREE OF MASTER OF PRODUCTION ENGINEERING IN

THE FACULTY OF ENGINEERING & TECHNOLOGY JADAVPUR

UNIVERSITY

PRODUCTION ENGINEERING DEPARTMENT

JADAVPUR UNIVERSITY

KOLKATA-700032

INDIA

2019

JADAVPUR UNIVERSITY

FACULTY OF ENGINEERING AND TECHNOLOGY

CERTIFICATE OF RECOMMENDATION

I HEREBY RECOMMEND THAT THE THESIS ENTITLED **"PARAMETRIC ANALYSIS OF LASER TREPAN DRILLING ON MONEL K-500"** CARRIED OUT UNDER MY SUPERVISION AND GUIDANCE, BY **MR. BITAB BISWAS,** MAY BE ACCEPTED IN THE PARTIAL FULFILLMENT OF THE REQUIREMENTS FOR THE DEGREE OF **"MASTER OF PRODUCTION ENGINEERING".**

Countersigned

(DR. BIPLAB RANJAN SARKAR)

HEAD,

Production Engineering Dept.,

JADAVPUR UNIVERSITY

KOLKATA-700032

Thesis Advisor

(PROF. ARUNANSHU SHEKHAR KUAR)

Professor,

Production Engineering Dept.,

JADAVPUR UNIVERSITY

KOLKATA- 700032

(PROF. CHIRANJIB BHATTACHARJEE)
DEAN,

Faculty of Engineering and Technology,
JADAVPUR UNIVERSITY,

KOLKATA-700032

JADAVPUR UNIVERSITY

FACULTY OF ENGINEERING AND TECHNOLOGY

CERTIFICATE OF APPROVAL*

The forgoing thesis is hereby approved as a creditable study of an engineering subject carried out and presented in a manner of satisfactory to warrant its acceptance as a pre-requisite to the degree for which it has been submitted. It is understood that by this approval, the undersigned do not necessarily endorse or approve any statement made, opinion expressed and conclusion drawn therein but approve the thesis only for the purpose for which it has been submitted.

COMMITTEEON **(External Examiner)**

FINAL EXAMINATION

FOR EVALUATIONOF

THETHESIS **----------**

(Internal Examiner)

***Only in case the recommendation is concurred in

ACKNOWLEDGEMENT

It is my greatest fortune to perform the thesis work in the Production Engineering Department, Jadavpur University.

It is great pleasure to express my gratitude and indebtedness to my esteemed guide Dr. Arunanshu Shekher Kuar, Professor, Production Engineering Department, Jadavpur University. It is because of his continuous guidance, encouragement and valuable advice at every aspect and strata of the problem from the embryonic to the development stage that my thesis has been in the light of the day.

My special thanks to Head of Production Engineering Department for allowing me to carry out the research investigation with various facilities of the department. I would like to express my warmest gratitude to all the respected faculty members and non-teaching staff members of this department who directly or indirectly helped and encouraged me during the thesis work.

I would also like to thank Mr. Debal Pramanik, PhD scholar of Production Engineering Department for their continuous help in completion of this work. I express my appreciation to my friends for their understanding, patience and active co-operation throughout my Masters course.

I feel pleased and privileged to fulfil my parents' ambition and I greatly indebted to them for bearing the inconvenience during my Masters course. Thank you, my beloved parents.

Everything in this nature is time bounded, so thanks to 'Almighty' for successful completion of the work in time.

(BITAB BISWAS)

Exam Roll No. - M4PRD19005

Table of Contents

CHAPTER 1:

1. INTRODUCTION

Machining is a process in which the raw material is cut in desired final shape and size by a control material removal process. The processes that have this common theme, controlled material removal, are today collectively known as subtractive manufacturing, in distinction from processes of controlled material addition, which are known as additive manufacturing. If the workpiece is metal, the process is often called metal cutting or metal removal. This can include material-removal as seen with such actions such as cutting, drilling or boring, milling. Although machining is most commonly used with metal products, machining can also be done with materials such as wood, ceramic, plastic, and composite materials. Materials such as hardened steel, carbides, nickel based super alloy and the ultra-hard non-conductive materials like composite materials are very difficult and sometimes not at all possible with the help of conventional machining processes such as turning, milling, drilling etc. All the conventional machining have some difficulty for fabricating precise micro components. Miniaturization is in great demand in various types of industrial applications. As a result of which researchers over the world focus on micro machining techniques using non-traditional machining processes like laser beam machining (LBM), ultrasonic machining, abrasive jet machining, electro-discharge machining etc. However the evolution of the above non-conventional machining has not came in a single days. This evolution is a contribution of many researchers for a long time.

1.1. History of Machining

The use of bones of animal, stones to remove material and forming desired shape and size was a common practice in ancient time. Up to almost the seventeenth century all tools were either hand operated or some other very elementary methods but power driven machine tool concept come into existence after the invention of electricity. In 1774 John Wilkinson first constructed a precision machine for boring engine cylinder. James Nasmyth invented the second basic machining tool for shaping and planning. Henry Maudslay, British engineer invented the metal lathe and other devices. Due to shape complexity, surface integrity and miniaturization requirements, non-conventional machining processes were invented. In 1917, Albert Einstein lays the foundations for laser technology when he predicts the phenomenon of “Stimulated Emission”.

This led them to invent an LBM machine used for working difficult to machine materials such as tungsten. Hybrid machining processes are developed made by the use of the combined advantages of two or more participating processes and at the same time avoiding its limitations.[2]

1.2. Types of Machining

Machining processes are classified by different ways. According to the use and history, machining process can be classified by two processes. They are conventional machining process and non-conventional machining process. The machining process which is normally used by human from the ancient era and there are direct contact between workpiece and tool with a relative motion and material is removed in the form of chips, is called conventional machining e.g. turning, boring, milling, shaping, broaching, slotting, grinding etc. The machining process which is a special type of machining process in which there is no direct contact between the tool and the workpiece, is called non-conventional machining process e.g. Abrasive Jet Machining (AJM), Ultrasonic Machining (USM), Water Jet and Abrasive Water Jet Machining (WJM & AWJM), Electro-discharge Machining (EDM). Machining process can also be further classified by a different way that is depicted in Fig.1.1.[5]

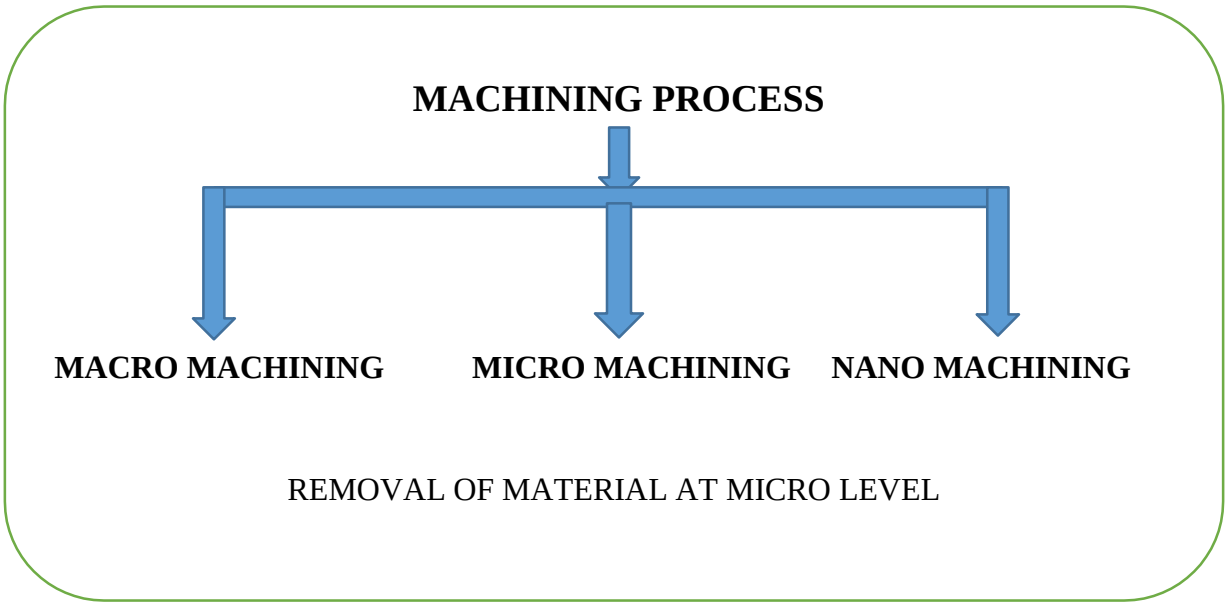

Fig.1.1. Types of Machining processes

(a) Macro Machining

Machining operations performed at conventional regimes at un-deformed chip thickness values that are larger than the cutting edge radius, hence dominated by shearing. Generally its value is larger than 10 mm and product size is greater than 1 mm.[2]

(b) Micro Machining

When the machining dimensions lay in between 1 micron to 999 micron, it is called micro-machining. But according to the CIRP (The International Academy for Production Engineering/College International pour la Recherché en Productique) the micro machining range is 1 micron to 500 micron. But recent definition according to metrological point of view if the ratio of tolerance to dimensions is less than 10-4 then it is called micro-machining. Micro-machining is the most basic technology for production of miniature parts and components.

(c) Nano Machining

When the machining amount is less than 1 micron then it enters into nano domain. This domain is referred as nano-technology not the nano-machining as a phenomena in this domain is completely different from others two domain. It is not simply another step of miniaturization. Instead of material removal, in this nano-domain addition or deposit of atom is done layer by layer. So volume of material removal is important not the component size.[2]

1.3. Micro Machining

Micro machining techniques have their roots in the 1960s when the need for miniaturized electronic components arose. Micro-machining deals with machining miniature component is not literally correct. The micromachining is material removal at micro/nano level with no constraint on the size of the component being machined (as shown in Fig.1.2). The most common applications of micromachining are in the medical and electronics industries. Micro-parts that are produced by micromachining are typically so small that they must be inspected using a microscope, Micromachining is differentiated from micro fabrication which is typically performed by machine shops that specialize in the machining fabrication of miniature parts to precise tolerances.

Micromachining is a precision machining in which the machining error is extremely small. The unit removal (UR) of material (UR is the volume or size of material removed by the unit removal phenomenon) in micromachining is very small. Since micromachining requires precision

machining, the identification and minimization of error generation factors is very important. There are several error generation factors in micromachining using machine tools, viz, mechanical deformation, thermal deformation, surface integrity, gap between tool and work piece, coordinate shift in tool handling, etc. [3]

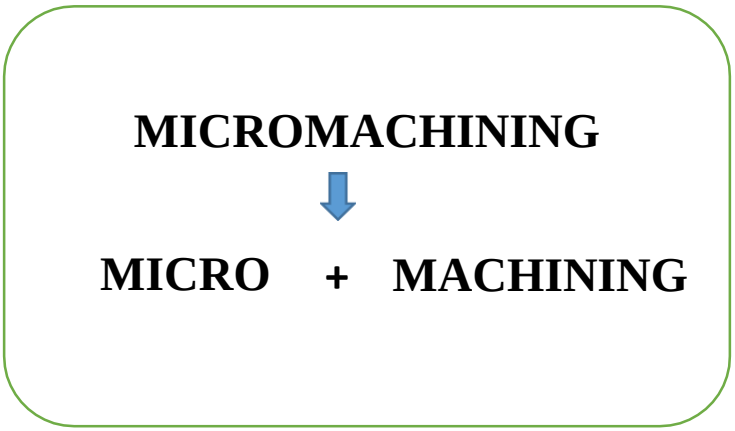

Fig 1.2: Definition of Micro Machining

1.4. Needs of Micro Machining

There is a growing demand for industrial products with increased number of functions and of reduced dimensions. Micro-machining is the most basic technology for the production of such miniature parts and components. Lithography based micro-machining technology uses silicon as material to produce integrated circuitry components and microstructures. However, these methods, in general, lack the ability of machining three-dimensional shapes because of poor machining control in the Z axis. Fabrication using hard and difficult-to-machine materials such as tool steels, composites, super alloys, ceramics, carbides, heat resistant steels and complex geometries for demanding aerospace, mechanical or biomedical applications requires alternative novel methods.

1.5. Various Micro Machining Processes

There are various techniques available to fabricate micro components and structures as shown in Fig.1.3 where some processes are mask based and some are tool based. However some of the important techniques are discussed in this section.

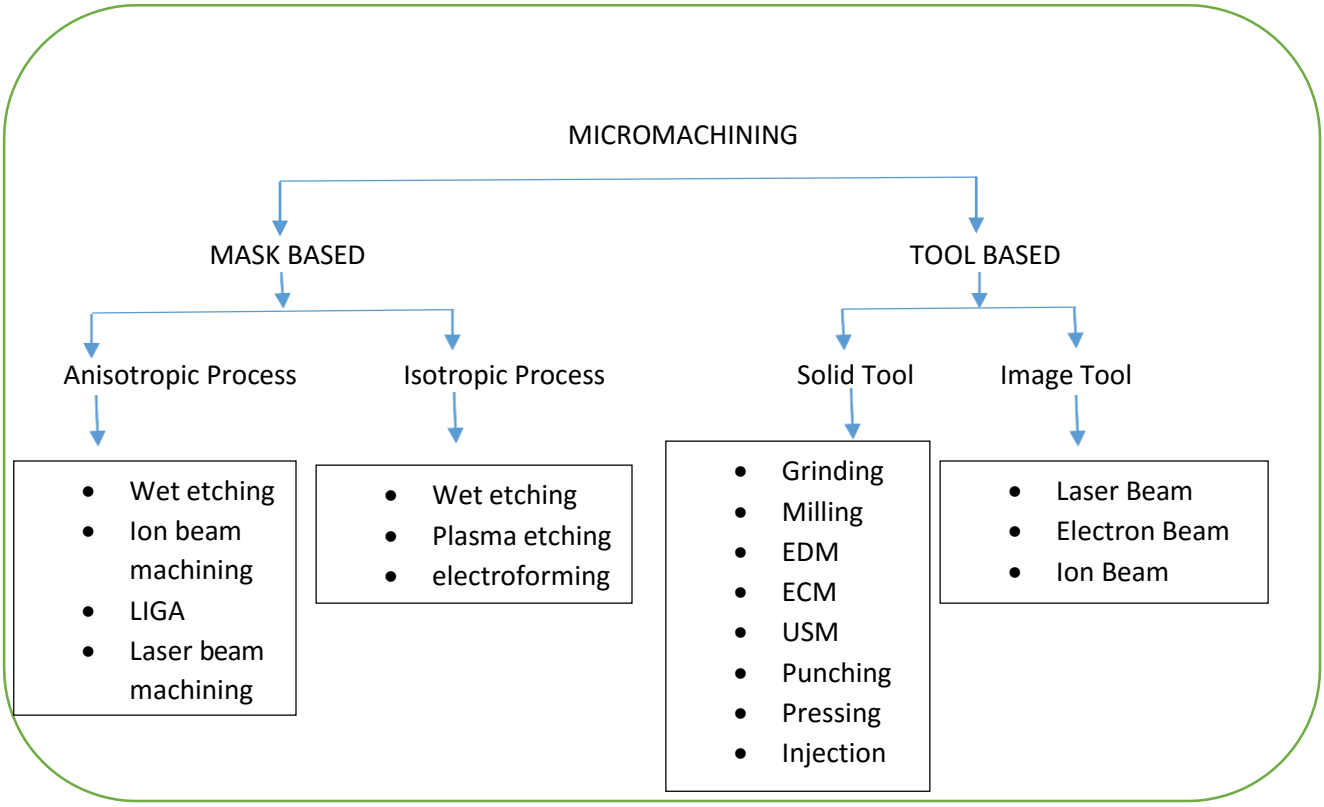

Fig.1.3.Various types of Micro-machining

1.5.1. Laser Beam Micro Machining

LASER stands for light amplification by stimulated emission of radiation. The underline working principle of laser was first put forward by Albert Einstein in 1917, though the first industrial laser for experimentation was developed around 1960s. Laser Beam Machining or more broadly laser material processing deals with machining and material processing like heat treatment, alloying, cladding, sheet metal bending etc. Such processing is carried out utilizing the energy of coherent

photons or laser beam, which is mostly converted into thermal energy upon interaction with most of the materials. Nowadays, laser is also finding application in regenerative machining or rapid prototyping as in processes like stereo-lithography, selective laser sintering etc. As laser interacts with the material, the energy of the photon is absorbed by the work material leading to rapid substantial rise in local temperature. Instant melting and vaporization of the work material and finally material is removed. Some of the advantages are in laser machining there is no physical tool, so there is no machining force or wear of the tool takes place. Large aspect ratio in laser drilling can be achieved along with acceptable accuracy or dimension, form or location. Micro-holes can be drilled in difficult-to-machine materials. Though laser processing is a thermal processing but heat affected zone especially in pulse laser processing is not very significant due to shorter pulse duration. [4]

1.5.2. Ultrasonic Micro Machining

Micro Ultrasonic Machining (micro-USM) is capable of making almost any three dimensional microstructure with high aspect ratio on most of materials, mainly on brittle materials. The USM uses a tool Ultrasonic Vibration with combination of favorable abrasive slurry to create accurate cavities of any shape through the impact grinding of fine grains. The machining process is non thermal, nonchemical, non-electrical and thus produces high quality surface finish. However, the micro-USM is not capable of drilling of micro holes smaller than 100 m for lack of corresponding co-axial micro tools. With special considerations given to slurry delivery and abrasive selection, tolerances up to 17 μm can be achieved in USM process. Machining of hard ceramics yield slightly better surface conditions than soft ceramics with surface finish as low as 0.4 μm Ra.

Micro-USM has been used for micro-hole drilling having diameter as 66 μm however micro-burrs are clearly visible. The process is also useful for producing micro cavity. In such applications, the amplitude of vibration and the working gap should be less than ten micrometer or so.[6]

1.5.3. Electrochemical Micro Machining

Electrochemical machining (ECM) is based on the electrochemical dissolution of a metal. In conventional ECM, the machining shape is specified by the shape of the electrode, similar to the case of EDM or USM. ECM has an invaluable advantage, that is, the machined surface is very smooth and there are no layers affected by machining. This makes micro-ECM suitable for

smoothing micro-metallic products. In order to adjust the unit removal suitable for micro removal, a short pulse and a low current are required. The low current can also be realized by using a high resistance electrolyte. Some trials are conducted using an electrolyte jet as the micro tool instead of a metal tool. A high speed jet can localize electrochemical dissolution and this enables the machining of micro indentations with controlled dimensions by switching the current synchronously to the movement of the work piece. When the Scanning Tunneling Microscope (STM) technique is used in combination with ECM, microgrooves with submicron width can be realized. This is due to the fact that the removal in ECM is basically an atom-by-atom phenomenon.[6]

1.5.4. Electron Beam Micro Machining

In Electron Beam Machining a stream of electrons is emitted from the cathode due to very high potential gradient (more than 100 kV). The concave shape of the cathode grid concentrates the electrons passing through the anode much like the way a concave mirror focuses a light beam from a flashlight. The anode potential accelerates the electrons which are forced through a valve that controls the beam.

After passing through the valve, the beam is then focused onto the surface of the work piece by a series of electromagnetic lenses and deflection coils. After hitting the work piece surface, the kinetic energy of electrons produces highly intense heat energy on a very small beam area on the work piece. This K.E is high enough to increase the localized area temperature to a value leading to melting/vaporization.

The basic mechanism of material removal is melting and/or vaporization depending on the beam energy and work piece material properties. The entire process occurs usually in a vacuum chamber otherwise the air molecules can adversely interact with the beam of electrons. A collision between an electron and an air molecule causes the electrons run out of the beam area and it lowers the beam strength. The machining rate during EBM depends on the variables such as thermal and physical properties of the work material, accelerating voltage, beam current, beam diameter, work piece thickness (or feature dimensions) and type of the machine (with vacuum or without vacuum). If the intensity of the electron beam is very high, the part may get over heated and get damaged.[1]

1.5.5. Electro Discharge Micro Machining

Electro discharge micro-machining (EDMM) removes material by thermal erosive action of electrical discharges (sparks) produced by a pulse DC power supply between the two electrodes: the tool electrode (cathode) and the work piece electrode (usually anode). The electrodes are immersed in the dielectric fluid

(kerosene, paraffin oil, deionized water, air, etc.). Due to very high electric field gradient across the two electrodes, a plasma channel is formed and a discharge takes place through the dielectric. Every discharge (or spark) melts and/or vaporizes a small amount of material from both the electrodes; a part of the molten material is removed from the IEG by the flowing/flushing dielectric fluid and the remaining re-solidifies on the machined surface, and this re-solidified material is known as recast layer. The net result is that each discharge leaves a small crater on both the electrodes. If the size of the spark is substantially reduced by appropriately selecting the machining parameters and the sparking frequency is considerably increased to create u-features with high accuracy and better surface finish on micro and macro components then the process is called electro discharge micromachining (EDMM). Thus, in EDMM, the key is to limit the energy in each discharge to make micro featured products with high accuracy and good surface finish. To achieve this, the energy required in a single discharge should be of the order of 10-7J. In EDMM, the relaxation type of power supply is used. The discharge energy ($E = 1/2\ CV2$) in the discharge circuit is reduced by minimizing capacitance (C) and voltage (V).

1.6. Need of Laser Beam Micro Machining (LBMM)

Presently manufacturing industries are facing challenges from newly developed conducting and non-conducting high strength temperature resistance materials viz. super alloys, ceramics and composites etc., which require high precision and surface quality thereby increase machining cost. In addition to this rapidly developing technology aims to develop products in miniaturized compact volumes with more functions are embedded in the products. This requires advancement of micro manufacturing; hence industrial research on micro-machining has become considerably important and widespread. To meet these challenges, non-conventional micro-machining processes are being employed to achieve higher metal removal rate, better surface finish and greater dimensional accuracy, with less tool wear. This process is capable to produce complex shapes with high degree of accuracy in difficult to cut but electrically conducting materials. It is an efficient micro-machining process for the fabrication of a micro-holes and micro-channel of various complex shape without tool wear. There are many electrical and technological parameters of Laser Beam μ-Machining (LBMM) process which are decisive in the machining characteristics and affect geometrical shape and surface quality of the machined parts. [5]

1.7. Applications of Laser Beam Micro Machining

Laser beam machining is now receiving acknowledgement of its importance because of some of its specific advantages, which can be exploited during the micromachining operation.
Since lasers can be used in wide range of manufacturing applications such as

- Micro drilling,
- Micro cutting
- Welding
- Cladding
- Engraving

Lasers are used not only in manufacturing processes but also in various other fields such as:

- Medicine-Bloodless surgery, laser healing, surgical treatment, eye treatment.
- Defense-Marking targets, alternative to radar, blinding troops.
- Fingerprint detection in the forensic identification.
- Research etc.

1.8. Types of Laser Beam Micro Machining Operations

Laser machining means material removal accomplished by laser material interaction, generally speaking, As per requirement of micromachining of components where the targeted size is less than 500 micron, these processes include laser drilling, laser cutting and laser grooving, marking or scribing, micro turning etc. have been develop

(a) Laser cutting
(b) Laser drilling
(c) Laser grooving
(d) Laser marking
(e) Laser turning
(f) Laser cleaning

(a) Laser Cutting

Laser micro-cutting can be called as two-dimensional micromachining technique. In this process, material removal takes place by controlling the intense laser beam as well as by moving the workpiece at particular direction. Laser cutting is most popular cutting process in various industries. Due to heating and melting as well as vaporization of material due to high intense laser beam, material is removed from the cutting front. The melted materials and vaporized gases are expelled from irradiated zone using jet of assist gas (air). The assist gas also helps for enhancing the chemical reactions in the cutting zone. During laser micro-cutting operation, the workpiece is moved in particular direction as while feed motion of laser focusing point vertically downward for facilitating the cutting of thick materials.

Micro-laser cutting is a non-conventional machining tool. It has higher precision and smooth cutting effect. The fast cutting speed can help to make easy model.

Advantages of laser micro-cutting over mechanical cutting include easier work holding and reduced contamination of work piece (since there is no cutting edge which can become contaminated by the material or contaminate the material). Precision may be better, since the laser beam does not wear during the process. There is also a reduced chance of warping the material that is being cut, as laser systems have a small heat affected zone. The main disadvantage of laser cutting is the high power consumption. Industrial laser efficiency may range from 5% to 45%. The power consumption and efficiency of any particular laser, for a particular job depends on the material type, thickness, and desired cutting rate. [6]

(b) Laser Drilling

Drilling is one of the most important and successful applications of industrial lasers. Laser hole drilling in metal, ceramic, silicon and polymer substrates is widely used in electronics industry. Laser drilling of metals is used to produce tiny orifices for nozzles, cooling channels in air turbine blades, via drilling of circuit board, etc. Holes less than 0.25mm in diameter are difficult to drill mechanically, laser drilling offers good choices for small hole drilling, especially for hard and brittle materials, such as ceramics and gemstones. Large holes can be drilled by trepanning, i.e., by over lapping drilling the circumference of a circle to form a large hole. High throughout of hole drilling are realized by mask projection and automation. Laser micro-drilling can be used to produce micro-hole in almost any material.

Laser drilled holes usually have tapers, i.e. the hole is not perfectly straight. Also a redemption area may exist around the hole, because laser drilling is realized through violent phase change, the material becomes melted, then ablated, then cool down and become solid state again. Re-deposition is serious for long pulses (pulse duration > 10 nanosecond). It was found that tapering and re-deposition can be lowered by suitably choose shorter wavelengths and pulse durations. For direct hole drilling, the quality of the laser beam, wavelength, intensity, pulse duration, pulse repetition rate are all important parameter.

High throughput of hole drilling are realized by mask projection and automation. Laser hole drilling in materials such as ceramics, copper, nickel, brass, aluminium, borosilicate glass, quartz, rubber and composite materials offer high accuracy for the medical device industry, semiconductor manufacturing and nanotechnology support systems. Laser drilling provides consistency for manufacturing specifications relying on tight tolerances for high depth-to diameter ratios. Laser drilled hole sizes vary depending on laser power, motion control and galvo systems. Laser drilling can provide dynamic, "on-the-fly "changing of hole diameter, hole depth and edge quality. [14]

(c) Laser Grooving

Laser grooving is similar to laser cutting except that grooving does not cut through the material. During laser grooving, a laser beam is scanned over the work piece surface, resulting in increasing its temperature above the material's melting point, in a small region near the beam spot. Laser grooving is a very complicated process to analyze, due to the molten material's behavior. Based on the assumption of complete removal of molten material, a theoretical analysis is performed to derive groove depth as a function of process parameters. Conduction heat direction and area change are approximated to obtain a closed form of the groove depth. The heat balance at the cutting front is used as the governing equation to determine groove depth. In cases where the heat flux, provided by the process parameters, is enough, vaporization of the material might also occur. A gas jet is applied coaxially or off-axially along with the laser beam in order to remove the molten material and produce the groove. Laser grooving is used in various manufacturing applications, such as the creation of micro channels for cooling systems and the creation of slots for assembly.

(d) Laser Marking

Laser marking is essentially a thermal process that employs a high intensity beam of focused laser light to create a contrasting mark on the material surface. Beam-steered marking employs mirrors mounted on high-speed, computer-controlled galvanometers to direct the laser beam across the target surface.[2]

(e) Laser Turning

One of the latest and emerging techniques of laser materials processing in micro-machining domain is laser micro turning process. This particular micro-machining process is applied to machine cylindrical shaped engineering material for removing micron level material from workpiece surface. For removal of bulk form (like a ring shape or tapered groove) of material from workpiece, laser micro-turning process is applied by using two intersecting laser beams. However, for carrying out micromachining process such as laser micro-turning, a single laser beam should be used to remove very thin planer layer from work material surface by irradiating and focusing the laser beam onto the machining surface of rotating workpiece through the desired length of turn along the axis of work sample.[6]

(f) Laser Cleaning

Laser cleaning is the process by which contaminants, debris or impurities (e.g. carbon, silicon and rubber) are removed from the surface of a material by using laser irradiation. This is a low-cost and environmentally-friendly laser application technique, which is in widespread use throughout global industry.

There are two types of laser cleaning process, which are typically used:

- One which is the removal of a layer on the surface of a material.
- While the second is the removal of the entire upper layer of a material.

An extremely brief laser pulse at high power is aimed at the surface to be cleaned. The laser energy applied ablates the surface. While part of the removed material is vaporized, some remains as particulate dust and may be collected in a filtration system. This process is repeated until the required depth and area has been reached. [7]

1.9. Types of Laser Beam Drilling (LBD) Operation

Laser Beam Drilling (LBD), due to its unique advantage, has wide application in aerospace, power generation, and several other modern manufacturing industries.

Laser Beam Drilling (LBD) mainly has three most commonly employed variations in several manufacturing industries, namely

- Laser Percussion Drilling (LPD)
- Laser Trepan Drilling (LTD)
- Laser Helical Drilling (LHD)

1.10. Needs of Laser Trepan Drilling (LTD) Operation

Laser Trepan Drilling (LTD), due to its unique advantages, has a wide applications in aerospace, power generation, and several other modern manufacturing industries. LTD has specific applications in the drilling of high-quality cooling holes in aeroengine parts such as guide vanes and blades of nozzle that efficiently control the operating temperature of the engine. Nickel-based superalloy Monel K500, Inconel718 (IN718) is the majorly employed manufacturing material in the aerospace sector, particularly in the high-temperature sections of gas turbine engines. However, this alloy is known as one of the difficult to conventionally machinable materials due to some peculiar properties such as high shear strength, toughness, work hardening tendency, and reduced thermal conductivity with enhanced chemical reactivity at elevated temperatures due to the presence of titanium. LTD has been found as a suitable method for the machining of Ni-based superalloys. Unlike conventional drilling, LTD does not require any cutting tool for generating the desired hole. High-intensity laser beam with micro-size spot is targeted on the work material and the unwanted material is removed by melting and vaporization. The melt part is ejected with the assistance of high-pressure gas jet.

1.11. Advantage of Laser Trepan Drilling (LTD) Operation over Laser Percussion Drilling (LPD) Operation

Due to direct impingement of laser pulses in LPD the processing time in LPD is lesser, but hole quality is poor compared with LTD due to the formation of a recast layer, spatter, and heat-affected zone. Higher dimensional accuracy and stringent hole-quality requirements in aerospace components result in holes with better-quality attributes. LTD may serve this purpose more efficiently than LPD if the processing parameters are optimized appropriately in order to overcome the geometrical inaccuracies such as hole taper (HT) and circularity error caused by inherent characteristics of laser machining. [16]

1.12. Literature Survey of the Past Research Works

Laser beam is the most versatile tool available to material scientists and engineers for processing of diverse range of materials i.e. metals, plastics, ceramics, composites etc. It can be used for both micro and macro level machining. Many studies have been conducted in the field of laser Beam micro-machining. Laser micro-drilling, Laser Trepan Drilling, Laser Percussion drilling, micro-cutting, Laser marking , Laser micro-grooving, laser micro-turning, etc. are some application of laser beam micro-machining.

Kuar et al. [13] did an experimental investigations of CNC pulsed Nd:YAG laser micro-drilling on zirconium oxide (ZrO2). Influence of laser machining parameters on the HAZ thickness and phenomena of tapering of the machined micro-holes was experimentally investigated. Response Surface Methodology-based optimal parametric analysis was performed to determine the optimal setting of process parameters such as pulse frequency and pulse width, lamp current, assist air pressure for achieving minimum HAZ thickness and taper of the micro-hole. Minimum HAZ thickness was obtained as 0.0675 mm when the lamp current, pulse frequency, assisted air pressure and pulse width were set at optimal parametric setting i.e. 17 amp, 2.0 kHz, 2.0 kg/cm2 and 2% of the duty cycle, respectively. Minimum taper was achieved as 0.0319 at optimal parametric setting i.e. the lamp current of 17 amp, pulse frequency of 2.0 kHz, assisted air pressure of 0.6 kg/cm2 and pulse width of 2% of the duty cycle. Analysis for multi-optimization of both the responses i.e. HAZ thickness and taper during pulsed Nd:YAG laser micro-drilling on ZrO2 also carried out.

Ghosal and Manna [14] investigated machining of Al/Al2O3- MMC by ytterbium fiber laser. The effects of the different parameters on the response characteristics were explained. A comprehensive mathematical models for correlating the interactive and higher-order influences of various machining parameters such as laser power, modulation frequency, gas pressure, wait time, pulse width on the machining performance criteria e.g. ,metal removal rate and tapering phenomena was developed for achieving controlled over fiber laser machining process. The response surface methodology (RSM) was employed to achieve optimum responses i.e., minimum tapering and maximum material removal rate. The parameters wait time and modulation frequency are identified as the most significant and significant parameters for MRR. Modulation frequency range from 600 to 680 Hz taper was minimum. The optimal parametric combination for maximized MRR and minimized taper was identified as 473.12W laser power, 604.54 Hz modulation frequency, 0.18s wait time, 19.82bar assist gas pressure and 93.47% of duty cycle pulse width and finally confirmation tests are conducted to validate the developed models.

Kleine et al. [15] carried out laser micro-cutting of stainless steel using a 50 W single-mode fiber laser. Kerf width and surface quality on the sidewall were their special interest and also presented the laser operating conditions to minimize Heat Affected Zone (HAZ). The cutting parameters for this experiment were 1500 Hz pulse frequency, 0.1 ms pulse length, 6 bar assist gas pressure (O2) and 4 mm/s cutting speed. Through this experiment they found the following conclusions- fiber laser, due to its good beam quality, is able to achieve very small focus diameters and small kerf widths. The cuts produced by the fiber laser show very similar features to those reported with other lasers. The surface quality and the thickness of the recast layer of stainless steel can be improved by optimizing the cutting parameters of the fiber laser. Lowering peak pulse power results in less pronounced striations and hence improved surface roughness · Higher pulse-to-pulse overlap improves the cut quality. There is no significant improvement of surface roughness beyond 85 % pulse-to-pulse overlap. · In order to reduce the recast layer, shorter laser pulse length and higher assist gas pressures are desirable.

Nikumb et al. [16] studied the effect of the pulse duration and other process parameters on the machined features to reveal the underlying thermal effects. Edge quality, circularity, aspect

ratio, formation of the redeposit material and machining rate were also studied with respect to the process variables such as laser power, wavelength and repetition rate. Arrays of drilled micro-hole patterns and fabricated micro-features were demonstrated with discussions on their potential applications. The lasers used in this work were a Q-switched Nd:YVO_4 laser operating at 532 nm wavelength with pulse width 3 ns and a repetition rate of 1 kHz. A frequency-tripled Nd:YAG laser, operating at 355 nm wavelength with pulse duration ranging from 10 to 30 ns, and an ultrafast Ti:Sapphire laser (Clark MXR 2000) at operating at its fundamental 775 nm wavelength having a fixed pulse duration of 150 fs and a repetition rate of
1000 Hz.

Corcoran. A et al [17] develop a laser drilling technique to generate cooling holes in multi-layer systems, for use in the aerospace industry. The cooling holes are required to conform to standards stipulated by the original engine manufacturer (OEM). A Nd:YAG laser was used to study the parameters affecting hole generation in superalloy materials. This paper reports on the investigation into the negative effects of percussion laser drilling on material interfaces, bond strength, and the negative effects on the individual microstructures such as recast layers and micro-cracking.

Yalukova, O. and Sarady, I. [18] performed experiments to compare the percussion drilled holes in fibre reinforced polymer and non-reinforced thermoplastic sheets using three wavelengths, 1064, 532 and 266nm. At near infrared and visible wavelengths, 1064 and 532nm, most of the bulk thermoplastic and thermoset polymers were partially transparent. The degree of transparency depended upon the degree of crystallinity. By using the fourth harmonics ultraviolet light (266nm) of a diode-pumped and AOQ-switched Nd:YAG laser with a pulse duration of about 100 ns, the hole drilling process was significantly improved and the risk for thermal damage had significantly reduced for both materials. Around the irradiated spot or drilled holes the material was influenced. There was clear evidence of a change in the interaction mechanism if UV light with high enough photon energy was utilized. By using UV light, bond breaking rather than thermal material removal occurred, i.e., a change from thermal to photo-chemical dissociation or photo-ablation became the

dominant interaction mechanism. The results achieved indicate that using even higher average UV power at 266nm and higher repetition frequency contour cutting of epoxy and polyester polymer sheets reinforced with different fibres would be possible. Higher power outputs were achieved by using a longer BBO crystal, increasing the average power of the present laser in the UV up to 10 W. This power level was enough to cut polymer sheets of up to 2mm thickness.

Zhu et al. [19] performed experimental investigation of drilling micro holes on Al, Mo, Ti, Cu, Ag, Au, and brass thin metal foils in air using 60-femtosecond Ti:Sapphire laser pulses. The influence of laser parameters and material properties on drilling processes at the sub-10-micron scale was examined. Comparison of hole drilling using 60-fs pulses with that using 50-ps and 10-ns pulses at an energy fluence of $\sim$ 15 J/cm^2 indicated that a significant amount of melting was present in both ps and ns regimes, whereas with fs pulses, fewer and much smaller droplets were observed. That indicates that fs machining has a physically different material removal process. It predominantly involves a transition from solid to vapor or smaller atomic clusters with minimum droplets from the molten phase. Although for thin and relatively low melting point metals, fs pulses was not as efficient as ns pulses in terms of material removal per unit energy, for hard materials and deeper holes, fs machining was evidently more advantageous.

Biswas et al. [20] fabricated Nd:YAG laser micro-drilling on gamma-titanium aluminide, a new material which has performed well in laboratory tests as well as in different fields of engineering. The effect of different process parameters in the optimization of the process was investigated. The aspects considered were the hole circularity at exit and the hole taper of the drilled hole. Lamp current, pulse frequency, air pressure and thickness of the job were selected as independent process variables. The central composite design (CCD) technique based on response surface methodology (RSM) was employed to plan the experiments to achieve optimum responses with a reduced number of experiments. Machining criteria have been checked for adequacy through ANOVA test successfully. They found lamp current and sample thickness have a significant effect on both responses, i.e., hole circularity at exit and hole taper. The pulse frequency and air pressure were dominant parameters for taper for hole circularity, respectively. The optimum value of hole circularity at exit was calculated at lower values of lamp current, higher value of thickness and moderate values of air pressure and pulse frequency. The optimum value of hole taper was found out at lower value of lamp current, lower value of air pressure, higher value of pulse frequency

and at higher thickness. Optimum values of both the responses may be obtained at moderate values of lamp current, pulse frequency, air pressure and at higher values of job sample thickness.

Matsuoka et al. [21] worked on laser micro-drilling on austenitic stainless steel with a Bessel beam to investigate the suitable processing conditions. They found that the threshold fluence to make a through hole increased with an increase in the sample thickness. For samples with the same thickness, the threshold fluence increased with an increase in the crossing angle. A small crossing angle Bessel beam can drill a deep hole with small threshold fluence. A through hole with a diameter smaller than 10 μm can be made on a stainless steel sheet 20 μm thick by using a Bessel beam with a large crossing angle. The taper of the hole drilled with the Bessel beam was smaller than that with the focused beam from the convex lens.

Jackson et al. [22] investigated the interaction phenomena of nanosecond time period, Q-switched, diode pumped Nd:YAG laser pulses of 1064, 532 and 355 nm wavelengths with M2 tool steel at an incident laser intensity range between 2 and 450 GW/cm^2. Interaction experiments were performed on 0.2 mm thickness M2 tool steel. For each sample experiment, drilling etch rate and surface structure was determined. Analysis of the results included the use of scanning electron microscopy (SEM) methods to detect changes related to melt solidification. A maximum etch rate of over 5m per pulse was obtained for the drilling etch rate experiments carried out using a laser wavelength of 355 nm, and just under 5m using 532 nm laser wavelengths. The maximum drilling etch rate obtained using a wavelength of 1064 nm was approximately 1m per pulse. They found decrease in the drilling etch rate as the interaction wavelength is increased, due to the reflective nature of tool steel and absorption of laser radiation by the plasma formed above the material during high intensity laser–material interaction.

Huang et al. [23] performed Micro-hole drilling and cutting in ambient air by using a femtosecond fiber laser. At first, the micro-hole drilling was investigated in both transparent (glasses) and non-transparent (metals and tissues) materials. The shape and morphology of the holes were characterized and evaluated with optical and scanning electron microscopy. Debris-free micro-holes with good roundness and no thermal damage were demonstrated with the aspect ratio of 8∶1. Micro-hole drilling in hard and soft tissues with no crack or collateral thermal damage is also demonstrated. Then, trench micromachining and cutting were studied for different materials and

the effect of the laser parameters on the trench properties was investigated. Straight and clean trench edges were obtained with no thermal damage.

Kumar Sanjay et al. [24] Observed that laser trepan drilling (LTD) produce better quality holes in advanced materials as compared with laser percussion drilling (LPD). But due to thermal nature of LTD process, it is rarely possible to completely remove the undesirable effects such as recast layer, heat affected zone and micro cracks. In order to improve the hole quality, these effects are required to be minimized. This research paper presents a computer-aided genetic algorithm-based multi-objective optimization (CGAMO) methodology for simultaneous optimization of multiple quality characteristics. The optimization results of the software CGAMO has been tested and validated by the published literature. Further, CGAMO has been used to simultaneously optimize the recast layer thickness (RLT) at entrance and exit in LTD of nickel based superalloy sheet. The predicted results show minimization of 99.82% and 85.06% in RLT at entrance and exit, respectively. The effect of significant process parameters on RLT has also been discussed.

Chein and Hou [25] investigate on the recast layer formation during the laser trepan drilling of Inconel 718 by a Nd:YAG laser. Laser drilling has evolved into the method of choice for the drilling of cooling holes in aerospace components. However, holes drilled with this particular technique are liable to display a variety of defects, including spattering, tapering, microcracks, and a recast layer. In order to meet the standards specified by the original engine manufacturer, this paper investigates the effects of the various laser drilling parameters on the recast layer thickness in the trepan drilling mode. A total of eight laser drilling parameters are considered in a series of experiments arranged using a Taguchi L18 orthogonal array. Taguchi analytical techniques are employed to establish the optimum set of parameters which yields a minimum recast layer thickness. The results indicate that the assist gas pressure, the peak power, and the focal position exert the greatest influence on the recast layer thickness. Having performed a confirmation experiment based on the initial Taguchi design experiments, the recast layer thickness is reduced further by adjusting the values of the assist gas pressure and the trepanning speed.

Goyal and Dubey [26] work on drilling of small-diameter holes meeting stringent quality standards in superalloys such as Inconel718 (having widespread applications in aero-engine component manufacturing) has always been a challenging task. Laser drilling has wide

applications in the aerospace industry. Laser trepan drilling (LTD) provides better control over the drilled hole geometry compared with laser percussion drilling to fulfill the higher dimensional accuracy requirement. This article presents an integrated approach of artificial neural network and genetic algorithm for the modeling and optimization of geometrical quality characteristics such as hole taper and circularity during LTD of 1.6mm thick Inconel718 Super alloy sheet. The optimum results show considerable improvements in hole taper, and hole circularities at laser beam entry and exit sides. Higher values of laser pulse frequency and trepanning speed in the present range have resulted in more circular holes with reduced taper.

Okasha .M.M et al. [27] observed that Laser percussion drilling is inherently associated with poor geometry and thermal defects. While mechanical micro-drilling produces good quality holes, premature drill breakage often occurs and it is difficult to drill holes at acute angles. This paper presents the feasibility and basic characteristics of a new approach for micro-drilling In718 alloy sheets at an acute angle, using sequential laser and mechanical drilling. The results demonstrate that sequential laser-mechanical micro-drilling alleviates the defects associated with laser-drilled holes, reduces burr size and machining time and increases the tool life compared with mechanical drilling.

Knowles et al. [28] fabricated micro-milled 2.5D structures in alumina, tungsten, steel and polyimide. Volume removal rates were presented for the different materials for different laser fluences. Three lasers were used in the tests; copper vapor laser (CVL), 532 nm Nd:YAG and 355 nm Nd:YAG. The CVL system used was an Oxford Lasers MP250 designed specifically for micro-machining. It is based on an oscillator amplifier laser emitting at 511 nm and 578 nm with 45 W maximum average power at a pulse frequency of 10 kHz and a pulse duration of 20 ns (FWHM). The 355 nm laser was a diode-pumped Nd:YAG of 5 W average power, 0–100 kHz pulse frequency and 27 ns pulse duration at 10 kHz (Light wave Q331). The 532 nm Nd:YAG laser (Spectra Physics Navigator II) was also diode-pumped. They demonstrated that, with the appropriate choice of laser parameters and processing strategies, nanosecond lasers can be used for high-quality micro-machining in metals, ceramics and polymers. Optimum laser intensities are 10–100 times higher for the processing of metals and ceramics compared to polymers. The detailed dependency of the surface quality for different materials and laser parameters was very complex

and has not been studied in their experiments. However, their work showed the potential for nanosecond-pulse-duration lasers to produce high-quality micro-machining results in a range of materials

Baumeister et al. [29] carried out laser micro-cutting on stainless steel foils with the aid of a 100W fiber laser. Experiments were performed on foil thicknesses of 100, 200 and 300 µm with the aid of assisting gases of nitrogen and oxygen. Using single mode fiber laser source of excellent beam quality and a high output power for micro-processing applications, minimal kerf widths of lesser then 20 µm were obtained with oxygen as the assisting gas. The kerf widths with nitrogen assisted cutting gas were wider. Thus, the common knowledge that nitrogen assisted cutting is better adapted to micro-processing is not justified for the case of fiber laser micro-cutting.

Yung et al. [30] performed Laser cutting on thin NiTi sheets with a thickness of 350 µm using a 355 nm Nd:YAG laser. A qualitative theoretical analysis and experimental investigations of the process parameters were done on the kerf profile and cutting quality. The results show that the kerf profile and cutting quality were significantly influenced by the process parameters, such as the single pulse energy, scan speed, frequency, pass number and beam offset, with the single pulse energy and pass number having the most significant effects. They found as the single pulse energy was increased and the laser beam velocity was decreased, the kerf width increased. The pass number mainly influenced the debris in the kerf as well as the depth. The number of laser passes was dependent on the other process parameters. If the process parameters were fixed, a sufficient number of passes was required for obtaining debris free cuts. Based on analysis, the process parameters were optimized. Debris-free kerf with narrow width (≈25 µm) and small taper (≈1˚) was obtained.

Meng et al. [31] presented a metallic cardiovascular stent cutting system based on fiber laser. In order to achieve the cutting of stent, the main modules and the key technologies were analyzed and achieved. Then with the cutting system, the kerf width size was studied for different cutting parameters including laser output power, pulse length, repeat frequency, cutting speed and assisting gas pressure. Finally, a high quality of cutting of 316L stainless steel cardiovascular stent was achieved. A 316L stainless steel tube (thickness 110µm, diameter 2 mm) was used in the cutting experiment. In this experiment frequency was 1500 Hz, pulse lengths were 0.15 ms and

assisting oxygen gas pressure was 0.3 MPa. They found that kerf width size increased as the laser output powers increased because of the high power density and decreased as the cutting speed increased, because of the low power density and oxygen density.

Kleine et al. [32] carried out laser micro-cutting of stainless steel using a 50 W single-mode fiber laser. Kerf width and surface quality on the sidewall were their special interest and also presented the laser operating conditions to minimize Heat Affected Zone (HAZ). The cutting parameters for this experiment were 1500 Hz pulse frequency, 0.1 ms pulse length, 6 bar assist gas pressure (O_2) and 4 mm/s cutting speed. Through this experiment they found the following conclusions- fiber laser, due to its good beam quality, is able to achieve very small focus diameters and small kerf widths. The cuts produced by the fiber laser show very similar features to those reported with other lasers. The surface quality and the thickness of the recast layer of stainless steel can be improved by optimizing the cutting parameters of the fiber laser. Lowering peak pulse power results in less pronounced striations and hence improved surface roughness · Higher pulse-to-pulse overlap improves the cut quality. There is no significant improvement of surface roughness beyond 85 % pulse-to-pulse overlap. · In order to reduce the recast layer, shorter laser pulse length and higher assist gas pressures are desirable.

Mauclair et al. [33] worked on femtosecond laser surface processing of materials allows for precise micrometer cutting with restricted detrimental side effects. They proposed and successfully employed an efficient technique to increase the cutting speed and energy efficiency of ultrafast laser micro-cutting by generating a line of N laser spots in the focal plane of a lens. Micro-cutting was conducted by translation of the sample along the spot line. This method avoids restriction on the cutting trajectory length and increases the cutting speed and energy efficiency of the process compared to single spot machining. Successful cutting of PZT ceramic and stainless steel was demonstrated with the spot line. The processing time was compared to single spot machining showing the advantage of the technique with various focal lenses. They also investigated the effect of intensity gradient on the spots line for micro-cutting on stainless steel. The efficiency and limitations of the method was discussed in light of the surface characterization using scanning electron microscopy on PZT.

Biswas et al. [34] carried out a research on pulsed Nd:YAG laser micro-cutting on alumina–aluminium. They investigated the influence of laser machining parameters such as lamp current, Q-switched pulse frequency and cutting speed on surface roughness. Response Surface Methodology (RSM) based optimal parametric analysis was performed for achieving minimum surface roughness (R_a) of the micro-cut surface. They found that lamp current has a very significant effect on surface roughness and pulse frequency and cutting speed also affect the surface roughness. From the surface plot they concluded that surface roughness first decreases and then increases following a curvilinear path with increase in lamp current and surface roughness decreases almost linearly with decrease in pulse frequency and cutting speed. The optimum value of surface roughness was obtained at higher value of lamp current, at lower value of pulse frequency and at lower value of cutting speed.

Sorgente et al. [35] carried out an experimental investigation of titanium alloy laser cutting using a 2 kW fiber laser. The cutting process was performed in continuous wave mode and using argon as shear gas. Laser cuts were performed on titanium alloy sheets 1mm thick. Image analysis and microscopy, were carried out to examine the cutting edge quality features including thickness of the recast layer and heat-affected zone. They found that, with increasing the cutting speed and then decreasing the heat input HAZ and RL thickness also increases. This behavior contrasts with the expected results.

Erika et al. [36] worked on fiber laser micro-cutting for coronary struts in AISI 316L stainless steel sheets. This work studied the influence of gases such compressed air and argon passing through the tube in order to drag molten material while laser micro-cutting was performed. The experimental work studied the influence of beam spot overlap and pulse energy on back wall dross and average surface roughness, using response surface methodology. The results indicate that the introduction of compressed air or argon gas was a relevant method to reduce the amount of dross adhered in the back wall of the miniature tube.

Chein and Hou [37] investigate on the recast layer formed during the laser trepan drilling of Inconel 718 by a Nd:YAG laser. Laser drilling has evolved into the method of choice for the drilling of cooling holes in aerospace components. However, holes drilled with this particular

technique are liable to display a variety of defects, including spattering, tapering, microcracks, and a recast layer. In order to meet the standards specified by the original engine manufacturer, this paper investigates the effects of the various laser drilling parameters on the recast layer thickness in the trepan drilling mode. A total of eight laser drilling parameters are considered in a series of experiments arranged using a Taguchi L18 orthogonal array. Taguchi analytical techniques are employed to establish the optimum set of parameters which yields a minimum recast layer thickness. The results indicate that the assist gas pressure, the peak power, and the focal position exert the greatest influence on the recast layer thickness. Having performed a confirmation experiment based on the initial Taguchi design experiments, the recast layer thickness is reduced further by adjusting the values of the assist gas pressure and the trepanning speed.

Ancona. A et al. [38] carried out an experimental study on the drilling of metal targets with ultrashort laser pulses at high repetition rates (from 50 kHz up to 975 kHz) and high average powers (up to 68 Watts), using an ytterbium-doped fiber CPA system. The number of pulses to drill through steel and copper sheets with thicknesses up to 1 mm have been measured as a function of the repetition rate and the pulse energy. Two distinctive effects, influencing the drilling efficiency at high repetition rates, have been experimentally found and studied: particle shielding and heat accumulation. While the shielding of subsequent pulses due to the ejected particles leads to a reduced ablation efficiency, this effect is counteracted by heat accumulation. The experimental data are in good qualitative agreement with simulations of the heat accumulation effect and previous studies on the particle emission. However, for materials with a high thermal conductivity as copper, both effects are negligible for the investigated processing parameters. Therefore, the full power of the fiber CPA system can be exploited, which allows to trepan high-quality holes in 0.5mm-thick copper samples with breakthrough times as low as 75 ms.

Emer et al. [39] worked on providing for laser drilling relatively large and deep holes in Superalloy components by percussion laser drilling a central hole through the component to a diameter less than the predetermined diameter, then trepanning laser drilling around the central hole to expand the predetermined diameter. The steps are repeated to deepen the hole.

Goyal and Dubey [40] carried out a study of laser trepan drilling process performance in terms of geometrical quality characteristics, such as hole taper and circularity for drilling small diameter hole in difficult-to-cut Titanium alloy sheet. Due to involvement of different process parameters

such as laser power, pulse width, pulse frequency, workpiece thickness, material composition, cutting speed, stand of distance and assist gas pressure, the laser cutting is a highly nonlinear and complex process. To handle this nonlinearity and complexity, genetic algorithm has been applied for the optimization. We used assist gas pressure, pulse width, pulse frequency and trepanning speed as input process parameters. The effect of significant process parameters on hole characteristics are discussed on the basis of data obtained through a well designed orthogonal array experimental matrix. Reliable empirical models have been developed for different quality characteristics. Improvements of 49% and 8% have been registered in hole taper and circularity, respectively, at optimum level of process parameters.

Ghoreishi M et al. [41] investigated the relationships and parameter interactions between six controllable variables on the hole taper and circularity in laser percussion drilling. Experiments have been conducted on stainless steel workpieces and a comparison was made between stainless steel and mild steel (IMechE Part B: J. Eng. Manufact. (in press)). Laser peak power, laser pulse width, pulse frequency, number of pulses, assist gas pressure and focal plane position were selected as independent process variables. The central composite design (CCD) was employed to plan the experiments in order to achieve required information with reduced number of experiments.The process performance was evaluated in terms of equivalent entrance diameter, hole taper and hole entrance circularity. The ratio of minimum to maximum Feret's diameter was considered as circularity characteristic of the hole. The models of these three process characteristics were developed by linear multiple regression technique. The initial models were computed according to the least squares procedure and were finalised by stepwise regression method. The significant coefficients were obtained by performing analysis of variance (ANOVA) at 1, 5 and 7% levels of significance. The final models were checked by complete residual analysis and finally were experimentally verified. It was found that the pulse frequency had a significant effect on the hole entrance diameter and hole circularity in drilling stainless steel unlike the drilling of mild steel where the pulse frequency had no significant effect on the hole characteristics.

Ng and Li [42] worked on experimental parametric analysis was carried out to correlate the laser parameters with the repeatability of a laser percussion drilling process. The experiment was conducted using a flash lamp pumped Nd:YAG laser to drill 2mm thick mild steel sheets. The relationship between the percentage standard deviation (PSD) of entrance hole diameter, hole

circularity and the operating parameters is established. Thirty-five holes were drilled and analysed for each set of identical laser parameters. The PSD of entrance hole diameter ranges between 1.47% and 4.78% for an operating window of 3.5–7kW peak power, and 1–3ms pulse width. The circularity of the entrance hole (defined as the ratio between the minimum and maximum diameters of the hole) ranges from 0.94 to 0.87, and is found to correlate with repeatability. The work shows that higher peak power, and shorter pulse width gives better hole geometry repeatability. The effect of melt ejection on hole geometry repeatability is also investigated. Melt ejection and spatter formation have been found to contribute to the poor repeatability of the process.

1.13. Objectives of the present research work

From the review of the past research works it is seen that a lot of theoretical and experimental works have been carried out for proper understanding of the basic process of Laser beam drilling (LBD) and also for identification of actual process parameter setting to optimize LBD performance criteria. Some researchers applied the LBD technique for machining of difficult-to-drill materials, which cannot be machine by any other conventional techniques.

Laser trepan drilling (LTD) is a very efficient technique for laser drilling operation. Researchers are going on using this technique for the effective improvement of the LBD performance measures like Diameter Deviation, Recast Layer formation, Circularity, Hole Taperness etc. Hence, the objectives of the present research work concentrated on

(i) To drill super-alloy shit (0.7 mm) with very less power (50 watt) laser machine by adjusting the performance criteria.

(ii) To study the feasibility of micro machining of Monel K-500 with Laser Beam µ-Machining.

(iii) To carry out LBMM experimentation based on RSM method for hole machining on Monel K-500 to investigate on the influences of various parameters such as sawing angle, power setting, scanning speed, Pulse Frequency, Duty cycle on the different micro machining performance criteria i.e. Top diameter, Bottom diameter, Circularity.

(iv) To develop mathematical model of performance criteria with the help of the response surface methodology (RSM) approach and analyze the effect of process parameters based on the developed models.

(v) To find out the most significant process parameters based on ANOVA Tables of RSM model for next level of experimentations.

(vi) To perform the multi-objective optimization to find out the optimal value of process parameters levels and performance criteria.

CHAPTER 2:

2. OVERVIEW OF LASER BEAM TREPANNING OPERATION

An improved method and apparatus for laser trepanning a passage through a workpiece, gas turbine engine component or the like includes the method steps of providing a linearly polarized beam of laser energy; focusing the laser beam on a selected location on the component; moving one of the laser beam or the work piece relative to one another along a first selected trepanning path and along a second selected trepanning path, which is substantially opposite in direction to the first selected path, to compensate for the linear polarization of the laser beam and to reduce the processing time. The steps of moving one of the laser beam or the work piece along the first and second trepanning paths are repeated until a passage is cut to a desired depth into the surface of the component or the passage is cut entirely through the component. An apparatus for accomplishing the method of the present invention includes a laser system for generating a linearly polarized beam of laser energy and a manipulator arrangement for moving one of the laser system or the component relative to one another. The apparatus further includes a computer controller which is programmed to move either the laser system or the component along the first and second selected trepanning paths.

2.1. Mechanism of Laser Beam Micro Machining (LBMM) Process

Laser beam machining is a thermal energy based on the non-conventional machining process in which the laser is focused on the conventional optical lens, at that instance high power density is generated by utilizing that high-energy, coherent light beam to melt and vaporize particles on the surface of metallic and non-metallic work pieces. Laser machining processes transport photon energy into the target material in the form of thermal energy, to remove material by melting and blow away, or by direct vaporization/ablation. Laser beam micro machining (LBMM) is a thermal energy based advanced machining process in which the material is removed by (i) Melting, (ii) Vaporization, and (iii) Ablation. When a high energy density laser bream is focused on work surface the thermal energy is absorbed which heats and transforms the work volume into a molten or vaporized state that can easily be removed by flow of high- pressure assist gas jet (which accelerates the transformed material and ejects it from machining zone).

Laser stands for light amplification by stimulated emission of radiation. Lasing process describes the basic operation of laser, i.e. generation of coherent (both temporal and spatial) beam of light by “light amplification “using “stimulated emission “The light generated by stimulated emission is very similar to the input signal in terms of wavelength, phase, and polarization. This gives laser light its characteristic coherence, and allows it to maintain the uniform polarization and often mono-chromaticity established by the optical cavity design.[8]

2.1.1 Material Removal

The basic material removal mechanism involved in laser beam machining is dependent upon the generation of high heat flux that causes melting and vaporization of the material where the beam is focused. A suitable lasing medium is used to get the laser beam of suitable wavelength.

Fig 2.1 shows the working of a laser. The beam coming out of a lasing medium has a small diameter. The beam is then focused on the material surface using a focusing lens. Laser beam has a well-defined wave front, which is either plane or spherical. When such a beam passes through a lens, the beam should get focused to a point. As a result, a high- energy concentration is obtained at that point. The laser radiation is first absorbed by the material surface where the optical energy is converted into heat. The amount of absorption of laser radiation by a work piece mainly depends on the wavelength, the angle of incidence of the laser beam on the work piece as well as polarization and finally the intensity of the focused laser beam. This intense heat melts and vaporizes the material.

The figure given bellow illustrates the principle of laser beam machining process. This machining method mainly comprises ruby laser tube, a pair of mirrors, an amplifying source, a flash tube, a cooling system, a lens and the main setup is incorporated in an enclosure (with high reflective inside surface). Depending upon the application, the lasers employed can be solid or gaseous type. The solid type provides shorter duration of laser beam while the gaseous type provides continuous laser beam and are best suited for cutting and welding operations.

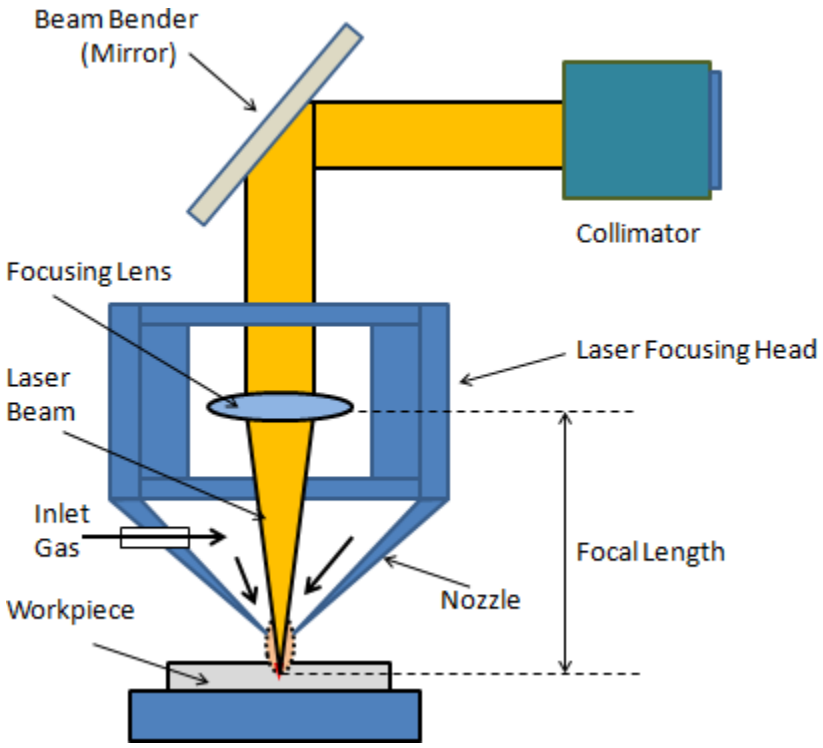

Fig. 2.1 working of a laser

When a light (i.e., optical energy) is projected on a laser tube by a flash lamp, the atoms get excited and absorb the radiation of incoming light energy. This causes to and fro motion of light in between the reflecting mirrors. Since partial reflecting mirror does not reflect the total light back at each travel that comes from a laser tube. Thus, a lens incorporated (in between work piece and partial reflecting mirror) converges the coherent stream of monochromatic light and focuses it to a particular point on the work piece surface. Therefore, the material gets melted and vaporized at the point where the converged laser beam of high intensity falls on work piece. The process continues to obtain the desired shape of the work piece. Since the process is accomplished by melting and vaporizing the work piece, this process is also known as "Thermal cutting process "The excitation energy provided by the laser is rapidly converted into heat and this is followed by various heat transfer processes such as conduction into the materials, convection and radiation from the surface. The temperature distribution within the material as a result of these heat transfer processes depends on the thermo physical properties of the material (density, emissivity, thermal conductivity,

specific heat, thermal diffusivity), dimensions of sample (thickness) and laser processing parameters (absorbed energy, beam cross-sectional area). The magnitude of temperature rise due to heating governs the different physical effects in the material for micro material removal/machining, such as

(a) Melting and sublimation

(b) Vaporization and dissociation

(c) Plasma formation

(d) Ablation

(a) MELTING & SUBLIMATION

Laser is focused on the conventional optical lens, at that instance high power density is generated by utilizing that high-energy, coherent light beam to melt and vaporize particles on the surface of metallic and non-metallic work pieces. At high laser power densities the surface temperature of the material may reach the melting point and material removal takes place by melting. The surface temperature increases with increasing irradiation time, reaches maximum temperature Tmax at laser ON-time and then decreases. The solid–liquid interface can be predicted by tracking the melting point in temperature versus depth Before initialization of surface evaporation, maximum melt depth increases with laser power density I (power per unit area) at constant pulse time while at a constant laser power density, maximum depth of melting increases with increasing pulse time. Prediction of melt depth using temperature profiles assists in determining depth of machined cavity in those glasses in which material removal takes place entirely or in part by melting shown in fig 2.2.[7]

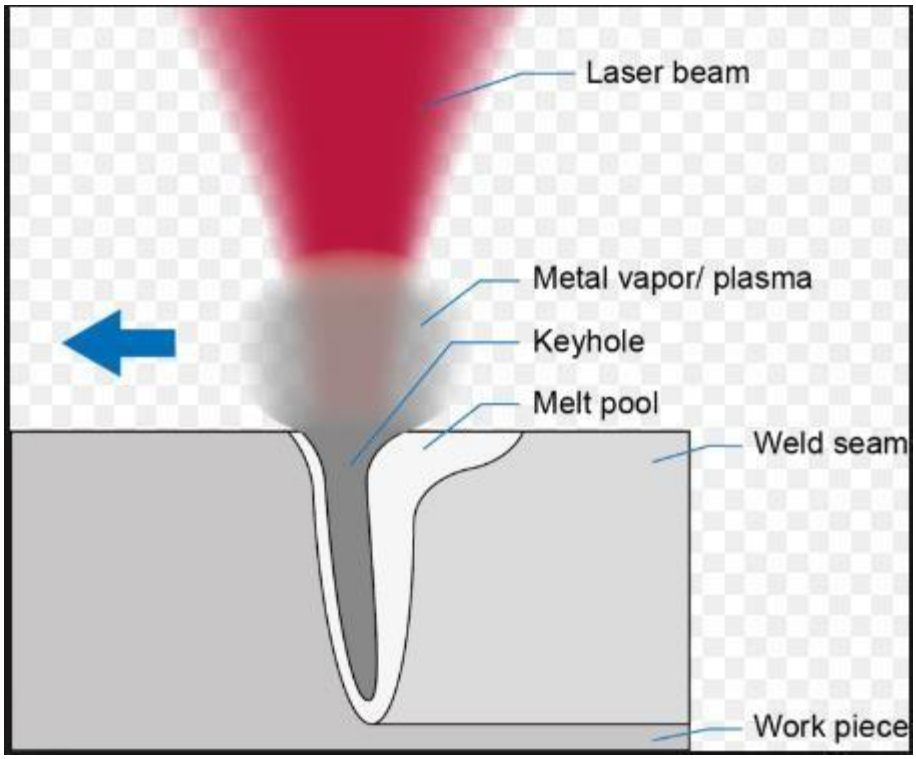

Fig.2.2: Melting and Vaporization of Materials

(B) VAPORIZATION & DISSOCIATION

As the surface temperature of material reaches the boiling point, further increase in laser power density or pulse time removes the material by evaporation instead of melting. After vaporization starts at the material surface, the liquid vapour interface moves further inside the material with supply of laser energy and material is removed by evaporation from the surface above the liquid vapour interface. Several works in the past have considered material removal only through this direct evaporation mechanism. In such cases, the depth of evaporation corresponding to depth of machined cavity depends on the laser conditions (processing time and absorbed laser energy) and material properties such as density, latent heat of vaporization, and boiling point during machining process and dissociation energy losses also affect the input laser energy and thus the temperature distribution, dimensions of machined cavity and machining time. The total enthalpy required for laser-induced vaporization being greater than that required for melting, the energy required for laser machining by melting is much less than the energy required for machining by vaporization.

It was reported that a combination of the different physical phenomena mentioned above was responsible for machining rather than any single predominant process.[6]

(C) PLASMA FORMATION

When the laser energy density surpasses a certain threshold limit, the material immediately vaporizes, gets ionized and forms plasma having temperatures as high as 50,000˚C and pressures up to 500MPa.The plasma plume forms a shield over the machining area and reduces the energy available to the work piece when the surface temperature exceeds a certain threshold value. Aerosols formed due to the condensation of ionized material vapour stick to the surface and reduces the efficiency of machined components for applications dominated by wear or tear load. Hence the degree of ionization is an important parameter which gives an indication whether plasma will be formed during the machining process and accordingly, necessary efforts to overcome the harmful effects of plasma could be undertaken. A special gas nozzle designed prevents the deposition of aerosols and this technique has been successfully applied to machine material surfaces without any debris. The additional gas stream obtained by combining a process gas stream and an exhaust stream transports the vaporized material and avoids radial distribution of the plasma.

Continuous application of laser pulses ensures that each successive spot is adequately displaced to reduce the plasma absorption effects. Furthermore, short duration pulses reduce the recast layer thickness; eliminate micro-cracks and the material removed per pulse increases with increasing energy density while machining ceramic materials.

(D) ABLATION

When the material is exposed to sufficiently large incident laser energy, the temperature of the surface exceeds the boiling point of the material causing rapid vaporization and subsequent material removal by the process referred to as thermal ablation. Ablation takes place when laser energy exceeds the characteristic threshold laser energy which represents the minimum energy required to remove material by ablation. Above ablation threshold energy, material removal is facilitated by bond breaking, whereas thermal effects take place below ablation threshold energy. Absorption properties of the glass and incident laser parameters determine the location at which the absorbed energy reaches the ablation threshold.

The sharp focusing of a laser light with sufficient fluencies is an attractive tool for material ablation. The type of interaction between the laser light and the material depends on laser parameters (wavelength, pulse duration and fluency) and on the properties (absorption coefficient, energy band gap, melting temperatures, the effective evaporation temperatures, and thermal conductivities) of the material. Ablation process can be categorized into three different mechanisms:

(i) Photo thermal

(ii) Photochemical

(iii) Photo physical

Photo thermal ablation is a thermal ablation process, in which instantaneous transformation of excitation energy into heat causes the removal of material. The rapid dissipation of the excitation and ionization energy from the electrons to the lattice, the material surface is heated rapidly and vaporized explosively with or without surface melting. These results in relatively high ablation rates and a rough surface finish. At moderate to high fluencies of nanosecond-pulsed lasers, screening of the incident radiation by vapour/plasma plume becomes significant. The screening effect would diminish laser light intensity that reaches the substrate by absorption and scattering within the vapour plume. Additionally, with decreasing wavelength of laser light, laser–plasma interaction becomes less pronounced.

If the photon energy of the laser light is sufficiently high, the probability of non-linear absorption increases strongly and multi-photon absorption is favoured. Under these conditions, laser excitation can result in direct bond scission, and the process is called photochemical ablation. For purely photochemical (non-thermal) processes, the temperature of the system remains essentially unchanged under laser irradiation. The ablation rate is relatively slow ($\leq$1μm/pulse), but high surface quality can be achieved. It is also called as photolytic processes. In photolytic processes the photon energy is directly applied to overcome the chemical bonding energy of (macro) molecules. When all laser energy is used to overcome the chemical binding energy, the ideal case, it is known as “cold ablation”.

Photo physical includes both thermal and non-thermal mechanisms contributing to overall ablation processes. In the laser ablation process, significant ablation is observed only above a certain laser fluence, which is referred as the threshold fluence. The values of the threshold fluence depend on laser parameters, in particular laser wavelength and pulse duration.

2.2. Basic Difference between Laser Trepan Drilling (LTD) and Laser Percussion Drilling (LPD) Operation

The Laser trepan drilling (LTD) and Laser percussion drilling (LPD) both the process have the same objective to make holes on the workpiece. Generally, they are the two basic approaches of laser beam drilling operation. In LPD, laser beam directly strikes and penetrates the material surface without any relative movement between laser beam and workpiece. While in LPD, the laser beam pierces the center of the hole and then move to the holes circumference. The material removal takes place by vaporization and/ or melts ejection.

The schematic of LTD is shown in Fig bellow.

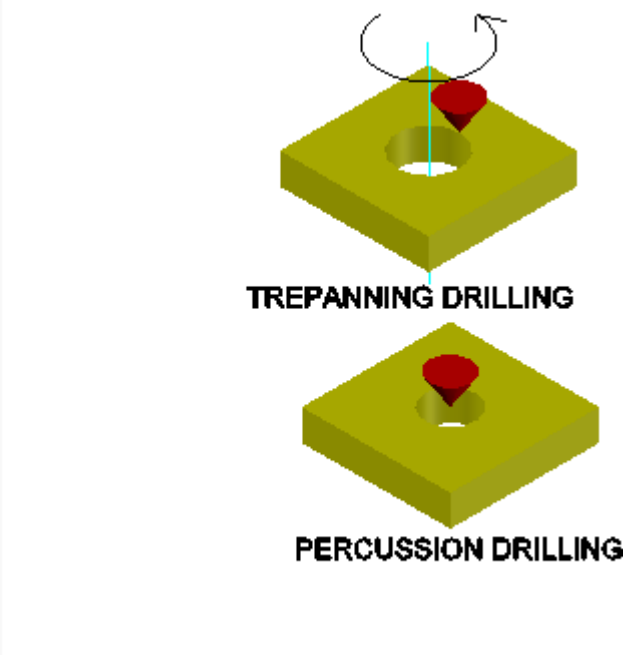

Fig. 2.3 Schematic of laser trepan drilling

Table 2.1 shows the basic differences between LTD and LPD

Points of distinction	LTD	LPD
Processing Time	More	Less
Recast Layer Formation	Less	More
Spatter	Less	More
Heat Affected Zone (HAZ)	Small	High

In LPD hole quality is poor compared with LTD due to the formation of a recast layer, spatter, and heat-affected zone. Higher dimensional accuracy and stringent hole-quality requirements in aerospace components result in holes with better-quality attributes. LTD may serve this purpose efficiently if the processing parameters are optimized appropriately in order to overcome the geometrical inaccuracies such as hole taper (HT) and circularity error caused by inherent characteristics of laser machining.

2.3. Relation between Process Parameters and Performance Criteria

The performance criteria of the LTD process are influenced by various process parameters which are discussed in brief as below.

2.3.1 Process Parameters of Laser Beam Trepanning Operation

i) Sawing Angle

Sawing Angle is used for smooth and easy Laser machining. In high power laser machining, laser impact on the metal and immediate evaporation of metal takes place. But in case of low power laser molten metal solidifies immediately after the melting. This phenomenon is called recasting. To overcome the recasting, an offset is provided on the metal, but the depth of the offset is taper in nature for easy removal of molten and evaporated metal. This angle of the taper is called sawing angle. Sawing angle is very important parameter for Laser trepan drilling operation. With increasing the sawing angle the power requirement for machining is decreases but the dimensional accuracy become poor.

The “sawing angle” for Laser trepan drilling has been shown in the fig. 2.4.

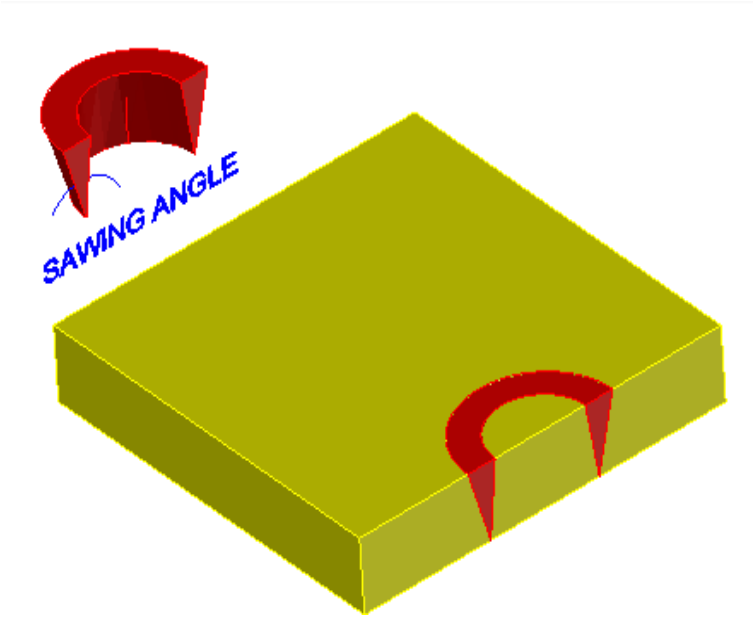

Fig.2.4. Sawing angle for laser trepan drilling operation

ii) Power Setting

Power setting is nothing but the power used for cutting. For high power laser operation, cutting is very easy. But for low power laser operation the cutting is very difficult. Some time it is not possible to cut a thick metal plate with low power laser operation. Here in this experiment our purpose is to make a hole by LTD process with a very low power (50 watt) laser machine.

iii) Scanning Speed

Scanning Speed is the speed of cutting or the speed of the laser nozzle. The quality of cutting is very much depends upon the Scanning Speed. High scanning speed reduce the quality of the cutting. Low to moderate value of scanning speed is used for high quality cutting operation.

iv) Pulse Frequency

Pulse frequency is the number of cycles produced across the gap in 1 s. The higher the frequency, finer is the surface finish that can be obtained. With an increase of number of cycles per second, the length of the on-time decreases. Short on-times remove very little material and create smaller craters. This produces a smoother surface finish with less thermal damage to the workpiece.

v) Duty Cycle

Duty cycle refers to the fraction of time its on and active in its application. It can be expressed as a fraction real number or as a percentage of the fraction multiplied by 100. A laser that's on continuously can be said to have 100% duty cycle. A laser that's modulated by a square wave will have a 50 percent duty cycle.

2.3.2 Performance Criteria of LTD process

In LTD, performance criteria significantly depend on the various factors like top diameter, bottom diameter, circularity, hole taper, HAZ etc. When micro components are generated in LBMM process, these factors are considered for the optimal performance criteria. The major LTD performance criteria are top diameter (TD), bottom diameter (BD), circularity, taperness, HAZ etc. Major performance criteria are described follows:

i) Top Diameter

It is the top portion of a hole. When laser beam strikes on a surface, the immediate melting and evaporation takes place on the surface. Due to overcut and high energy impact on the top surface, the shape of the hole became larger and non-uniform. An investigation on the overcut of top diameter has been done in that experiment. In general the overcut is mostly depends upon the power setting, sawing angle, duty cycle, pulse frequency and scanning speed. In the present experiment the relation between that process parameters and Top Diameter has been developed.

ii) Bottom Diameter

It is the bottom portion of a hole. When laser strikes and penetrate into the material, melting and evaporation takes place from the inner and bottom portion of the material also. A small overcut are also there at the bottom surface like the top surface. An investigation on the overcut of bottom diameter has been done in that experiment. In general the overcut is mostly depends upon the power setting, sawing angle, duty cycle, pulse frequency and scanning speed. In the present experiment the relation between that process parameters and Top Diameter has been developed.

iii) Circularity

The circularity symbol is used to describe how close an object should be to a true circle. Sometimes called roundness, circularity is a 2-Dimensional tolerance that controls the overall form of a circle ensuring it is not too oblong, square, or out of round. An investigation on the circularity has been done in that experiment. In general the circularity is mostly depends upon the power setting, sawing angle, duty cycle, pulse frequency and scanning speed. In the present experiment the relation between that process parameters and circularity has been developed.

CHAPTER 3:

3. LBM SETUP FOR EXPERIMENTATION

3.1. Multi Diode fiber laser system

A 50 W ytterbium doped multi diode pumped fiber laser system with a wavelength of 1064 nm, made by M/S Sahajanand Laser Technology Limited (Model: SCRIBO SLF 175), has been used for the micro-cutting operation. Fig. 3.3 is the photographic view of the laser machining setup. This laser system is comprised of (a) power supply unit, (b) laser head, (c) collimator, (d) beam bender, (e) beam delivery unit and focusing lens, (f) assist gas supply unit and (g) computer numerical control (CNC) controller for X–Y–Z movement.

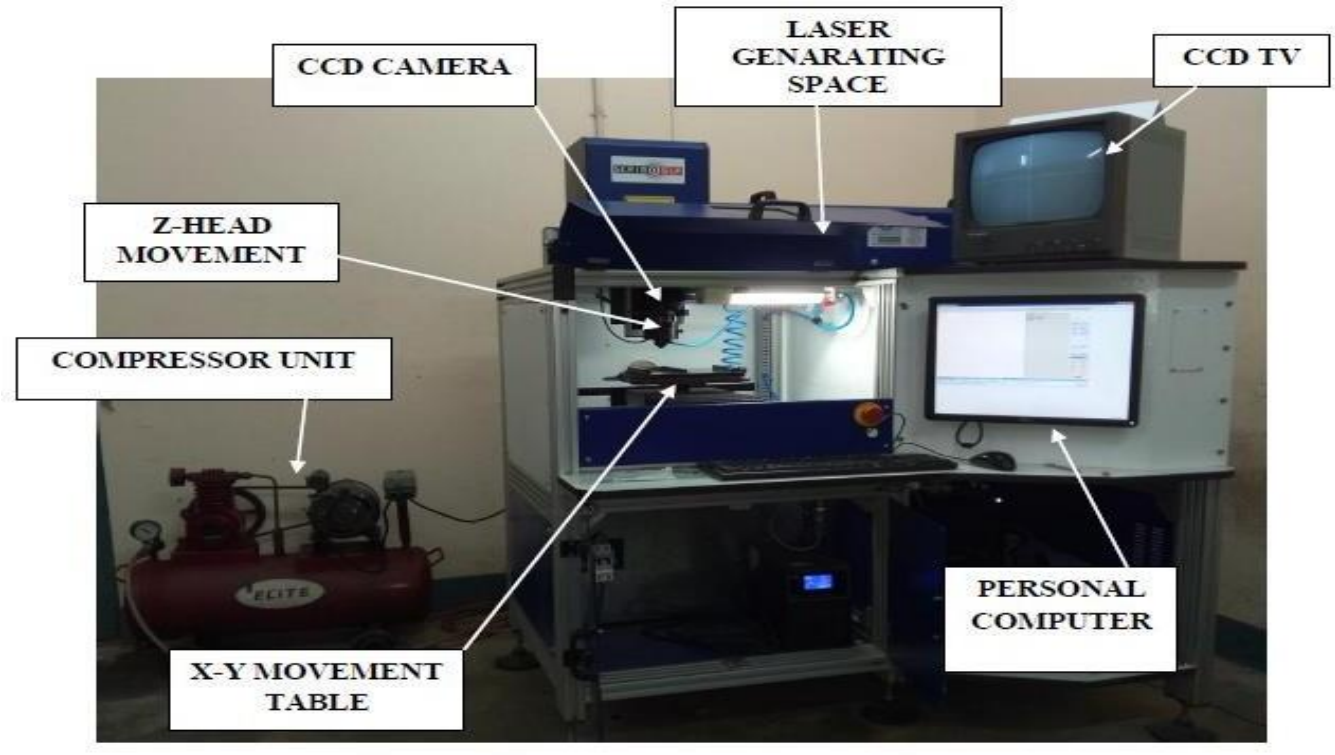

Fig. 3.1. Photographic View of the Laser Machining Set up

Chapter 3:

3.2. Components of Multi Diode Fiber Laser System

3.2.1 Power Supply with Isolation Transformer

The power supply unit as shown in the fig. 3.2 consist of a 1.5 kVA of isolation transformer and 1 kVA of un-interruptible power source (UPS). The isolation transformer is connected with the main power supply unit and the UPS is connected to the isolation transformer. The pumping of laser diodes inside the laser head is achieved via the power supply unit.

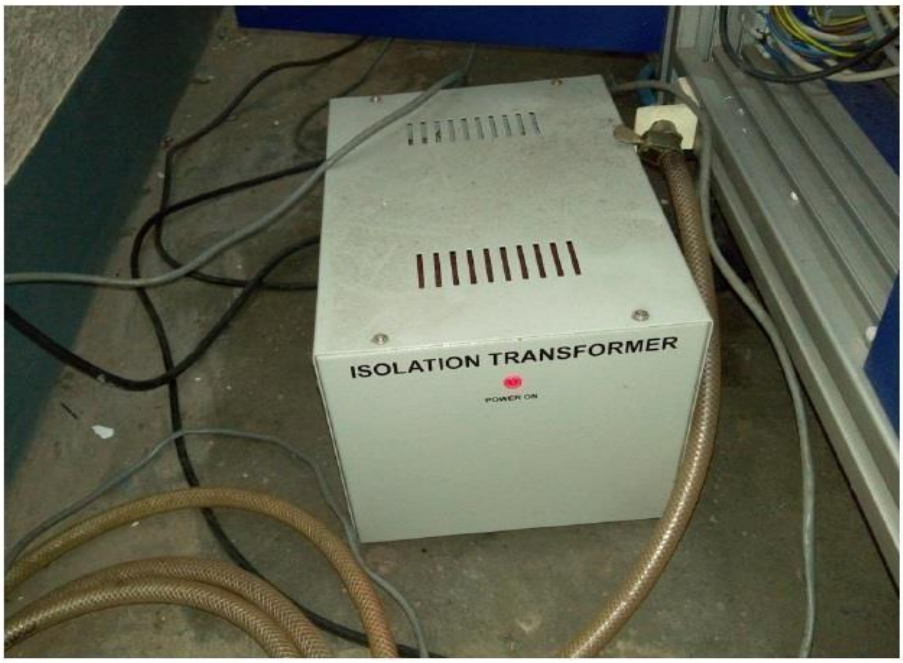

Fig. 3.2. Photographic view of isolation transformer

3.2.2 Laser Source

Fiber laser is pumped with special high power multimode diodes via cladding surrounding as single mode core. Life of this individual multimode diode is quite long corresponding to conventional diode pump solid-state laser (DPSSL). Fiber laser is pumped by multiple identical diodes all feeding same gain medium, whereas DPSSL is pumped by a single diode bar. In the

unlikely event of failure of any single pump diode in the fiber laser, the laser continues to work with slightly lower specification. In case of DPSSL, the total laser fails if diode stops working.

3.2.3 Laser Head

The diode pumped fiber laser system is comprised of a fiber which is doped with Yb^{3+}, fiber Bragg grating and light emitting diodes. The number of diodes is dependent on the total output power of the system. A total number of 8 diodes are utilized in the present system for pumping. Fiber Bragg gratings are sliced into two ends of the fiber optics so that the laser can be generated. The total length of the fiber can be up to 3 mm depending upon the output power generated by the fiber laser.

3.2.4 Collimator

After the generation of the laser within the optical fiber, the laser is transferred into a collimator. In the collimator, two prisms are fitted at the two ends of it. This collimator acts as a beam expander, i.e., the laser can propagate to the required distance. The diameter of the laser beam is 9 mm at the end of the collimator.

3.2.5 Beam Bender

After the collimator, a beam bender with 100% reflectivity is placed at an angle of 45º with the horizontal plane so that the laser can be perpendicular to the focus lens. At the top of the beam bender, a charge couple device camera (CCD) is placed which is further connected to a CCTV.

3.2.6 Beam Delivery System

The biggest benefit of fiber laser is that the Gain Medium is fiber & delivery is also through the fiber. This leads to less chances of failure at coupling point between gain medium and delivery when extended to the workplace.

3.2.7 Laser Beam Focusing Control System

By changing the focal length of the focusing lens one can alter the power density and the depth of focus produced by the laser of given beam diameter. A lower focal length lens has higher power density but large

depth of focus for as same beam diameter falling over a focusing lens. The alignment of the focusing lens is very important because if the beam center is not coincident with the center of the lens then the beam after the lens will not be straight and therefore the cutting efficiently drastically decreases. To get proper focus on the work piece this Fibre laser system equipped with CNC interface, CCD camera, CCTV.

3.2.8 CNC Controller for Axis Movement

An X-Y table and the movement of X and Y-axis is controlled by CNC controller unit, for proper focusing of laser beam by means of focusing lens. Fig. 3.3 is the photographic view of X-Y table and Z-head. The hardware specification of CNC table unit is shown in table 3.1. Z axis controls the focus length of the job.

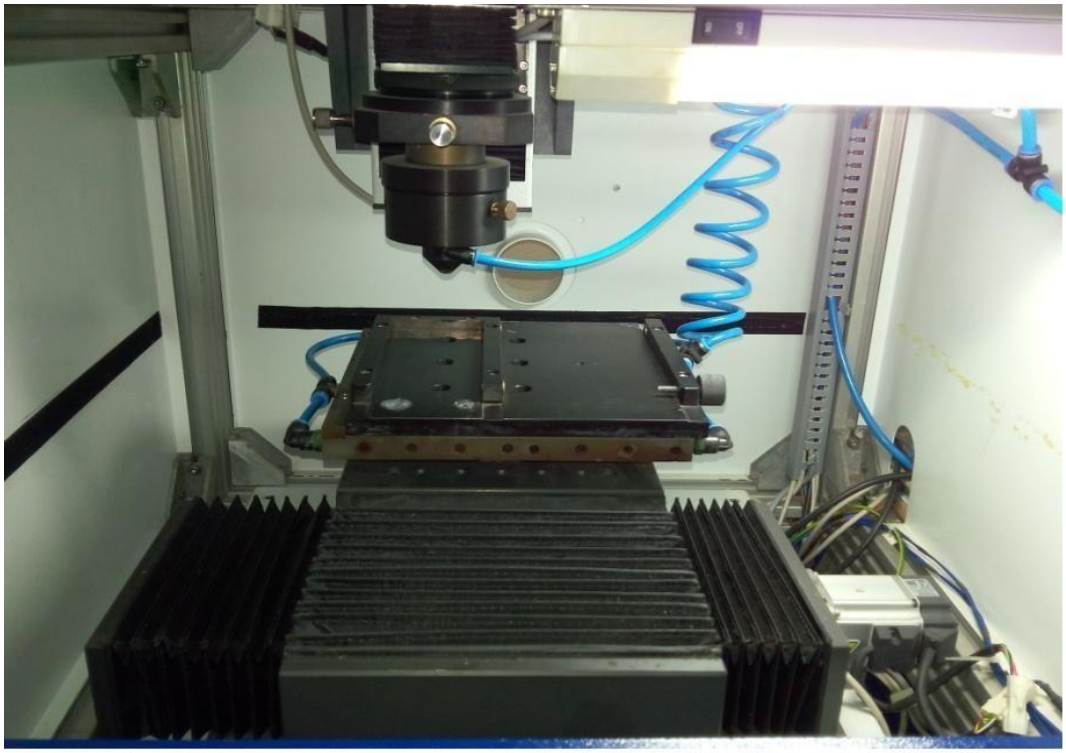

Fig. 3.3. Photographic view of X-Y Table and Z-head

Table 3.1: Specification of CNC table unit

Axis of travel (X-Y axis)	150mm X 150mm
Focusing vertical travel	75mm
Beam Diameter	21μm
Resolution	1μm
Table working area	150 X 150 mm^2
Clamping of Workpiece	By developed fixture
Feed rate (X, Y, & Z axis)	0.1-30 mm/s
Control system	Open Loop Control

3.2.9 CCTV and CCD Camera

CCD camera gets its three-phase supply through 12V adapter. It is connected to the CCTV by a bnc cable. CCTV gets supply from single phase. A camera together with monitor is used for viewing the work piece and therefore need to align before the laser is used. The alignment consists of setting the image of the laser spot at the center of the monitor over which a cross wire is drawn. The laser spot with lens and without lens should coincides with the center of the cross wire.

3.2.10 Compressor Unit

Sometimes the ablated micro-chips or particles may deposited or recasted on the machining zone. To remove this impurity and clean the machining zone a compressor unit is used to remove this adhere particles as shown in the fig. 3.4. Here compressor of 3 bar is used.

Fig. 3.4. Photographic view of Compressor Unit

3.2.11 Moisture Separator and Air Pressure Controlling Unit

The jet of assisting gas helps to remove the molten material from the cutting zone and overcome re-solidification of the molten material from the micro-machining zone. Further the supply line passes through a moisture separator and is connected to a pressure regulating valve. It results in the jet flow of dry pressurized air to the laser micro-machining zone. Fig. 3.5 is the photographic view of the moisture separator and pressure regulating Unit.

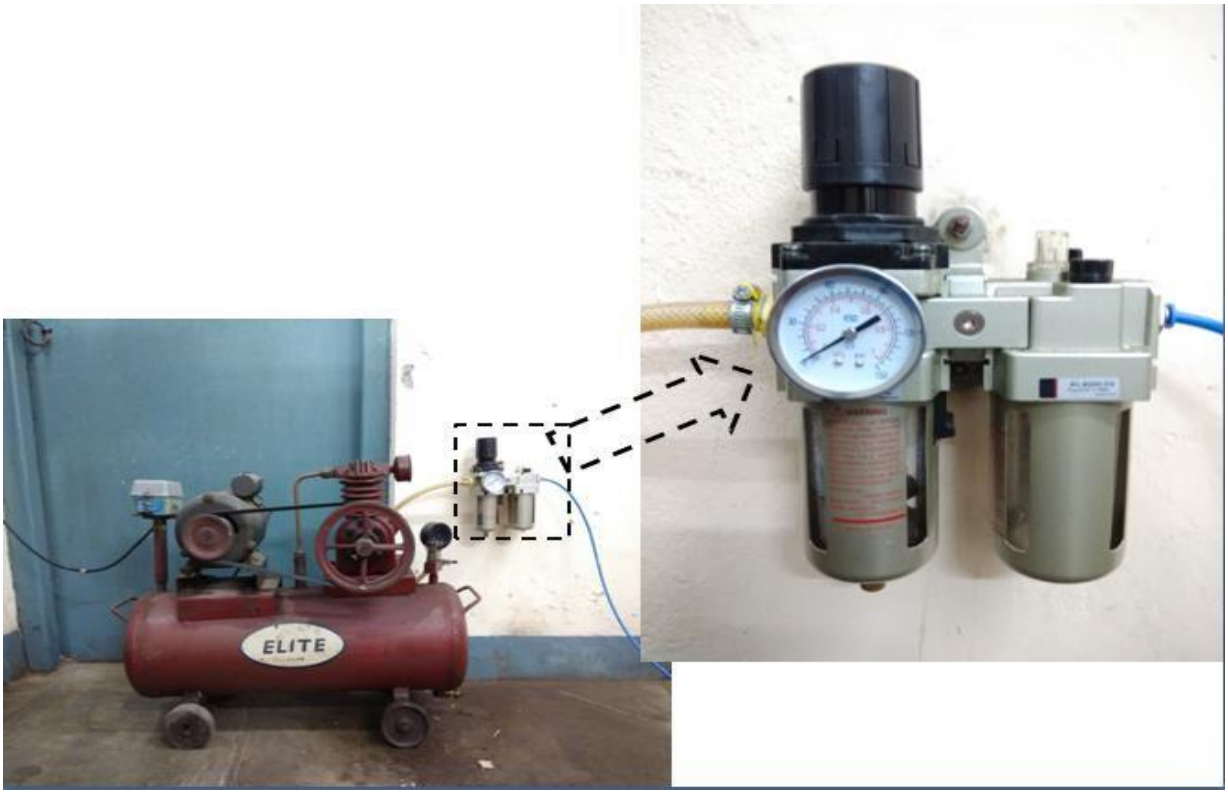

Fig. 3.5. Moisture separator and pressure regulating Unit

3.3 Principle of fiber laser

A working laser needs an optical resonator with gain media and a source of energy to excite electrons in the gain media. Classic design of fiber lasers uses a double clad optical fiber. Pump light is directed into the inner cladding, bouncing inside outer cladding through active core and is gradually absorbed along fibers length. Laser light is bound inside active core, serving as a gain media too.

Most robust design of a fiber laser as shown in the fig. 3.6 uses reflection from fiber Bragg grating as a mirror, so the whole laser resonator is made inside a fiber. Another possible design of a fiber-integrated mirror is a loop mirror.

A Bragg Grating is a section of glass that has stripes in it where the refractive index has been changed. Each time the light goes across a boundary between one refractive index and another, a bit is reflected back. If you have enough stripes, the grating acts like a very efficient mirror.

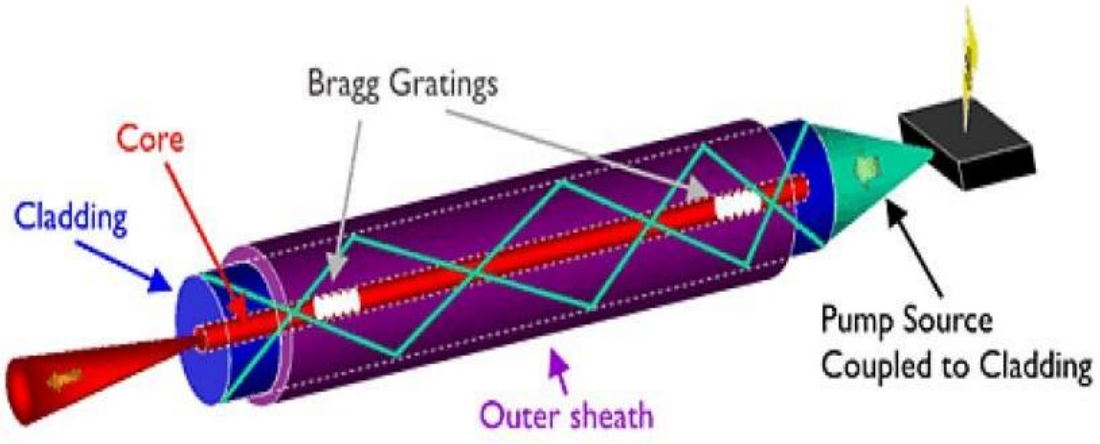

Fig. 3.6 Schematic diagram of fiber laser

The most important element of this type of devices is active optical fiber doped with rare earth elements, inside of which the laser beam is created. It is a specific kind of fiber, which consists of three layers of materials, characterized by different refractive index, the outer layer – it is a special cladding, characterized by the lowest refractive index. Its role is to reflect of its surface light. At the same time the cladding blocks the emission of radiation outside; the middle layer –which is created from a material characterized by higher refractive index in comparison to the outer cladding. Its goal is to initiate the work of the laser, as well as guarantee optimal transmission of the pumping energy; the Centre is an active optical core, it is characterized by the highest refractive index of all of the layers.

Fiber is highly flexible, and at the same time it is characterized by very solid and compact construction, which allows to create a thin laser rods of substantial length. On both sides of the fiber there are connectors, responsible for the transportation of the energy from pumping diodes to the external layer. Beam, which is emitted by the core, is transferred to the collimator through the fiber. The beam itself is characterized by a very strong power and large divergence. It is

transformed in the collimator into a beam and rays are transmitted in parallel to each other. After the process is finished, the beam is transferred to the optical system, in which it is focused into a point of a required diameter. A great advantage is the fact, that a thin construction of long beams makes its cooling process easier and more effective. At the same time the heating process, resulting from pumping the laser's beam with energy, is minimal. These parameters influence the general efficiency of the devices, which in turn leads to achieving very high power conversion ratio (it is calculated by taking into account the ratio of the power of the beam, emitted by the active fiber, to the electrical power, which had to be used to generate the radiation). Fig.3.7 is the Schematic diagram of a fiber laser micro-machining setup.

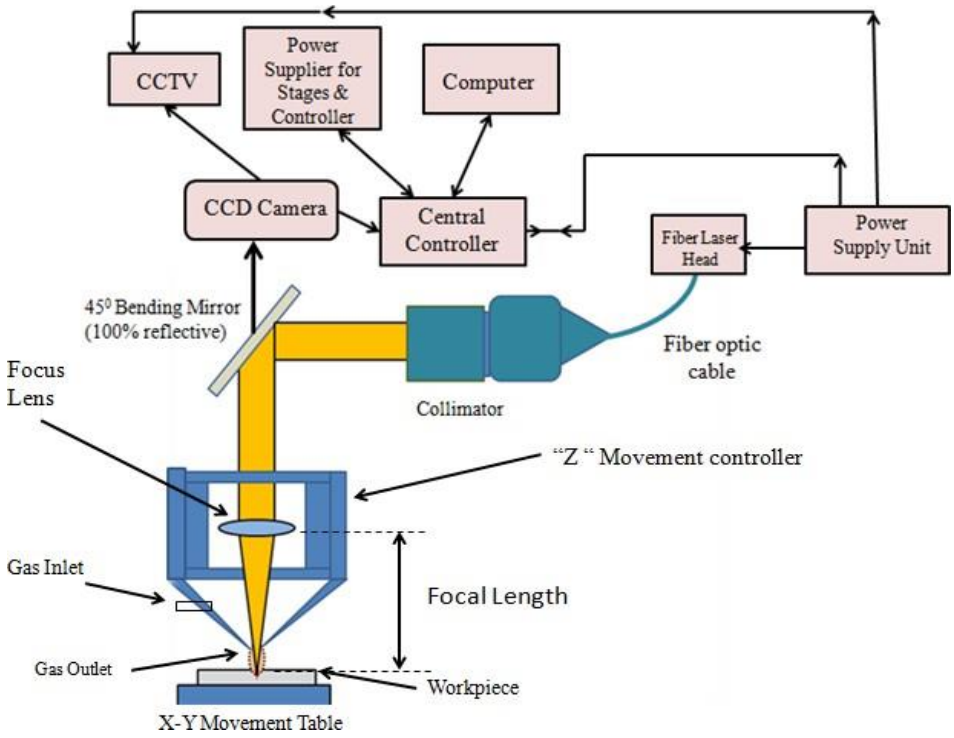

Fig.3.7 Schematic diagram of a fiber laser micro-machining setup

3.4 ADVANTAGES OF FIBER LASER

The importance of fiber laser system for the micro-machining domain is inevitable. Fiber lasers are ideally suited for the generation of micro-features required for the bio-medical applications, electronics industries, automotive and aerospace industries. Excellent constant beam properties, long focal lengths, and rapid warm-up make it ideal for the applications in the micro-machining domain.

The advantages of fiber lasers over other types include:

a) Superior Beam Quality: The primary characteristics of the high quality beams are that, it can be focused on a small spot on the workpiece, providing high power density thereby leading to faster processing time. Compared to the other laser technologies, fiber laser beams have a longer focal length (working distance) along with greater depth of focus (workpiece positioning tolerance).
b) Light is already coupled into a flexible fiber: The fact that the light is already in a fiber allows it to be easily delivered to a movable focusing element. This is important for laser cutting, welding, and folding of metals and polymers.
c) High output power: Fiber lasers can have active regions several kilometers long, and so can provide very high optical gain. They can support kilowatt levels of continuous output power because of the fiber's high surface area to volume ratio, which allows efficient cooling.
d) High optical quality: The fiber's wave guiding properties reduce or eliminate thermal distortion of the optical path, typically producing a diffraction-limited, high-quality optical beam.
e) Compact size: Fiber lasers are compact compared to rod or gas lasers of comparable power, because the fiber can be bent and coiled to save space.
f) Reliability: Fiber lasers exhibit high vibrational stability, extended lifetime, and maintenance-free turnkey operation.
g) High peak power and nanosecond pulses enable effective marking and engraving.
h) The additional power and better beam quality provide cleaner cut edges and faster cutting speeds.

i) Lower cost of ownership.

j) Fiber lasers are now being used to make high-performance surface-acoustic wave (SAW) devices. These lasers raise throughput and lower cost of ownership in comparison to older solid-state laser technology.

CHAPTER 4:

4. PLANNING FOR THE PRESENT RESEARCH WORK

4.1. Experimentation

Although, Laser trepan drilling (LTD) significantly improve the performance criteria such as diameter deviation, recast layer formation, circularity, hole taper etc. but it has low processing speed. So this is a very challenging issue to improving the machining efficiency for drilling of Monel K-500 thickness of 0.7 mm by LTD process. For this, optimization of all the process parameters is required Laser trepan drilling (LTD) operation. The targeted diameter of the hole is 0.5 mm.

4.1.1. Experimental Scheme

To fulfill the objective of the present research work an attempt has been made to investigate on the influences of process parameter such as Sawing Angle, Power Settings, Scanning Speed, Pulse Frequency and Duty Cycle on various LTD responses e.g. Top diameter, Bottom diameter and circularity.

To investigate the influences of various process parameters as mentioned in above paragraph on the above machining criteria, the LTD process was used for drilling on rectangular shaped workpiece for experimentation. At first many trial experiments were carried out to find out the ranges of Sawing Angle, Power Setting, Scanning Speed, Pulse Frequency and Duty Cycle. A 50 watt multi diode fiber laser of beam diameter 21µm was used. Monel K-500 was selected as the workpiece material. During trial experimentation with above mentioned laser beam and workpiece, it was observed that a good spark quality and the desired hole diameter occurred at the range of (0.1 to 1.3 deg.) of Sawing Angle, (32.5 to 42.5 watt) of Power Setting, (0.2 to 1 mm/sec) of Scanning Speed, (50 to 70 kHz) Pulse Frequency and (80 to 92 %) of Duty Cycle. Otherwise the hole quality was found poor. For this reason, it was decided to conduct thee experiments at different Sawing Angle, Power Setting, Scanning Speed, Pulse Frequency and Duty Cycle and total 52 number of experiments to for Response Surface Methodology (RSM) based model.

At each parametric condition, only one experiment was carried out and the value of experiment results were used for analysis.

The experiments were performed based on Response Surface Methodology (RSM) and analysis was done with the results of experiment. Optimal condition of parameters and responses for single objective as well as multi-objective, were obtained with the mathematical models developed by RSM and the particle swarm optimization (PSO) technique.

4.1.2 Measurement of Different Performance Characteristic

In this research work three LTD performance characteristics, i.e. Top diameter (TD), Bottom diameter (BD) and circularity have been taken.

And all the performance characteristic have been measured in LEICA microscope setup.

Fig.4.1. Photographic view of LEICA microscope setup

(i) Top diameter (TD)

Top diameter (TD) was measured by using the Olympus STM 6 microscope setup. The technique used for measuring the top diameter is shown in the given figure bellow.

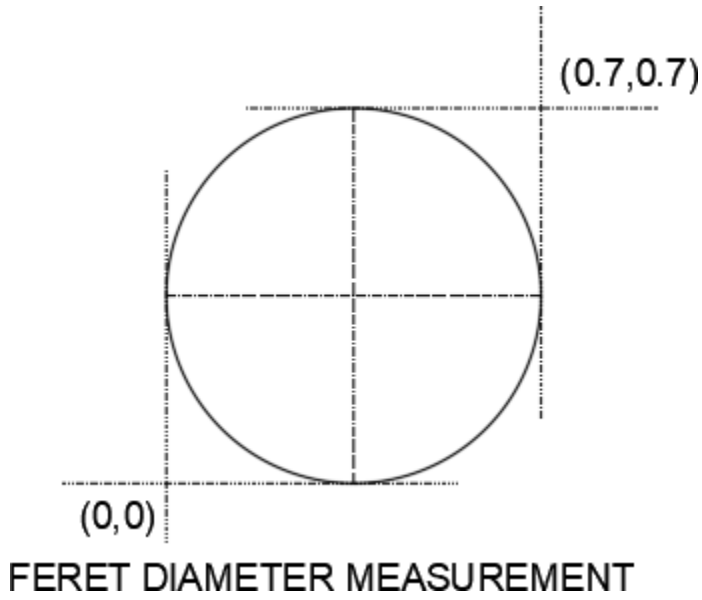

Fig. 4.2. Feret diameter measurement by LEICA microscope setup

At first the origin of X and Y axis has been set up in such a way that the axis should be tangent with the hole or circle and set the origin at (0,0). Similarly set the origin at diagonally opposite side after the first setting. The origin after second setting gives the measurement of the ferret diameter.

(ii) Bottom diameter (BD)

Bottom diameter (BD) was also measured by using the Olympus STM 6 microscope setup. The bottom diameter is measured in the same way as the top diameter measured.

(iii) Circularity or Roundness

In the Laser trepan drilling (LTD) operation for top and bottom portion of hole, circularity is defined by the maximum inscribed circle diameter to the minimum circumscribed circle diameter.

The value of circularity or roundness must be in between 0 to 1. The value of circularity closer to one indicate that the hole is very much closer to the true hole and machined surface is smooth. The circularity is expressed by the given expression and Fig. 4.3.

$$\text{Circularity} = \frac{\text{Maximum inscribed circle diameter of entry or exit}}{\text{Minimum circumscribed cirle diameter of entry or}} \quad \text{Eq. 4.3.}$$

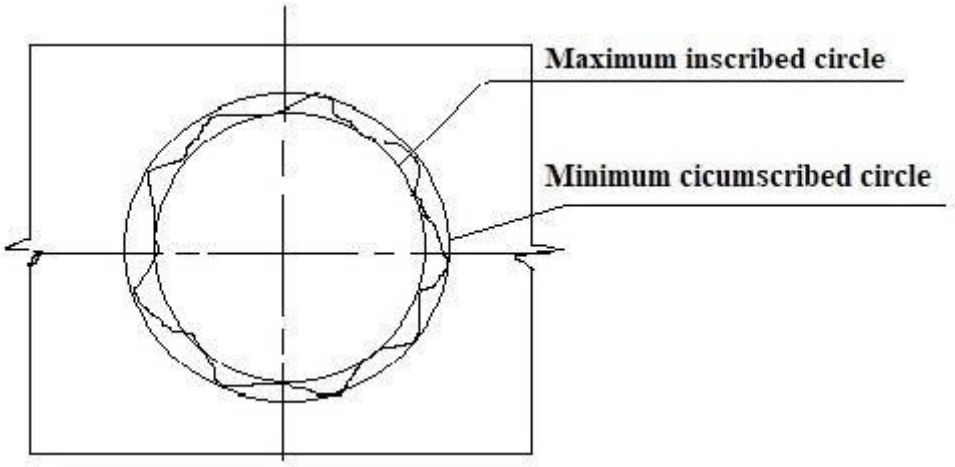

Fig.4.3. Schematic top view of micro hole

4.2 Selection of job sample (Monel K-500)

The selection of the material of job sample in LTD is an important task because the machining performance totally depends on the combination job and process parameters.

MONEL K-500 is a Nickel & cobalt base corrosion, temperature and wear-resistant alloy. During machining this alloy becomes work harden rapidly, generates high heat during cutting, weld to the cutting tool surface and offers high resistance to metal removal because of its higher shear strengths. If the range of machining is in micro-level then laser beam micro machining (LBMM) is the one of the best alternatives over all other micro machining processes for machining Monel K-500. Because the density, thermal conductivity and electrical resistivity of copper is greater than that of Monel K-500 and the process mechanism of the LTD is by melting and vaporization, so it

would be possible that more material is removed from the workpiece. The chemical composition of Monel K-500 is given in Table 4.1.

Table 4.1. The chemical composition of Monel K-500

Material	Ni	Cu	Al	Ti	C	Fe	Mn	Si	S
Percentage	**63.0**	**29.5**	**2.7**	**0.6**	**0.18**	**2.0**	**1.5**	**0.50**	**0.01**

The physical, thermal, electrical and mechanical properties of the Monel K-500 are shown in Table 4.2.

Table 4.2. Properties of Monel K-500

Properties	Monel K-500
Density (gm/cm^3)	8.44
Melting Range (°C)	1315-1350
Electrical resistivity (ohm-m)	$0.615 \times \mathbf{10}^{-6}$
Thermal conductivity (W/m.°C)	17.2
Poisson ratio	0.32
Hardness (BHN)	260-325

4.2.1 Applications of job sample material (Monel K-500)

Monel K-500 is used extensively in countless applications because of its quality. It has excellent corrosion resistant characteristics and has enhanced strength and hardness after precipitation hardening. Monel K 500 has approximately three (3) times in the yield strength and double in the tensile strength when compared with Monel 400. Monel K 500 can be further strengthened by cold working before the precipitation hardening. It has excellent mechanical properties from sub-zero temperatures up to about 480°C and corrosion resistance in an extensive range of marine and

chemical environments. Typical application of Monel K 500 are to manufacture pump shafts, impellers, propeller shafts, valve components for ships and offshore drilling towers, bolting, oil well drill collars and instrumentation components for oil and gas production. It is particularly well suited for centrifugal pumps in the marine industry because of its high strength and low corrosion rates in high-velocity seawater.

4.3. Design of Experiment

For the purpose of making 0.5 mm diameter hole on 0.7 mm thick Monel K-500 shit by laser trepan drilling (LTD process, a design of experiment (DOE) is developed.

Design of Experiments (DOE) is a powerful statistical technique introduced by R.

A. Fisher in England in the 1920's to study the effect of multiple variables simultaneously. Design of experiments (DOE) is a systematic method to determine the relationship between factors affecting a process and the output of that process.

In other words, it is used to find cause-and-effect relationships. This information is needed to manage process inputs in order to optimize the output.

The most commonly used terms in DOE methodology include: controllable and uncontrollable input factors, responses, hypothesis testing, blocking, replication and interaction.

- Controllable input factors, or *x* factors, are those input parameters that can be modified in an experiment or process. The controllable input factors can be modified to optimize the output. The relationship between the factors and responses is shown in Fig. 4.4.

- Uncontrollable input factors are those parameters that cannot be changed. These factors needs to be recognized to understand how they may affect the response.

- Response, or output measures, are the elements of the process outcome that gage the desired effect. In the cooking example, the taste and texture of the rice are the responses.

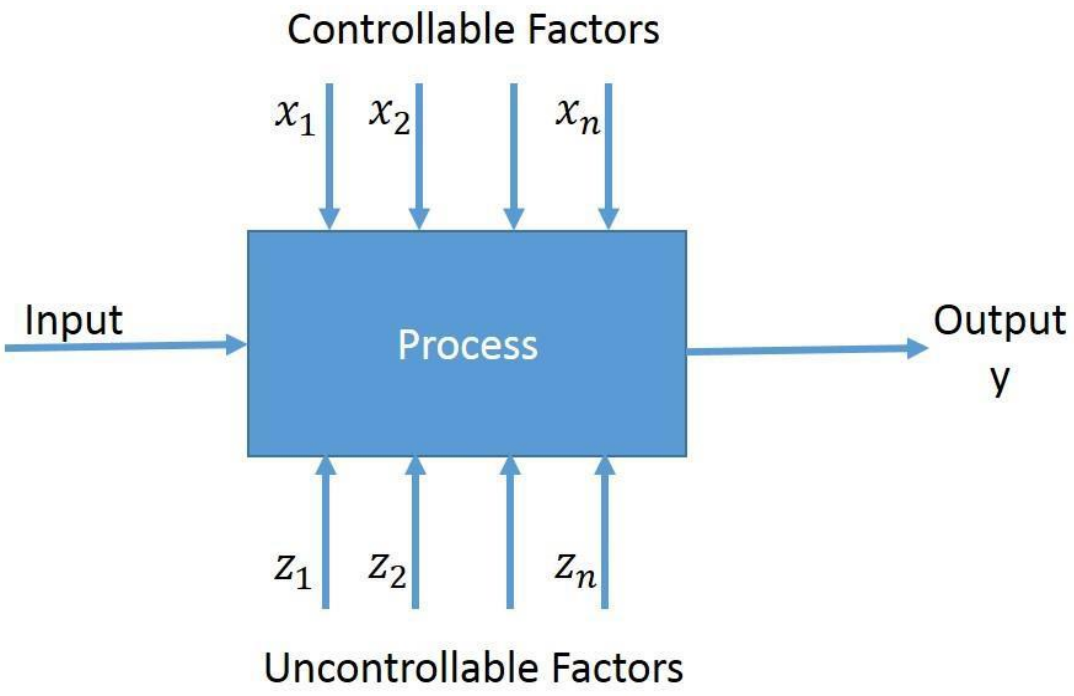

Fig.4.4. Schematic diagram of a design process

4.3.1. Response Surface Methodology

Response surface methodology (RSM) is a collection of mathematical and statistical techniques for empirical model building. By careful design of experiments, the objective is to optimize a response which is influenced by several independent variables. An experiment is a series of tests, called runs, in which changes are made in the input variables in order to identify the reasons for changes in the output response. Originally, RSM was developed to model experimental responses (Box and Draper, 1987) and then migrated into the modelling of numerical experiments.

In statistics, response surface methodology (RSM) explores the relationships between several explanatory variables and one or more response variables. The main idea of RSM is to use a set of designed experiments to obtain an optimal response. Central composite design can be implemented to estimate a second degree polynomial model, which is still only an approximation at best. In this work, response surface modelling (RSM) is utilized for determining the relations between the various LTD process parameters with the various machining criteria and exploring the effect of these process parameters on the responses, i.e. the material removal rate, electrode wear ratio, gap

size and the surface finish. In order to study the effects of the LTD parameters on the above mentioned machining criteria, second order polynomial response surface mathematical models can be developed. In the general case, the response surface is described by an equation of the form:

$$Y = \beta 0 + \sum_{i=1}^{s} \beta_{ii} X_i + \sum_{i=1}^{s} \beta_{ii} X_i^2 + \sum_{i,j=1, i \neq 1}^{s} \beta_{ij} X_i X_j \text{ ---------- Eq. 4.4.}$$

Where, Y is the corresponding response, e.g. the TD, BD and Circularity produced by the various process variables of LTD and the Xi (**1, 2,,,,,S**) are coded levels of **S** quantitative process variables, the terms, $\beta 0$, βi, βii and βij are the second order regression coefficients. The second term under the summation sign of this polynomial equation is attributable to linear effect, whereas the third term corresponds to the higher-order effects; the fourth term of the equation includes the interactive effects of the process parameters.

CHAPTER 5:

5. EXPERIMENTAL RESULTS AND DISCUSSION

Based on the designed experimental conditions of the present research, all the experiments have been performed after setting all the process parameters (variable and fixed) at different combinations. Then based on the experimental procedure, various data are obtained from the various measurements such as the magnitude of top and bottom diameter, circularity. At first pilot experiment was done and then RSM experimental design for finding out the regression equations and the most significant process parameter on the performance characteristics. Then by considering the regression equations and significant process parameter from RSM experimental design, the final optimal process parameters and performance characteristics are found from particle swarm optimization (PSO) algorithm.

5.1. Experimental Results Based on Response Surface Methodology (RSM) Approach

In this section the full Central Composite Design (CCD) of RSM is employed to conduct experiment further by taking the most influenced process. Here, five process parameters namely Sawing Angle, Power Setting, Duty Cycle, Pulse Frequency and Scanning Speed were selected and experiment were carried out on Monel K-500. The levels of different process parameters and their combinations have been shown in the Table 5.1, 5.2 and 5.3 respectively. According to CCD, a total of 52 experiments have been performed.

Table 5.1. Process parameters and their levels for trepanned hole

Parameter	Unit	Coded Symbol	Level 1	Level 2	Level 3	Level 4	Level 5
Coded value			-2	-1	0	+1	+2
Sawing Angle (S.A)	Degree	A	0.1	0.4	0.7	1	1.3
Power Setting (P.S)	Watt	B	32.5	35	37.5	40	42.5
Duty Cycle (D.C)	%	C	80	83	86	89	92
Pulse Frequency (P.F)	kHz	D	50	55	60	65	70
Scanning Speed (S.S)	mm/sec	E	0.2	0.4	0.6	0.8	1

Table 5.2. Values of experimental results of various performance characteristics (coded)

Exp. No	S.A (deg.)	P.S (watt)	D.C	P.F (Hz)	S.S (mm/sec)	TD (mm)	BD (mm)	Circularity
1	-1	-1	-1	-1	-1	0.6117	0.0323	0.935
2	1	-1	-1	-1	-1	0.6667	0.0559	0.891
3	-1	1	-1	-1	-1	0.6252	0.0349	0.926
4	1	1	-1	-1	-1	0.6713	0.0721	0.865
5	-1	-1	1	-1	-1	0.6369	0.0355	0.938
6	1	-1	1	-1	-1	0.6792	0.0545	0.897
7	-1	1	1	-1	-1	0.6467	0.0381	0.912
8	1	1	1	-1	-1	0.6902	0.0796	0.859
9	-1	-1	-1	1	-1	0.6142	0.0457	0.913
10	1	-1	-1	1	-1	0.6571	0.0617	0.895
11	-1	1	-1	1	-1	0.6186	0.5424	0.918
12	1	1	-1	1	-1	0.6676	0.5752	0.871
13	-1	-1	1	1	-1	0.6379	0.5504	0.932
14	1	-1	1	1	-1	0.6738	0.5603	0.908
15	-1	1	1	1	-1	0.6456	0.5493	0.895

Exp. No	S.A (deg.)	P.S (watt)	D.C	P.F (Hz)	S.S (mm/sec)	TD (mm)	BD (mm)	Circularity
16	1	1	1	1	-1	0.6898	0.5781	0.857
17	-1	-1	-1	-1	1	0.6257	0.5429	0.918
18	1	-1	-1	-1	1	0.6754	0.5612	0.890
19	-1	1	-1	-1	1	0.6522	0.5651	0.926
20	1	1	-1	-1	1	0.6928	0.5985	0.886
21	-1	-1	1	-1	1	0.6469	0.5361	0.950
22	1	-1	1	-1	1	0.6679	0.5557	0.928
23	-1	1	1	-1	1	0.6466	0.5474	0.919
24	1	1	1	-1	1	0.6852	0.5887	0.881
25	-1	-1	-1	1	1	0.6214	0.5503	0.905
26	1	-1	-1	1	1	0.6731	0.5635	0.895
27	-1	1	-1	1	1	0.6424	0.5651	0.906
28	1	1	-1	1	1	0.6814	0.5814	0.884
29	-1	-1	1	1	1	0.6383	0.5453	0.931
30	1	-1	1	1	1	0.6651	0.5507	0.927
31	-1	1	1	1	1	0.6532	0.5519	0.903
32	1	1	1	1	1	0.6715	0.5725	0.891
33	-2	0	0	0	0	0.6132	0.5314	0.934
34	2	0	0	0	0	0.6965	0.5821	0.865
35	0	-2	0	0	0	0.6473	0.5352	0.911
36	0	2	0	0	0	0.6714	0.5621	0.878
37	0	0	-2	0	0	0.6293	0.5507	0.891
38	0	0	2	0	0	0.6429	0.5492	0.904
39	0	0	0	-2	0	0.6635	0.5503	0.943
40	0	0	0	2	0	0.6602	0.5594	0.924
41	0	0	0	0	-2	0.6465	0.5487	0.895
42	0	0	0	0	2	0.1525	0.5651	0.906
43	0	0	0	0	0	0.1302	0.5372	0.919

Exp. No	S.A (deg.)	P.S (watt)	D.C	P.F (Hz)	S.S (mm/sec)	TD (mm)	BD (mm)	Circularity
44	0	0	0	0	0	0.1338	0.5381	0.905
45	0	0	0	0	0	0.1425	0.5373	0.916
46	0	0	0	0	0	0.1314	0.5361	0.904
47	0	0	0	0	0	0.1374	0.5414	0.913
48	0	0	0	0	0	0.1436	0.5343	0.912
49	0	0	0	0	0	0.1351	0.5387	0.919
50	0	0	0	0	0	0.1341	0.5346	0.902
51	0	0	0	0	0	0.1425	0.5383	0.918
52	0	0	0	0	0	0.1359	0.5412	0.911

Table 5.3. Values of experimental results of various performance characteristics (un-coded)

Exp. No	S.A (deg.)	P.S (watt)	D.C	P.F (Hz)	S.S (mm/sec)	TD (mm)	BD (mm)	Circularity
1	0.4	35	83	55	0.4	0.6117	0.5323	0.935
2	1	35	83	55	0.4	0.6667	0.5559	0.891
3	0.4	40	83	55	0.4	0.6252	0.5349	0.926
4	1	40	83	55	0.4	0.6713	0.5721	0.865
5	0.4	35	89	55	0.4	0.6369	0.5355	0.938
6	1	35	89	55	0.4	0.6792	0.5545	0.897
7	0.4	40	89	55	0.4	0.6467	0.5381	0.912
8	1	40	89	55	0.4	0.6902	0.5796	0.859
9	0.4	35	83	65	0.4	0.6142	0.5457	0.913
10	1	35	83	65	0.4	0.6571	0.5617	0.895
11	0.4	40	83	65	0.4	0.6186	0.5424	0.918
12	1	40	83	65	0.4	0.6676	0.5752	0.871
13	0.4	35	89	65	0.4	0.6379	0.5504	0.932

Exp. No	S.A (deg.)	P.S (watt)	D.C	P.F (Hz)	S.S (mm/sec)	TD (mm)	BD (mm)	Circularity
14	1	35	89	65	0.4	0.6738	0.5603	0.908
15	0.4	40	89	65	0.4	0.6456	0.5493	0.895
16	1	40	89	65	0.4	0.6898	0.5781	0.857
17	0.4	35	83	55	0.8	0.6257	0.5429	0.918
18	1	35	83	55	0.8	0.6754	0.5612	0.890
19	0.4	40	83	55	0.8	0.6522	0.5651	0.926
20	1	40	83	55	0.8	0.6928	0.5985	0.886
21	0.4	35	89	55	0.8	0.6469	0.5361	0.950
22	1	35	89	55	0.8	0.6679	0.5557	0.928
23	0.4	40	89	55	0.8	0.6466	0.5474	0.919
24	1	40	89	55	0.8	0.6852	0.5887	0.881
25	0.4	35	83	65	0.8	0.6214	0.5503	0.905
26	1	35	83	65	0.8	0.6731	0.5635	0.895
27	0.4	40	83	65	0.8	0.6424	0.5651	0.906
28	1	40	83	65	0.8	0.6814	0.5814	0.884
29	0.4	35	89	65	0.8	0.6383	0.5453	0.931
30	1	35	89	65	0.8	0.6651	0.5507	0.927
31	0.4	40	89	65	0.8	0.6532	0.5519	0.903
32	1	40	89	65	0.8	0.6715	0.5725	0.891
33	0.1	37.5	86	60	0.6	0.6132	0.5314	0.934
34	1.3	37.5	86	60	0.6	0.6965	0.5821	0.865
35	0.7	32.5	86	60	0.6	0.6473	0.5352	0.911
36	0.7	42.5	86	60	0.6	0.6714	0.5621	0.878
37	0.7	37.5	80	60	0.6	0.6293	0.5507	0.891
38	0.7	37.5	92	60	0.6	0.6429	0.5492	0.904
39	0.7	37.5	86	50	0.6	0.6635	0.5503	0.943
40	0.7	37.5	86	70	0.6	0.6602	0.5594	0.924
41	0.7	37.5	86	60	0.2	0.6465	0.5487	0.895
42	0.7	37.5	86	60	1	0.6525	0.5651	0.906

Exp. No	S.A (deg.)	P.S (watt)	D.C	P.F (Hz)	S.S (mm/sec)	TD (mm)	BD (mm)	Circularity
43	0.7	37.5	86	60	0.6	0.6302	0.5372	0.919
44	0.7	37.5	86	60	0.6	0.6338	0.5381	0.905
45	0.7	37.5	86	60	0.6	0.6425	0.5373	0.916
46	0.7	37.5	86	60	0.6	0.6314	0.5361	0.904
47	0.7	37.5	86	60	0.6	0.6374	0.5414	0.913
48	0.7	37.5	86	60	0.6	0.6436	0.5343	0.912
49	0.7	37.5	86	60	0.6	0.6351	0.5387	0.919
50	0.7	37.5	86	60	0.6	0.6341	0.5346	0.902
51	0.7	37.5	86	60	0.6	0.6425	0.5383	0.918
52	0.7	37.5	86	60	0.6	0.6359	0.5412	0.911

5.1.1. Development of Models for different LTD criteria based on Response Surface Methodology (RSM) Approach

The modeling is very important for optimizing the process parameters of Laser Trepan Drilling operation. Modeling can determine the predicting value of performance criteria for any given set of process parameter. In this research investigation, mathematical modeling of LTD process criteria has been achieved in order to establish the relationship between process parameters and responses. Based up on the second order polynomial model, the mathematical models of TD, BD and Circularity have been calculated by the computer software "MINITAB 17" using the data of process parameters and performance characteristics as given in Table 5.4. The developed mathematical models of TD, BD and Circularity are expressed by the given equation below as Eqs 5.1 to 5.3. Tables 5.4 to 5.6 depict the ANOVA table of TD, BD and Circularity respectively and Figs. 5.1 to 5.3 represent the residual plots of TD, BD and circularity respectively.

(i) Development of models for Top diameter (TD)

Considering the Eq.4.4 and the experimental values, a mathematical model is proposed for TD and it is expressed as follows:

(a) Un-coded regression equation

Top diameter = 1.470 + 0.3768 S.A - 0.0548 P.S + 0.0161 D.C - 0.03168 P.F + 0.619 S.S + 0.04865 S.A*S.A + 0.000881 P.S*P.S - 0.000034 D.C*D.C + 0.000245 P.F*P.F + 0.0760 S.S*S.S - 0.00025 S.A*P.S - 0.003590 S.A*D.C - 0.000604 S.A*P.F- 0.0381 S.A*S.S - 0.000098 P.S*D.C - 0.000027 P.S*P.F + 0.00213 P.S*S.S + 0.000043 D.C*P.F - 0.00820 D.C*S.S - 0.000719 P.F*S.S----------Eq. 5.1

(b) Coded regression equation

Y = 0.63676 + 0.020280 A + 0.005930 B + 0.005130 C - 0.001905 D + 0.002965 E + 0.004378 A*A + 0.005503 B*B - 0.000309 C*C + 0.006128 D*D + 0.003041 E*E - 0.000188 A*B - 0.003231 A*C - 0.000906 A*D - 0.002288 A*E - 0.000731 B*C - 0.000331 B*D + 0.001063 B*E + 0.000650 C*D - 0.004919 C*E - 0.000719 D*E -------Eq. 5.2

Table 5.4. ANOVA results for TD

Source	DF	Adj SS	Adj MS	F-Value	P-Value
Model	20	0.024313	0.001216	56.94	0.000
Linear	5	0.019407	0.003881	181.80	0.000
A	1	0.016451	0.016451	770.55	0.000
B	1	0.001407	0.001407	65.88	0.000
C	1	0.001053	0.001053	49.31	0.000
D	1	0.000145	0.000145	6.80	0.014
E	1	0.000352	0.000352	16.47	0.000
Square	5	0.003516	0.000703	32.93	0.000
2-WayInteraction	10	0.001390	0.000139	6.51	0.000
Error	31	0.000662	0.000021		
Lack-of-Fit	22	0.000458	0.000023	0.92	0.591
Pure Error	9	0.000204			
Total	51	0.024975			

Table 5.5. Model Summary

s	R-sq	R-sq(adj)	R-sq(pred)
0.0046206	97.35%	95.64%	92.43%

Standard values of F-ratio for different confident limits have been listed below.

F0.01 (1, 31) = 7.53, F0.05 (1, 31) = 4.16, F0.10 (1, 31) = 2.87,

F0.01 (20, 31) = 2.52, F0.05 (20, 31) = 1.66, F0.10 (20, 31) = 1.65

From the ANOVA Table 5.4 for TD, it is observed that the calculated values of the F-ratio of sawing angle, power setting, duty cycle and scanning speed are greater than the standard value of F-ratio at 99% of confident interval.

Hence, sawing angle, power setting, duty cycle and scanning speed have significant effect on TD at 99% of confident interval.

Similarly, calculate value of F-ratio of pulse frequency is greater than the standard value of F-ratio at 95% confident interval. Hence, pulse frequency has significant effect on TD at 95% of confident interval. Also the calculated F-ratio for developed regression model for TD is found as 56.94 which is more than standard F value for the DOF of (20,31) at confidence level of 99% and the P value is calculated as zero. So the model is significant at that confident level. Further the calculated F value for lack-of-fit of the developed model is obtained as 0.92 which is less than standard F value for the DOF of (22,31) at confidence level of 99%. Therefore the developed model for TD is adequate at that confidence level.

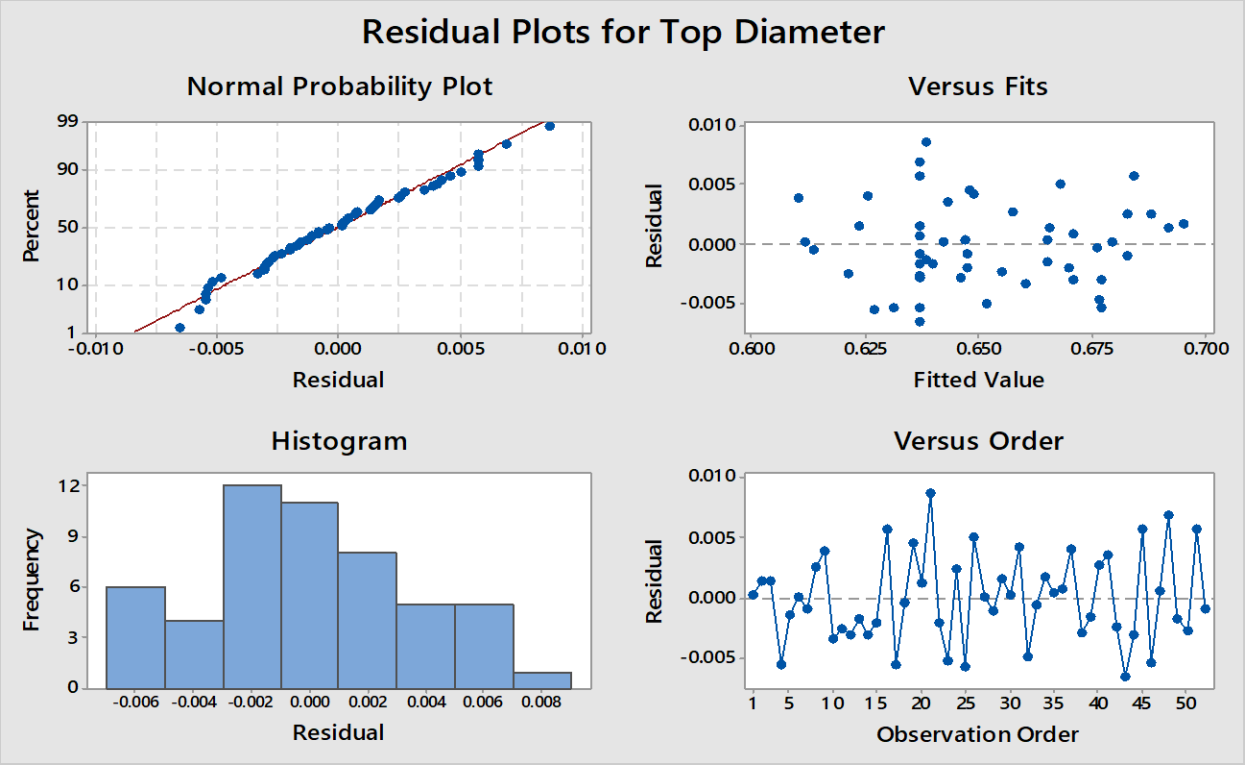

Fig.5.1. Residual plots for TD

(ii) Development of models for Bottom diameter (BD)

Considering the Eq.4.4 and the experimental values, a mathematical model is proposed for BD and it is expressed as follows:

(a) Un-coded regression equation

Bottom Diameter = 3.679 - 0.0927 S.A - 0.02671 P.S - 0.05576 D.C - 0.01196 P.F + 0.2856 S.S + 0.05335 S.A*S.A + 0.000444 P.S*P.S + 0.000345 D.C*D.C + 0.000173 P.F*P.F + 0.1210 S.S*S.S + 0.005287 S.A*P.S - 0.000163 S.A*D.C - 0.001894 S.A*P.F - 0.02120 S.A*S.S - 0.000017 P.S*D.C - 0.000156 P.S*P.F + 0.005719 P.S*S.S + 0.000001 D.C*P.F - 0.005484 D.C*S.S - 0.002347 P.F*S.S ---------- Eq. 5.3

(b) Coded regression equation

Y = 0.537691 + 0.011957 A + 0.007302 B - 0.001427 C + 0.001587 D + 0.003578 E
+ 0.004801 A*A + 0.002776 B*B + 0.003101 C*C + 0.004326 D*D + 0.004839 E*E
+ 0.003966 A*B - 0.000147 A*C - 0.002841 A*D - 0.001272 A*E - 0.000128 B*C
- 0.001947 B*D + 0.002859 B*E + 0.000016 C*D - 0.003291 C*E - 0.002347 D*E -----Eq. 5.4

Table 5.6. ANOVA results for BD

Source	DF	Adj SS	Adj MS	F-Value	P-Value
Model	20	0.013392	0.000670	84.08	0.000
Linear	5	0.008547	0.001709	214.63	0.000
A	1	0.005719	0.005719	718.15	0.000
B	1	0.002133	0.002133	267.84	0.000
C	1	0.000082	0.000082	10.23	0.003
D	1	0.000101	0.000101	12.66	0.001
E	1	0.000512	0.000512	64.28	0.000
Square	5	0.003125	0.000625	78.48	0.000
2-WayInteraction	10	0.001720	0.000172	21.60	0.000
Error	31	0.000247	0.000008		
Lack-of-Fit	22	0.000195	0.000009	1.55	0.253
Pure Error	9	0.000052	0.000006		
Total	51	0.013639			

Table 5.7. Model Summary

s	R-sq	R-sq(adj)	R-sq(pred)
0.0028220	98.19%	97.02%	94.42%

Standard values of F-ratio for different confident limits have been listed below.

F0.01 (1, 31) = 7.53, F0.05 (1, 31) = 4.16, F0.10 (1, 31) = 2.87,

F0.01 (20, 31) = 2.52, F0.05 (20, 31) = 1.66, F0.10 (20, 31) = 1.65

From the ANOVA Table 5.6 for BD, it is observed that the calculated values of the F-ratio of sawing angle, power setting, duty cycle, pulse frequency and scanning speed are greater than the standard value of F-ratio at 99% of confident interval.

Hence, sawing angle, power setting, duty cycle and scanning speed have significant effect on TD at 99% of confident interval.

Similarly, the calculated F-ratio for developed regression model for TD is found as 84.08 which is more than standard F value for the DOF of (20,31) at confidence level of 99% and the P value is calculated as zero. So the model is significant at that confident level. Further the calculated F value for lack-of-fit of the developed model is obtained as 1.55 which is less than standard F value for the DOF of (22,31) at confidence level of 99%. Therefore the developed model for BD is adequate at that confidence level.

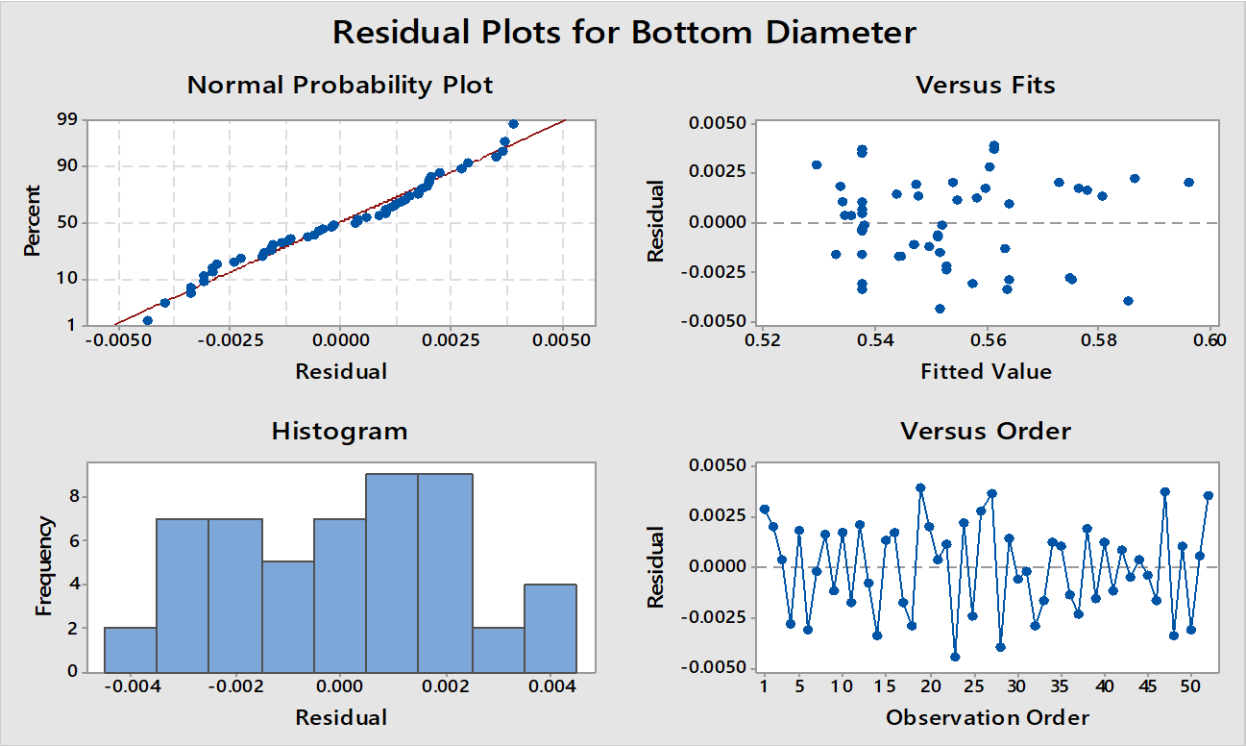

Fig.5.2. Residual plots for BD

(iii) Development of models for Circularity

Considering the Eq.4.4 and the experimental values, a mathematical model is proposed for Circularity and it is expressed as follows:

(a) Un-coded regression equation

Circularity = -4.392 - 0.172 S.A + 0.1312 P.S + 0.0950 D.C- 0.03066 P.F - 0.662 S.S - 0.03154 S.A*S.A - 0.000654 P.S*P.S - 0.000371 D.C*D.C + 0.000226 P.F*P.F - 0.0647 S.S*S.S - 0.00500 S.A*P.S + 0.001319 S.A*D.C + 0.003167 S.A*P.F + 0.0781 S.A*S.S - 0.000975 P.S*D.C - 0.000020 P.S*P.F + 0.00363 P.S*S.S + 0.000021 D.C*P.F + 0.00708 D.C*S.S - 0.000687 P.F*S.S---------- Eq. 5.5

(b) Coded regression equation

Y= 0.91173 - 0.016000 A - 0.010500 B + 0.003250 C - 0.003200 D + 0.003750 E - 0.002839 A*A - 0.004089 B*B - 0.003339 C*C + 0.005661 D*D - 0.002589 E*E - 0.003750 A*B + 0.001188 A*C + 0.004750 A*D + 0.004688 A*E - 0.007313 B*C - 0.000250 B*D + 0.001813 B*E + 0.000313 C*D + 0.004250 C*E - 0.000688 D*E -----Eq. 5.6

Table 5.8. ANOVA results for Circularity

Source	DF	Adj SS	Adj MS	F-Value	P-Value
Model	20	0.022833	0.001142	46.97	0.000
Linear	5	0.016045	0.003209	132.03	0.000
A	1	0.010240	0.010240	421.31	0.000
B	1	0.004410	0.004410	181.44	0.000
C	1	0.000423	0.000423	17.38	0.000
D	1	0.000410	0.000410	16.85	0.000

Source	DF	Adj SS	Adj MS	F-Value	P-Value
E	1	0.000563	0.000563	23.14	0.000
Square	5	0.002453	0.000491	20.19	0.000
2-WayInteraction	10	0.004335	0.000433	17.83	0.000
Error	31	0.000753	0.000024		
Lack-of-Fit	22	0.000389	0.000018	0.44	0.946
Pure Error	9	0.000365	0.000041		
Total	51	0.023586			

Table 5.9. Model Summary

s	R-sq	R-sq(adj)	R-sq(pred)
0.0049300	96.81%	94.74%	92.06%

Standard values of F-ratio for different confident limits have been listed below.

F0.01 (1, 31) = 7.53, F0.05 (1, 31) = 4.16, F0.10 (1, 31) = 2.87,

F0.01 (20, 31) = 2.52, F0.05 (20, 31) = 1.66, F0.10 (20, 31) = 1.65

From the ANOVA Table 5.8 for Circularity, it is observed that the calculated values of the F-ratio of sawing angle, power setting, duty cycle, pulse frequency and scanning speed are greater than the standard value of F-ratio at 99% of confident interval.

Hence, sawing angle, power setting, duty cycle and scanning speed have significant effect on TD at 99% of confident interval.

Similarly, the calculated F-ratio for developed regression model for TD is found as 46.97 which is more than standard F value for the DOF of (20,31) at confidence level of 99% and the P value is calculated as zero. So the model is significant at that confident level. Further the calculated F value for lack-of-fit of the developed model is obtained as 0.44 which is less than standard F value for the DOF of (22,31) at confidence level of 99%. Therefore the developed model for Circularity is adequate at that confidence level.

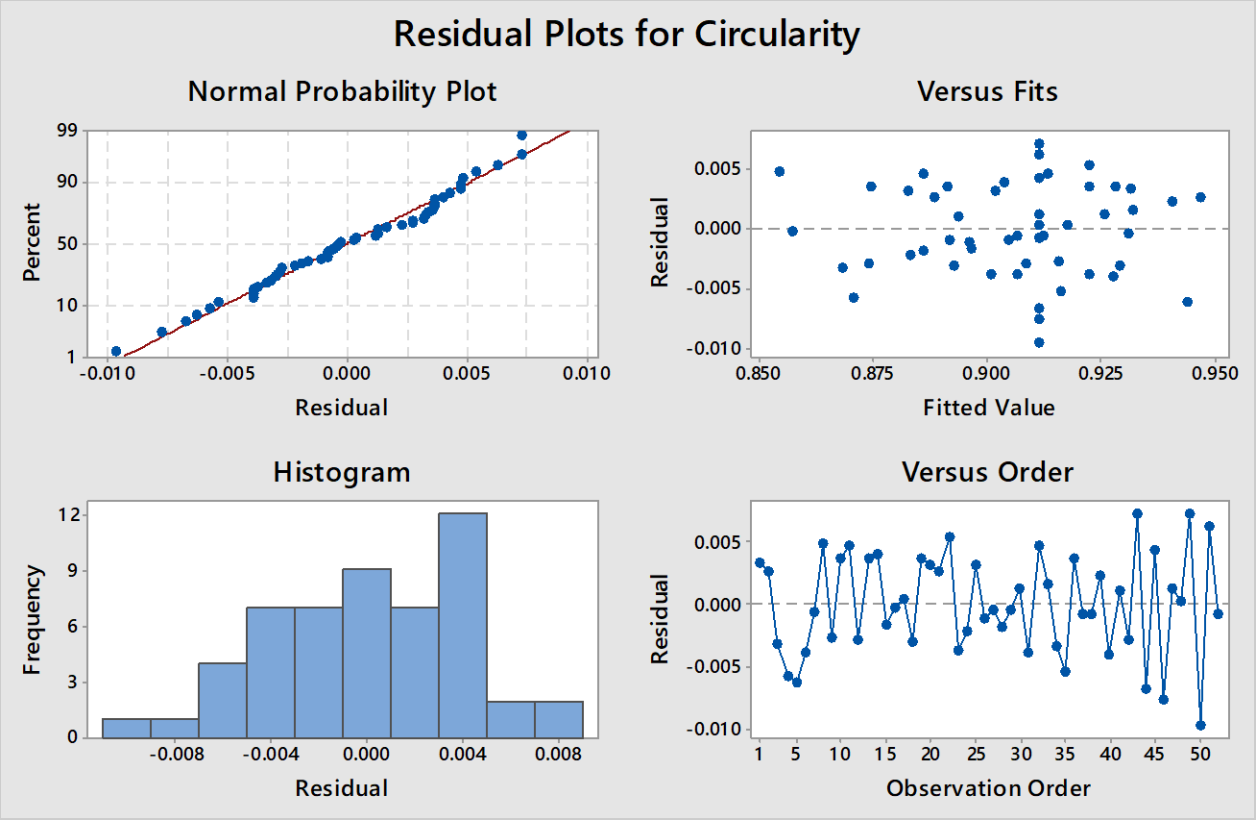

Fig.5.3. Residual plots for Circularity

5.1.2. Influences of LTD process parameters on performance criteria

The influences of LTD process parameters on the various responses like TD, BD and Circularity has been analyzed based on developed model Eqs.5.1 to 5.6. Various response surface plots have been drawn with one response and two process parameters at a time keeping third parameter fixed at its mid-value. The response surface of TD, BD and Circularity with respect to the process parameters and their influences have been discussed as follows:

5.1.2.1 Influences of process parameter on Top diameter (TD)

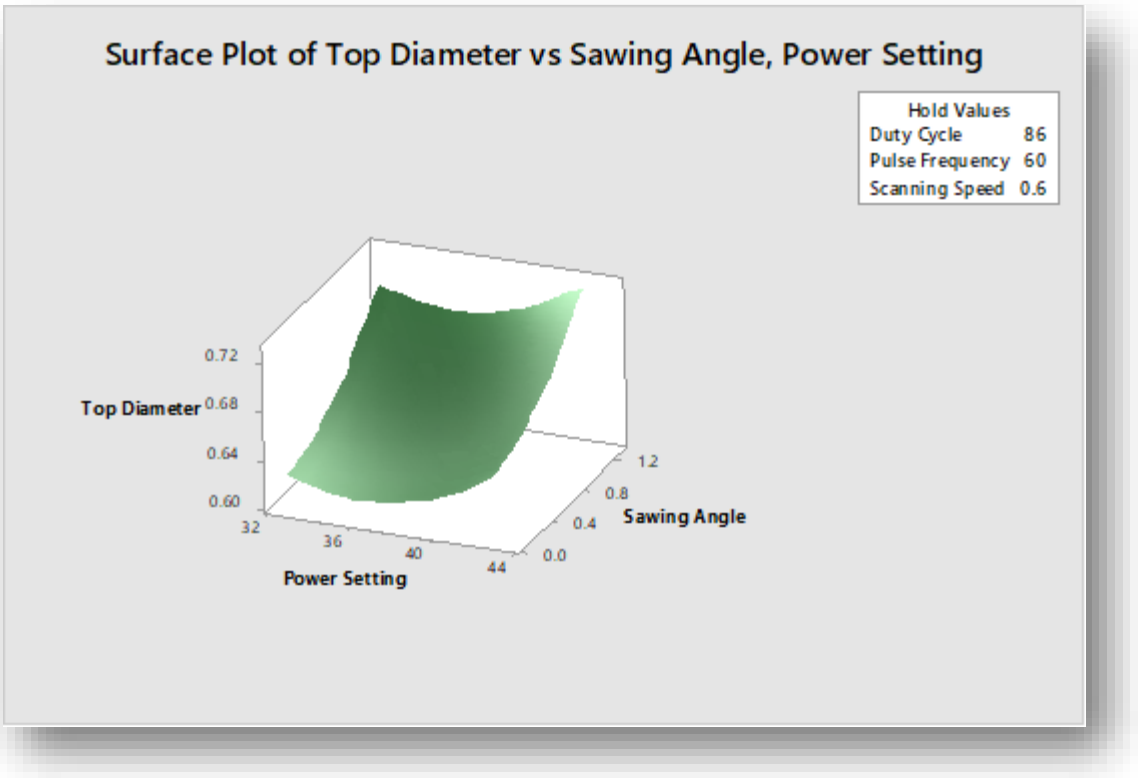

Fig.5.4. Effects of power setting and sawing angle on TD

The combination effect of significant process parameters power setting and sawing angle on overcut top diameter is shown in figure 5.4. Duty cycle Pulse frequency and scanning speed is taken as constant at 86%, 60 kHz and 0.6 mm/sec respectively. Revelation by the surface plot shows a curvilinear relationship of top diameter with the Power setting and Sawing angle. If the Sawing angle remains to be higher the kerf width in the top surface would also be higher, as a result of which overcut on the top surface occurs. When average power increases instant melting will occur in the top surface, leading to vaporization and top diameter overcut will also be higher. So keeping with low value of sawing angle and mid range of power setting, overcut top diameter may be decrease.

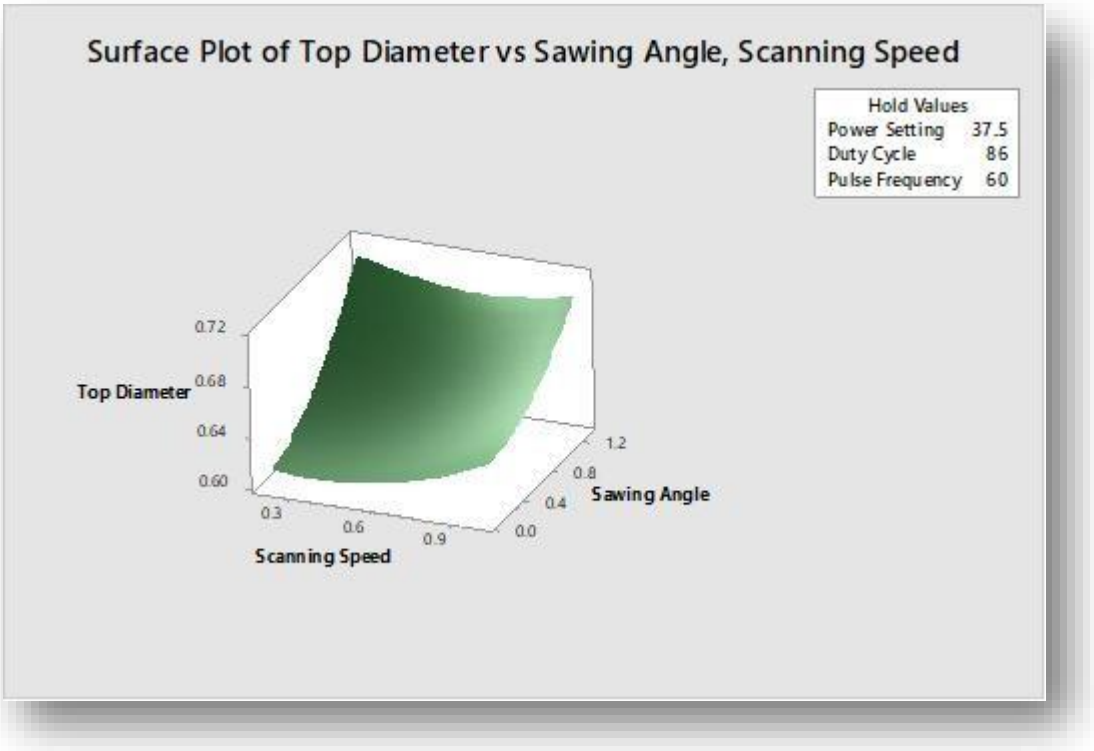

Fig.5.5. Effects of scanning speed and sawing angle on TD

The combination effect of significant process parameters scanning speed and sawing angle on overcut top diameter is shown in figure 5.5. The power setting, duty cycle and pulse frequency are kept constant at 37.5 watt, 86 % and 60 kHz respectively. From the response surface plot, it can be noticed that the kerf deviation of top diameter follows the curvilinear relationship with scanning speed; it increases with the increment of scanning speed at low value of sawing angle and decreases with the increment of scanning speed at high value of sawing angle. The energy concentration on the surface is controlled by the scanning speed but the overcut on the surface is controlled by the sawing angle. So keeping with mid range of scanning speed and low value of sawing angle, overcut top diameter may be decrease.

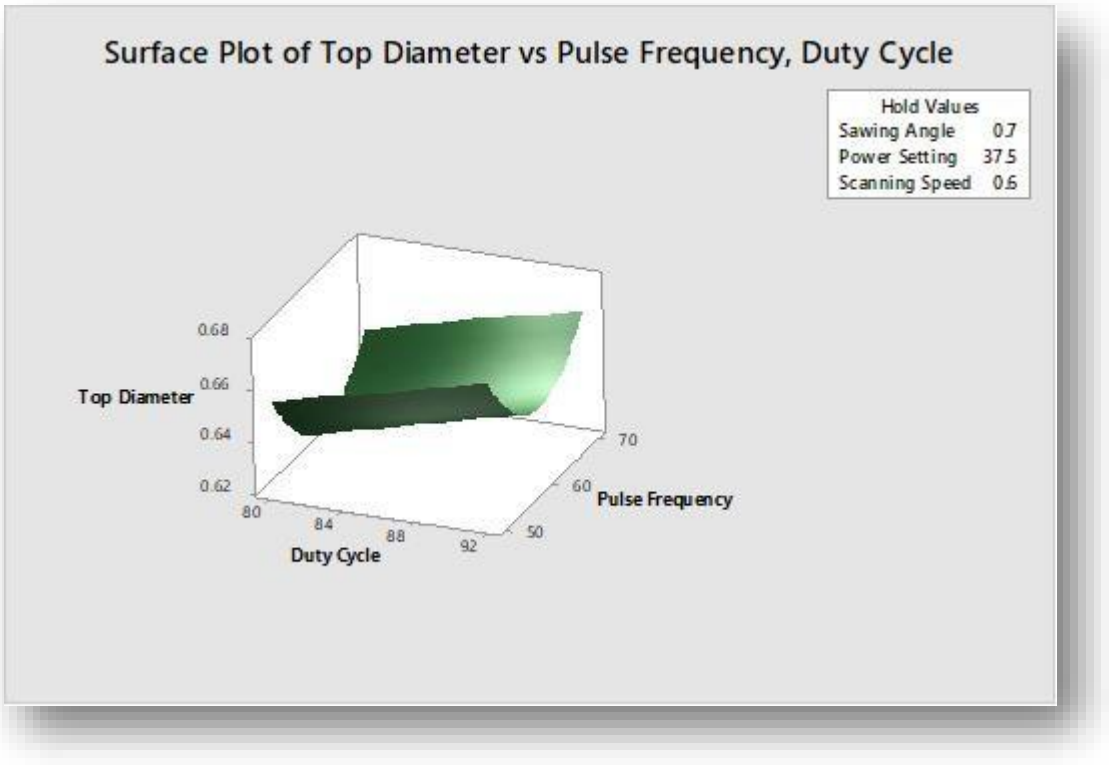

Fig.5.6. Effects of duty cycle and pulse frequency on TD

The combination effect of significant process parameters duty cycle and pulse frequency on overcut top diameter is shown in figure 5.6. The sawing angle, power setting and scanning speed are kept constant at 0.7 degree, 37.5 watt and 0.6 mm/sec. From the response surface plot, it can be noticed that the kerf deviation of top diameter follows the linear relationship with duty cycle; it increases with the increment of duty cycle for different values of pulse frequency. The pulse fiber laser cutting process involves generation of individual holes produced by each pulse. If the pulse frequency increases the overcut decreases due to fast pulses impact on the surface but further increment of pulse frequency increases the overcut. So keeping with low value of duty cycle and mid range of pulse frequency, overcut top diameter may be decrease.

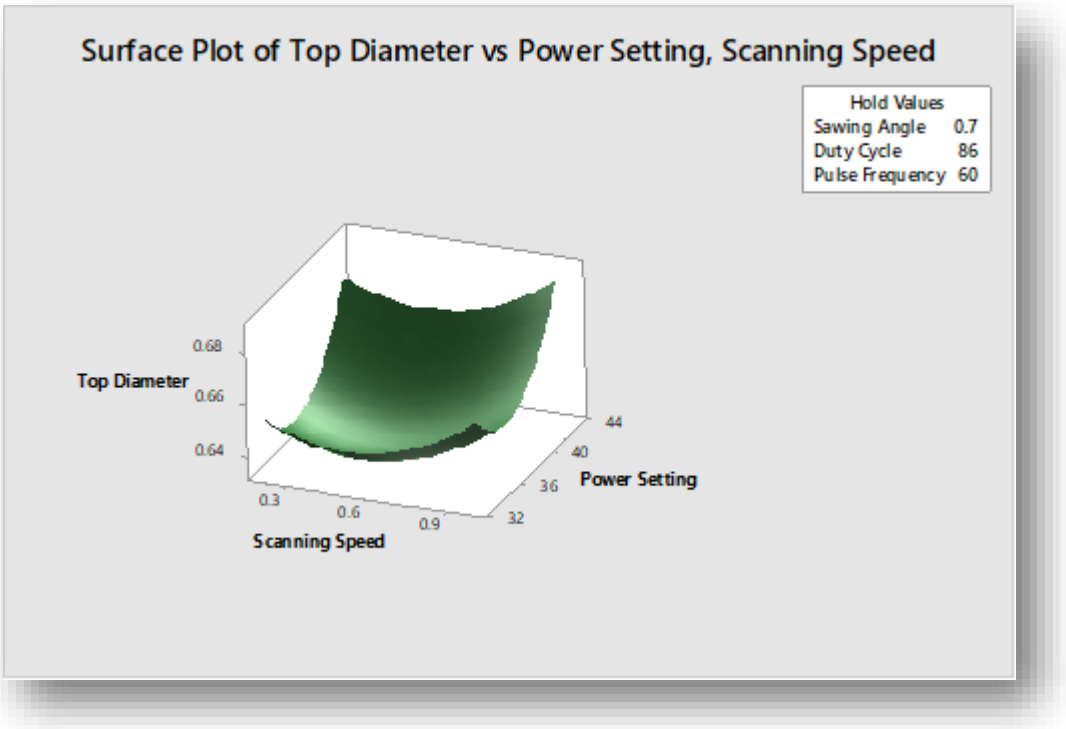

Fig.5.7. Effects of scanning speed and power setting on TD

The combination effect of significant process parameters scanning speed and power setting on overcut top diameter is shown in figure 5.7. The sawing angle, duty cycle and pulse frequency are kept constant at 0.7 degree, 86 % and 60 kHz. From response surface plot, it has been observed that the kerf deviation follows the curvilinear path with power; it increases sharply with the increment of power for the different values of scanning speed. It can also be noticed that kerf deviation increases with scanning speed for different values of power. Energy concentration on the surface is controlled by power input of the laser beam and scanning speed, mid range power and low cutting speed leads to generation of even kerf width.

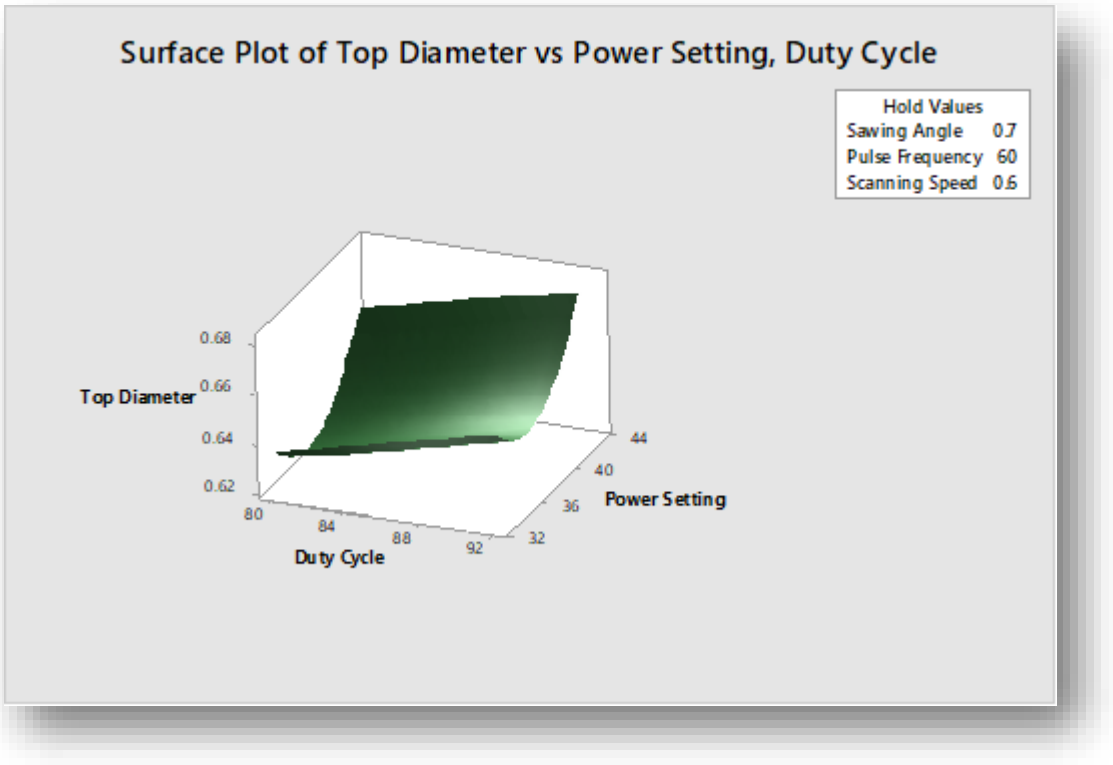

Fig.5.8. Effects of duty cycle and power setting on TD

The combination effect of significant process parameters duty cycle and power setting on overcut top diameter is shown in figure 5.8. The sawing angle, pulse frequency and scanning speed are kept constant at 0.7 degree, 60 % and 0.6 mm/sec. From the response surface plot, it can be noticed that the kerf deviation of top diameter follows the linear relationship with duty cycle; it increases with the increment of duty cycle for different values of power setting. It can also be noticed that kerf deviation increases sharply with power setting for different values of duty cycle. When average power increases instant melting will occur in the top surface, leading to vaporization and top diameter overcut will also be higher. Also with increasing the duty cycle the overall energy impact on the surface will be increasing. The net effect of power setting and duty cycle is to increase the kerf width. . So keeping with low value of duty cycle and mid range of power, overcut top diameter may be decrease.

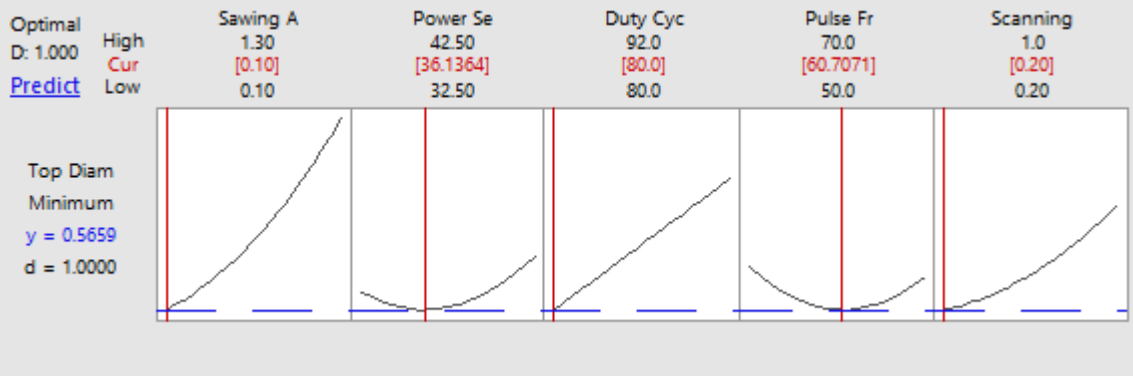

Fig.5.9. Optimization results for minimized Top Diameter (TD)

From the Fig. 5.9., the optimum value of TD and process parameters are obtained individually

Table 5.10. Optimum value of Top Diameter and corresponding process parameters

	Top Diameter (mm)	Sawing Angle (deg.)	Power Setting(watt)	Duty Cycle(%)	Pulse Frequency (kHz)	Scanning Speed(mm/sec)
Optimum value	0.5659	0.10	36.1364	80	60.7071	0.20

This result is obtained using 'MATLAB 17' software environment for minimum TD, BD and maximum Circularity. A conformation experiment has been conducted in order to validate the optimal combination of process parameters and optimal results. Prediction error of the achieved model is found out by the expression below.

$$\textbf{Error}(\%) = \frac{\textbf{Experimental value} - \textbf{optimised value}}{\textbf{experimental value}} \times 100$$

Table 5.11. Confirmation Test for the Top Diameter

Responses	Actual Value	Predicted Value	% Error
Top Diameter	0.5902	0.5659	4.11 %

5.1.2.2 Influences of process parameters on Bottom Diameter (BD)

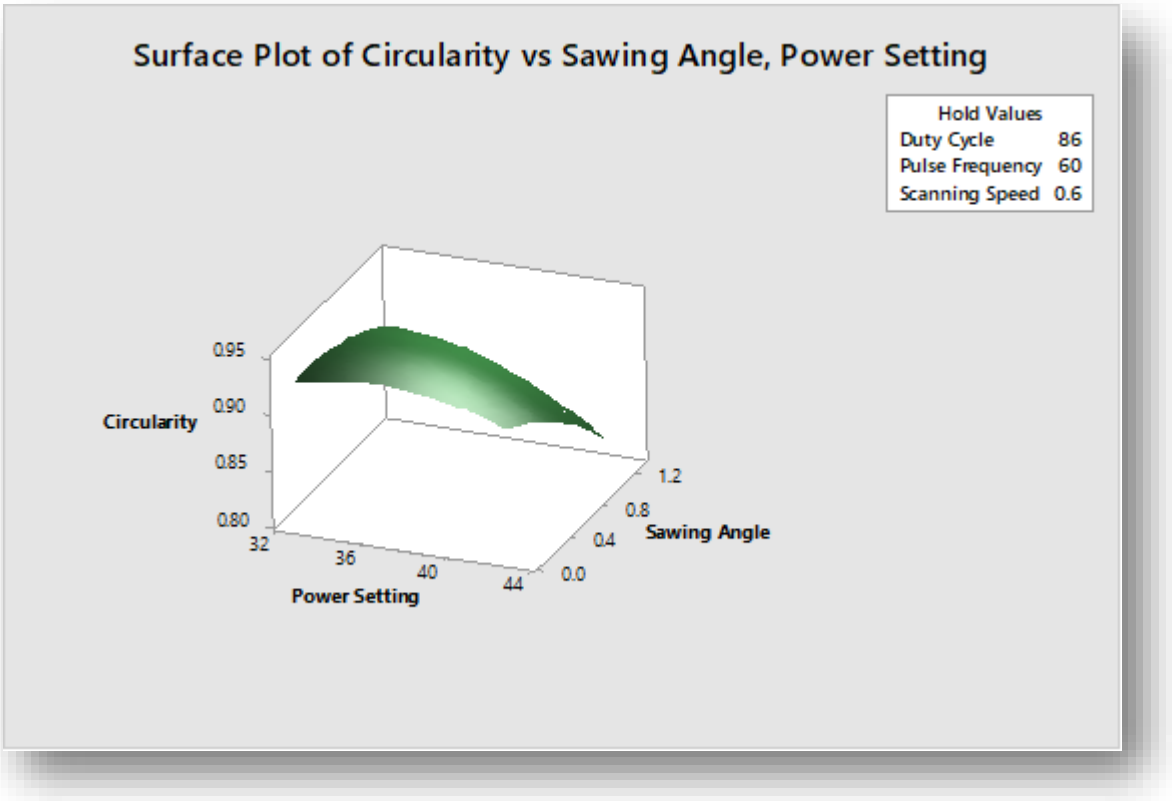

Fig.5.10. Effects of power setting and sawing angle on BD

The effect of power setting and sawing angle upon overcut bottom diameter with the respective maintenance of constant duty cycle, pulse frequency and scanning speed at 86 %, 60 kHz and 0.6mm/sec are shown in fig. 5.10. Surface plot reveals that with the increase in sawing angle and power setting, bottom diameter will increase. If the sawing angle is higher, kerf width will also be higher and if then the power remains to be higher material removal will also be higher, as a result of which, diameter of the bottom surface will increases. Therefore keeping of sawing angle at

moderate value and power on the higher site, chance of material re-deposition at the cutting surface will be lower. Here constant air pressure helps to keep the material cool and to be away from burr formation. So keeping with low value of duty cycle and mid range of power, overcut bottom diameter may be decrease.

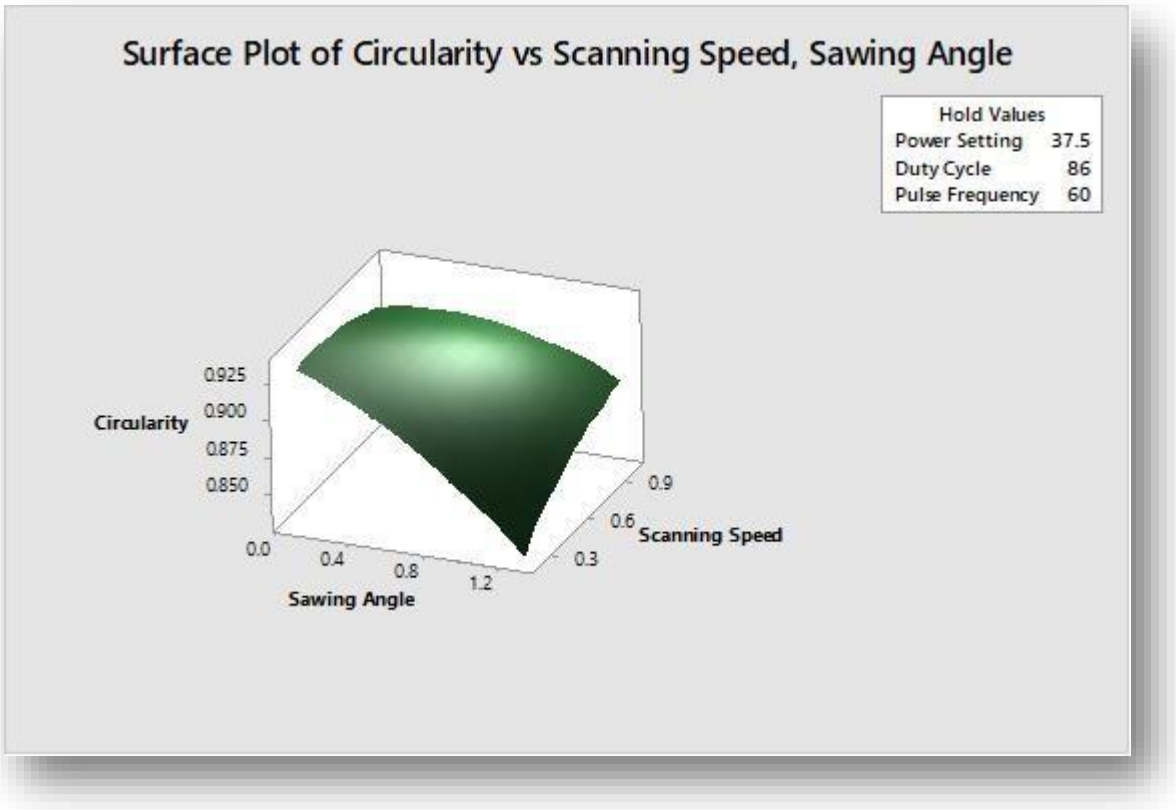

Fig.5.11. Effects of power setting and duty cycle on BD

The effect of power setting and duty cycle upon overcut bottom diameter with the respective maintenance of constant sawing angle, pulse frequency and scanning speed at 0.7 degree, 60 kHz and 0.6 mm/sec are shown in figure 5.11. Surface plot reveals that with the increase in power setting, kerf deviation of bottom diameter also increases for different values of duty cycle. When power setting and duty cycle both are increases, the overall energy reaches to the bottom face also increases. Therefore the kerf deviation of the bottom face also increases.

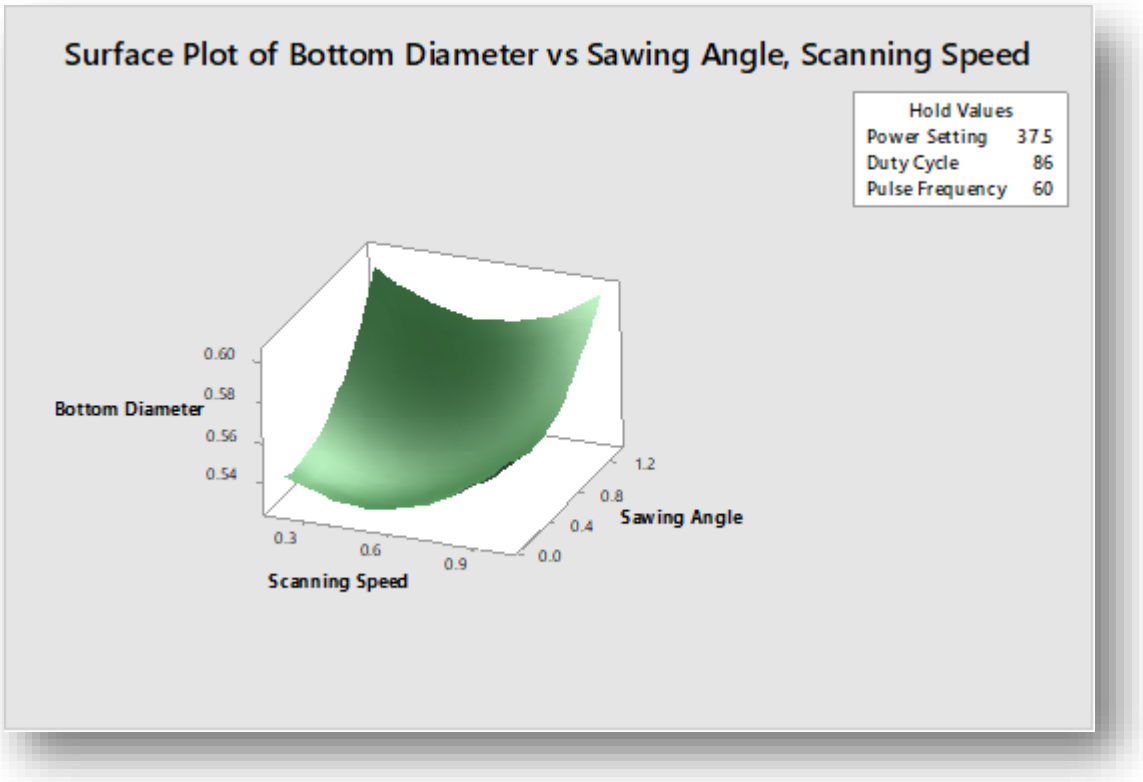

Fig.5.12. Effects of scanning speed and sawing angle on BD

The combination effect of significant process parameters scanning speed and sawing angle on overcut bottom diameter is shown in figure 5.12. The power setting, duty cycle and pulse frequency are kept constant at 37.5 watt, 86 % and 60 kHz. From the response surface plot, it can be noticed that the kerf deviation for the bottom diameter is decreases with increase of scanning speed for different value of sawing angle. It is also observed that for high value of sawing angle the kerf deviation is also very high. When sawing angle increases the overcut value also increases but with increasing scanning speed the energy density decreases. But high scanning speed is caused for uneven cutting action. So keeping with mid range of scanning speed and low value of sawing angle, overcut bottom diameter may be decrease.

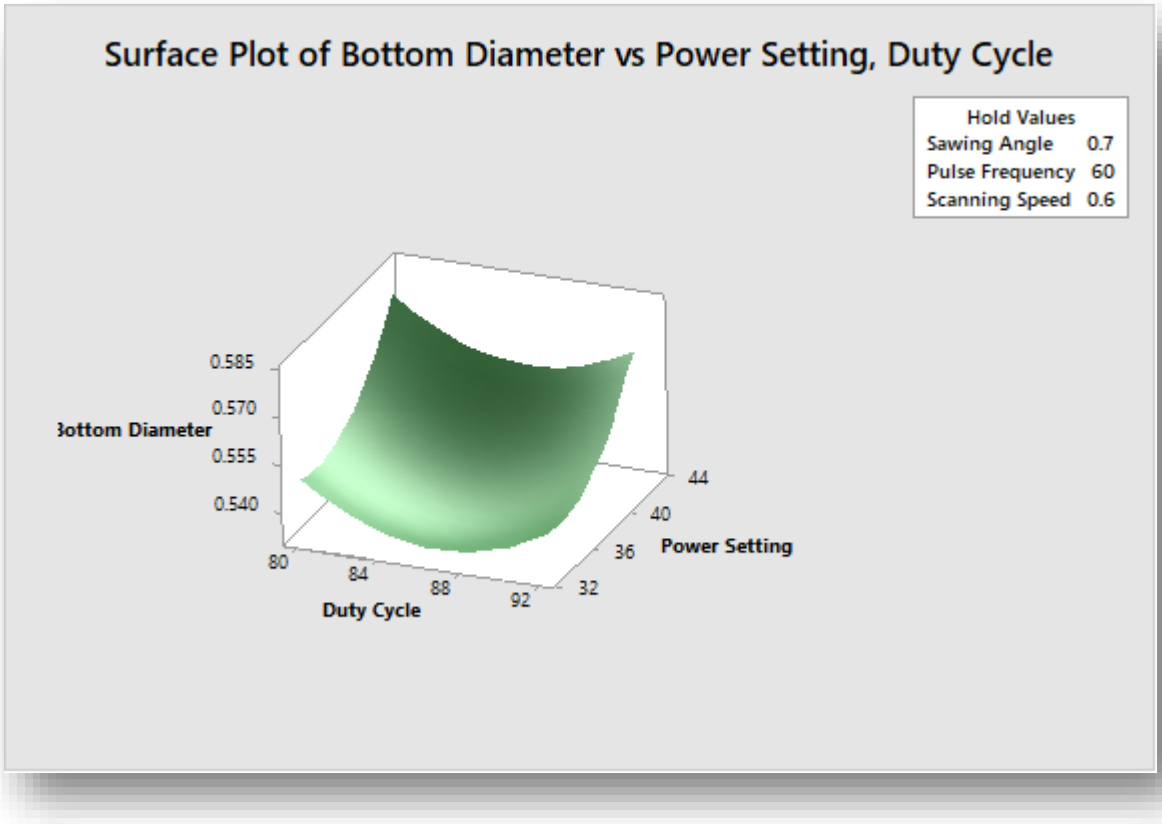

Fig.5.13. Effects of scanning speed and sawing angle on BD

The combination effect of significant process parameters duty cycle and pulse frequency on overcut bottom diameter is shown in figure 5.13. The sawing angle, duty cycle and pulse frequency are kept constant at 0.7 degree, 37.5 watt and 0.6 mm/sec. From the response surface plot, it can be noticed that the kerf deviation of bottom diameter follows the curvilinear relationship with duty cycle as well as with the pulse frequency. When the duty cycle is low but the pulse frequency is very high then the net effect is to reach high amount of energy at the bottom surface. It also increase the kerf deviation. So keeping with mid range of duty cycle and mid range of pulse frequency, overcut bottom diameter may be decrease.

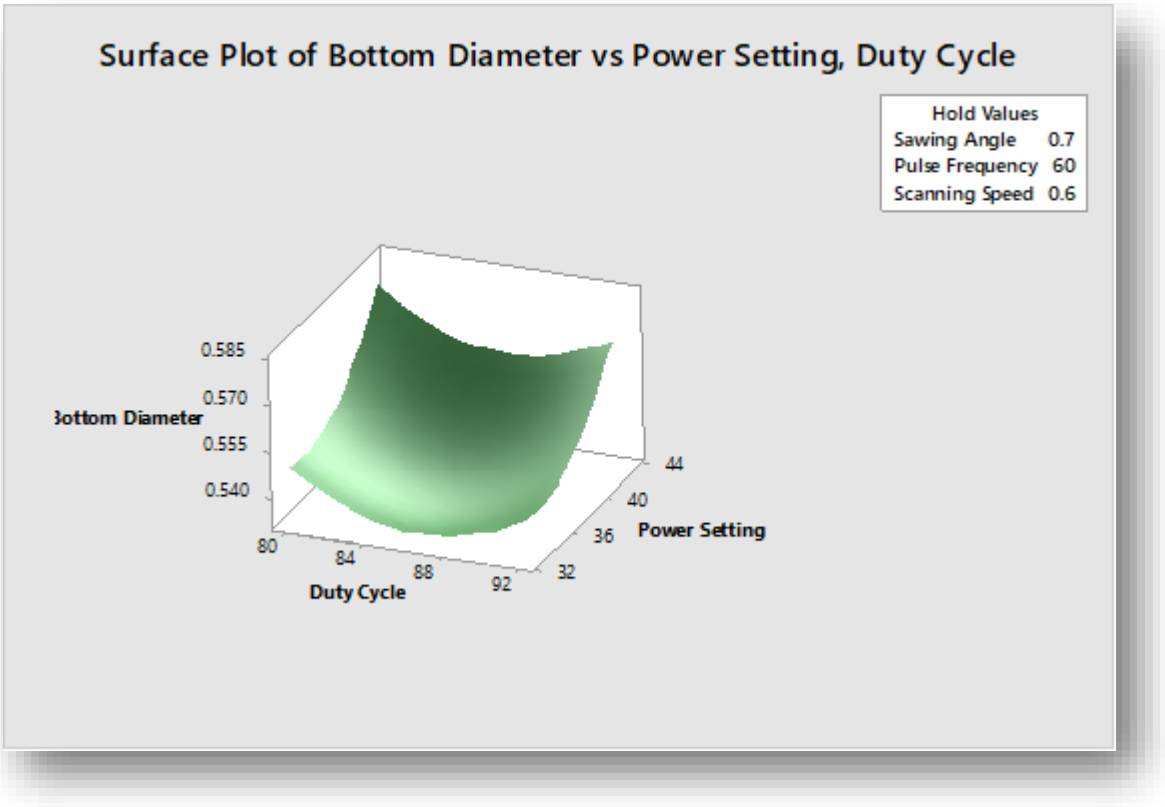

Fig.5.14. Effects of duty cycle and power setting on BD

The effect of duty cycle and power setting upon overcut bottom diameter with the respective maintenance of constant sawing angle, pulse frequency and scanning speed at 0.7 mm/sec, 60 kHz and 0.6mm/sec are shown in fig. 5.14. From the response surface plot, it can be noticed that the bottom diameter follows the nonlinear relationship with duty cycle and the power setting. When average power increases the major portion of energy reaches to the bottom surface. Keeping with mid range value of duty cycle and mid range value of power setting, overcut of bottom diameter may be decrease.

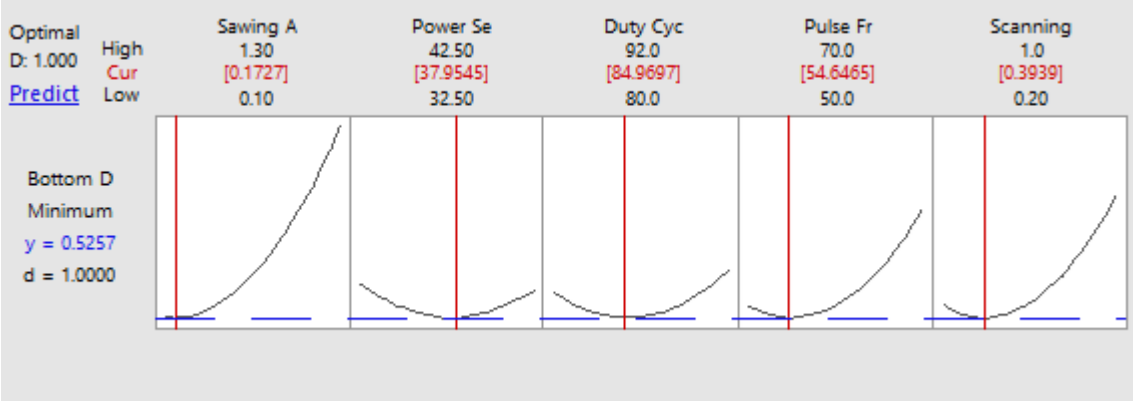

Fig.5.15. Optimization results for minimized Bottom Diameter (BD)

Table 5.12. Optimum value of Bottom Diameter and corresponding process parameters

	Bottom Diameter (mm)	Sawing Angle (deg.)	Power Setting (watt)	Duty Cycle (%)	Pulse Frequency (kHz)	Scanning Speed (mm/sec)
Optimum value	0.5257	0.1727	37.9545	84.9697	54.6465	0.3939

The result of conformation test for bottom diameter is shown in the table 5.13

Table 5.13. Confirmation Test for the Bottom Diameter

Responses	Actual Value	Predicted Value	% Error
Bottom Diameter	0.5471	0.5257	3.91%

5.1.2.3 Influences of process parameters on Circularity

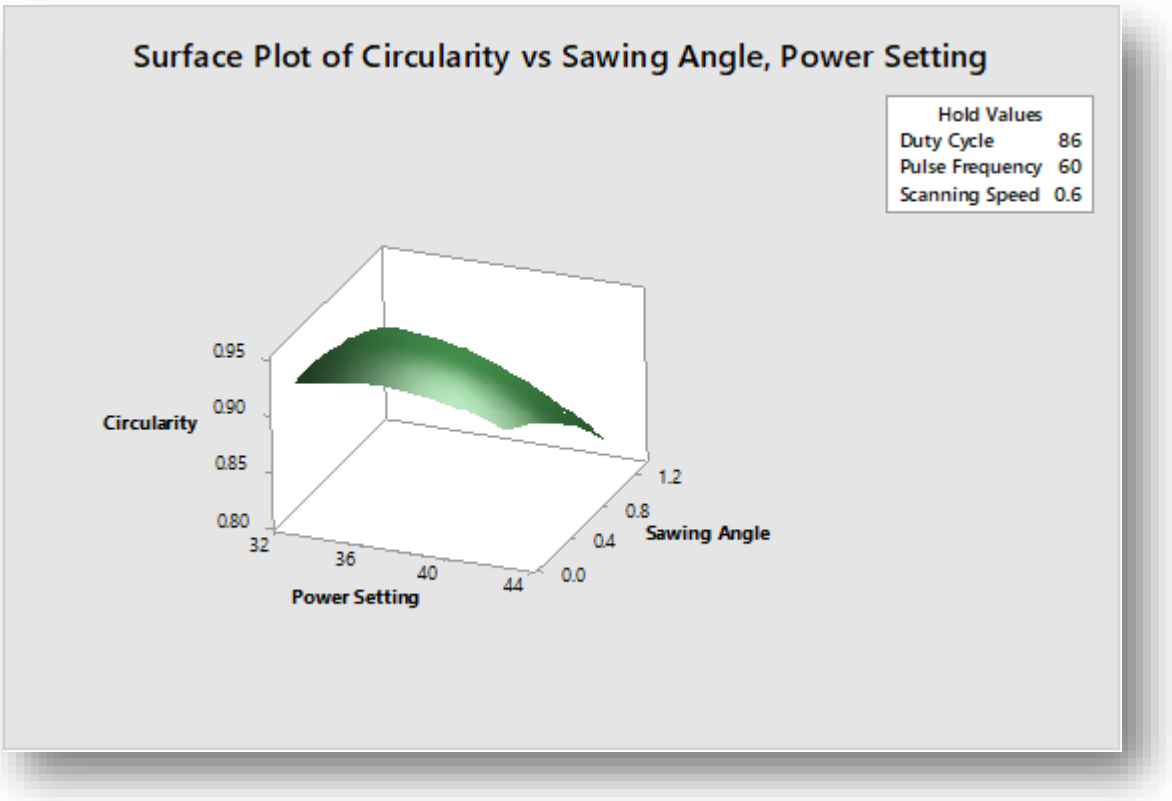

Fig.5.16. Effects of power setting and sawing angle on circularity

The combination effect of significant process parameters power setting and sawing angle on circularity is shown in figure 5.16. The duty cycle, pulse frequency and Scanning speed are kept constant at 86 %, 60 kHz and 0.6 mm/sec. From the response surface plot, it can be noticed that at low value of sawing angle the circularity near about same for different values of power setting, but at high sawing angle the circularity sharply decreases with increase in power setting. Circularity also decreases with increase in sawing angle for different values of power setting. At high power and high sawing angle the shape of the hole is hampered because of frequent high energy impact. So keeping with mid range of power and low sawing angle, circularity of the hole may be increases.

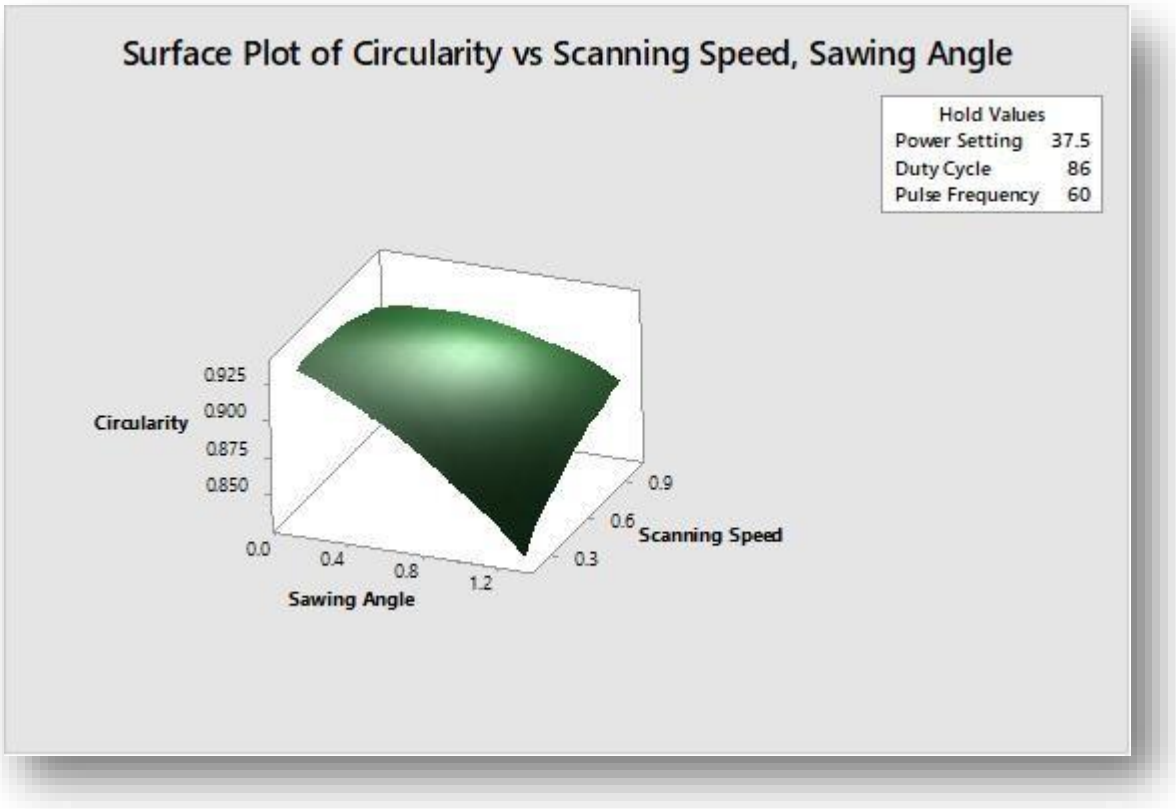

Fig.5.17. Effects of sawing angle and scanning speed on circularity

The combination effect of significant process parameters sawing angle and scanning speed on circularity is shown in figure 5.17. The power setting, duty cycle and Scanning speed are kept constant at 37.5 watt, 86 % and 60 kHz. Revelation by the surface plot shows a curvilinear relationship of circularity with the sawing angle and scanning speed. It is clearly shown from the figure that at high sawing angle and low scanning speed the circularity is very low. When the scanning speed is low the energy density becomes very high and uneven shapes of the hole is formed. So keeping with high scanning speed and low sawing angle, circularity of the hole may be increases.

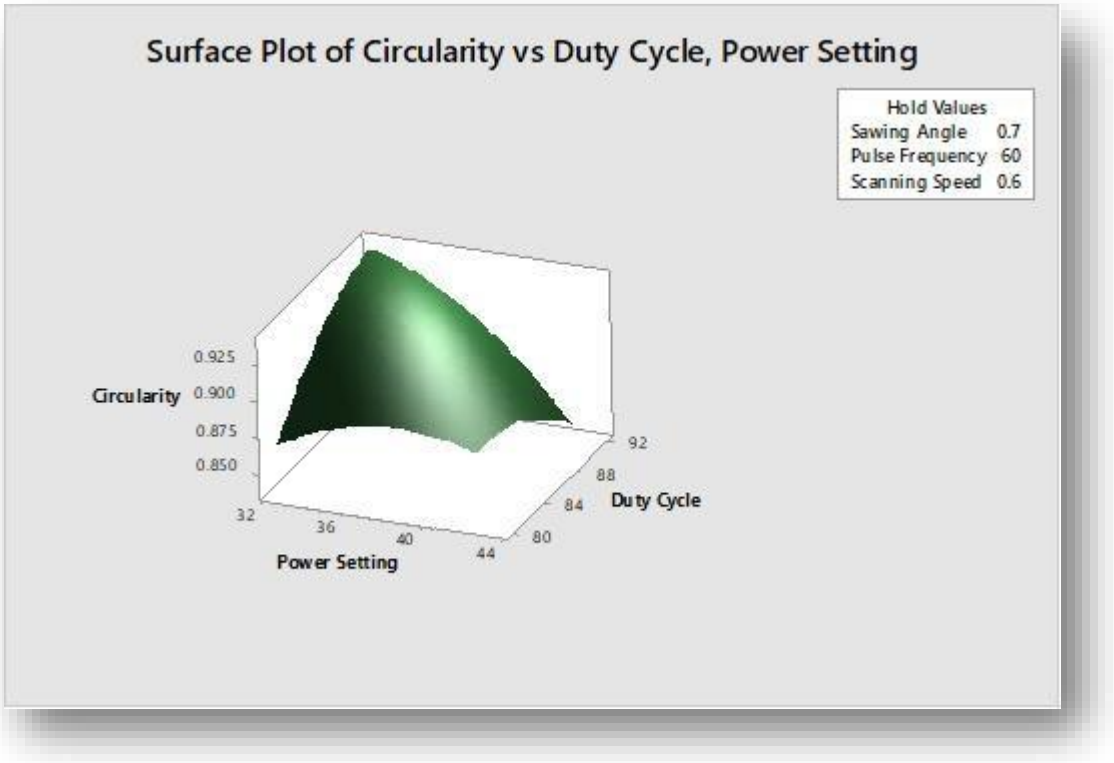

Fig.5.18. Effects of power setting and duty cycle on circularity

The effect of power setting and duty cycle upon circularity with the respective maintenance of constant sawing angle, pulse frequency and scanning speed at 0.7 mm/sec, 60 kHz and 0.6mm/sec are shown in fig. 5.18. From the surface plot it is clearly seen that there is an uneven curvilinear relationship of power setting and duty cycle with circularity. So keeping with mid range power and high duty cycle, circularity of the hole may be increases

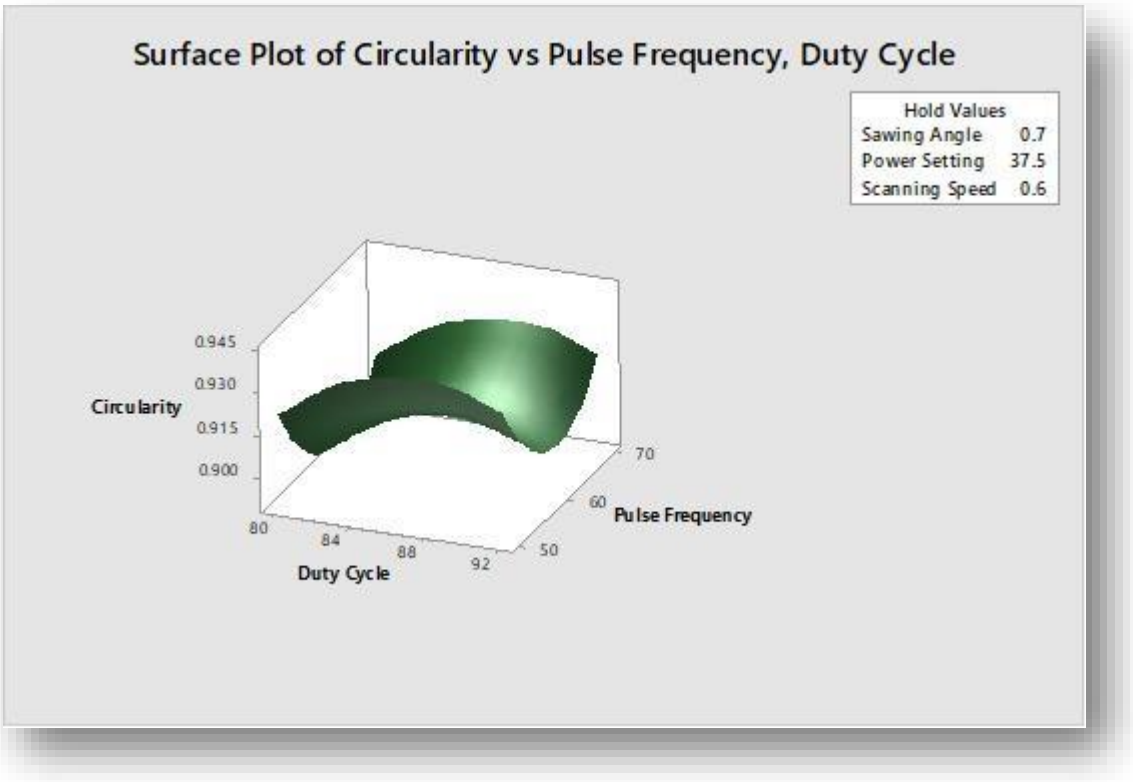

Fig.5.19. Effects of duty cycle and pulse frequency on circularity

The combination effect of significant process parameters duty cycle and pulse frequency on circularity is shown in figure 5.19. The sawing angle, power setting and Scanning speed are kept constant at 0.7 degree, 37.5 and 0.6 mm/sec. From the response surface plot, it can be noticed that the circularity follows the curvilinear relationship with duty cycle; it remains almost same with the increment of duty cycle for different values of pulse frequency. At high value of duty cycle and high value of pulse frequency the circularity also becomes very high because the pulse fiber laser cutting process involves generation of individual holes accurately produced by each pulse. So keeping with mid range value of duty cycle and high value of pulse frequency, circularity of the hole may be increases.

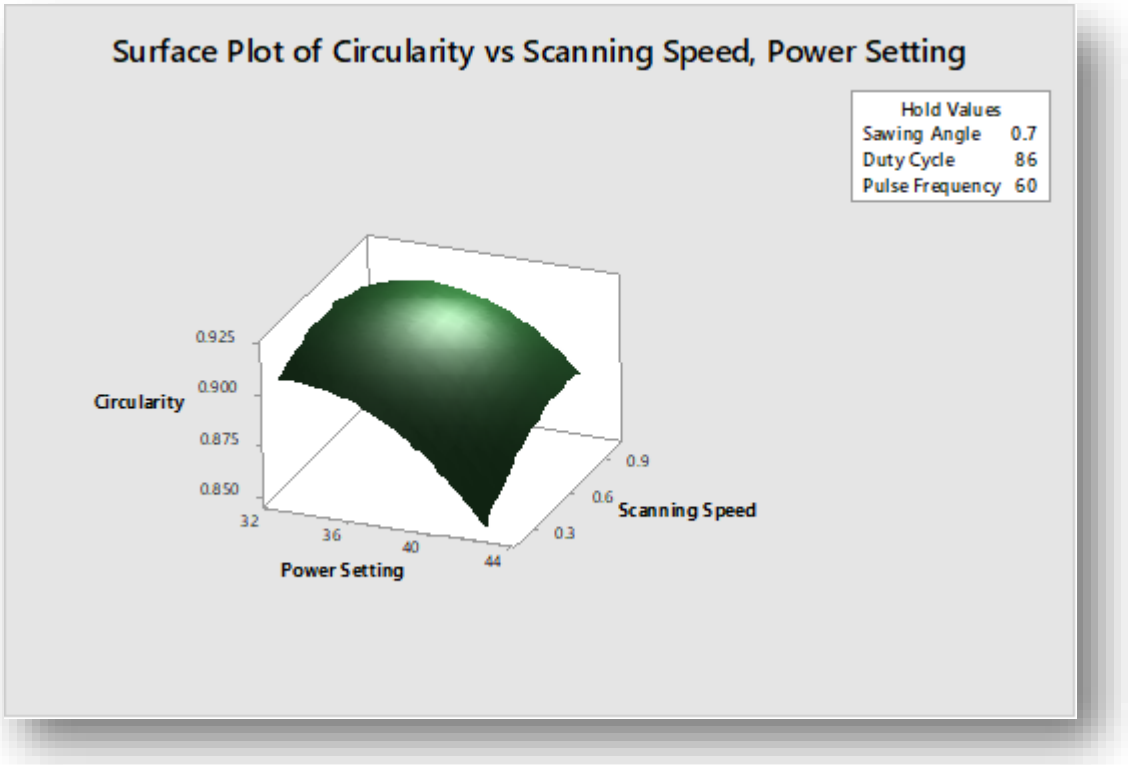

Fig.5.20. Effects of power cycle and scanning speed on circularity

The effect of power setting and scanning speed upon circularity with the respective maintenance of constant sawing angle, Duty cycle and pulse frequency at 0.7 degree, 86 % and 60 kHz are shown in fig. 5.20. From the response surface plot, it can be noticed that the circularity follows the curvilinear relationship with duty power setting; with increase in power setting the circularity decreases for different values of scanning speed. At low scanning speed and high power setting the energy density on the surface is very high. Due to this high energy, in-proper melting and evaporation takes place on the surface. So keeping with mid range value of power and high value of scanning speed, circularity of the hole may be increases.

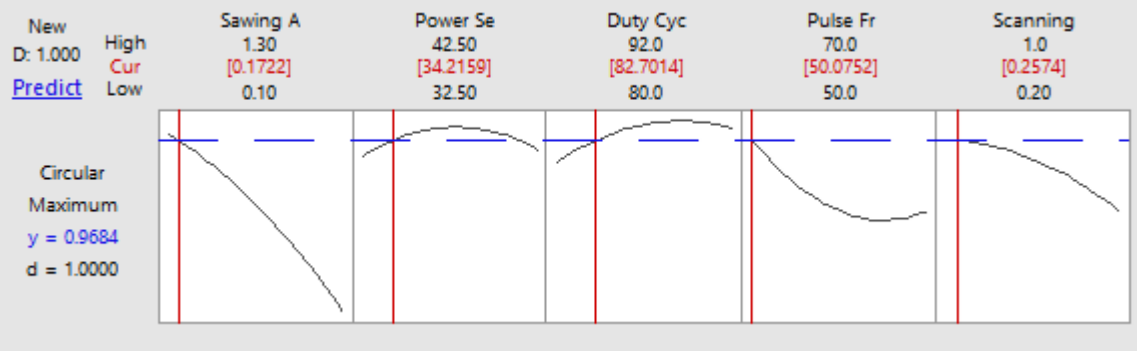

Fig.5.21. Optimization results for maximize circularity

Table 5.14. Optimum value of Circularity and corresponding process parameters

	Circularity	Sawing Angle (deg.)	Power Setting (watt)	Duty Cycle (%)	Pulse Frequency (kHz)	Scanning Speed (mm/sec)
Optimum value	0.9684	0.1722	34.2159	82.7014	50.0752	0.2574

The result of conformation test for circularity is shown in the table 5.15

Table 5.15. Confirmation Test for the Circularity

Responses	Actual Value	Predicted Value	% Error
Circularity	0.9492	0.9684	2.02 %

5.1.3. Development of models for different LTD criteria based on response surface methodology (RSM) approach

In this research investigation, multi-objective optimization has been carried to find out the optimum value of the three responses like Top Diameter, Bottom Diameter and Circularity with corresponding value of three process parameters like Sawing Angle, Power Setting, Duty Cycle,

Pulse Frequency, Scanning Speed at a time during trepan drilling in Monel K-500 sheet. Multi-objective optimization has been carried out in computer software "Minitab 17" and mathematical models are developed on the basis of RSM.

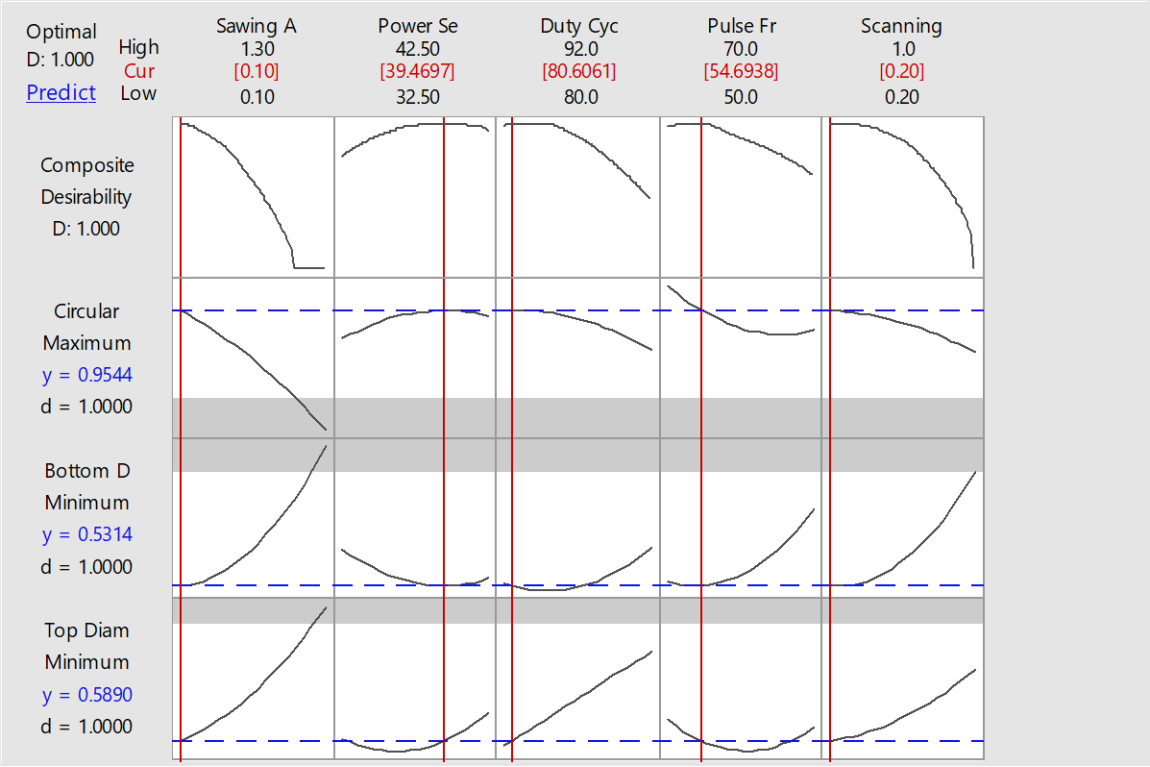

Fig.5.22. Multi-objective optimization of process parameters, based on RSM

From the Fig. 5.22., the optimize value of the process parameters and the resulting responses are obtained. The optimize values are listed below as Table 5.16.

Table 5.16. Optimization value of process parameters and responses

	TD (mm)	BD (mm)	Circularity	S.A (deg.)	P.S (watt)	D.C (%)	P.F (kHz)	S.S (mm/sec)
Optimum value	0.5890	0.5314	0.9544	0.10	39.4697	80.6061	54.6938	0.20

The result of conformation test for multi objective is shown in the table 5.17

Table 5.17. Confirmation Test for the Multi Objective Optimization Responses

Responses	Actual Value	Predicted Value	% Error
Top Diameter	0.5890	0.6122	3.78 %
Bottom Diameter	0.5314	0.5489	3.18 %
Circularity	0.9544	0.9344	2.09 %

The percentage of errors for top diameter, bottom diameter and circularity are 3.78, 3.18 and 2.09 % respectively in multi objective optimization. It is observed that developed RSM model predict the top diameter, bottom diameter and circularity quite satisfactorily.

5.2. Development the optimum Results Based on Particle Swarm Optimization Algorithm

The particle swarm concept was originated as a simulation of a simplified social system. The original intent was to simulate the graceful but unpredictable choreography of a bird flock graphically. Each particle keeps track of its coordinates in the problem space, which are associated with the best solution (fitness) it has achieved so far. This value is called ‘pBest’. Another ‘best’ value that is tracked by the global version of the PSO is the overall best value and its location obtained so far by any particle in the population. This location is called ‘gBest’. The

PSO concept consists of, at each step, changing the velocity (i.e. accelerating) of each particle towards its ‘pBest’ and ‘gBest’ locations (global version of PSO). Acceleration is weighted by a random term with separate random numbers being generated for acceleration towards ‘pBest’ and ‘gBest’ locations. The updates of the particles are accomplished as per the following equations

$$V_{i+1} = wV_i + C_1r_1(pBest_i - X_i) + C_2r_2(gBest - X_i) \text{ ----------Eq. 5.7}$$

$$X_{i+1} = X_i + V_{i+1} \text{ ----------Eq. 5.8}$$

Equation (5.7) calculates a new velocity (Vi+1) for each particle (potential solution) based on its previous velocity, the best location it has achieved ('pBest') so far, and the global best location ('gBest') the population has achieved. Equation (5.8) updates an individual particle's position (Xi) in the solution hyperspace. The two random numbers r1 and r2 in equation (5.7) are independently generated in the range [0,1].

The acceleration constants cl and c2 in equation (5.7) represent the weighting of the stochastic acceleration terms that pull each particle towards 'pBest' and 'gBest' positions. 'w' represents the inertia weight. The inertia weight w plays an important role in the PSO convergence behaviour since it is employed to control the exploration abilities of the swarm. The large inertia weights allow wide velocity updates to explore the design space globally while small inertia weights concentrate the velocity updates to nearby regions of the design space. The optimum use of the inertia weight w provides improved performance in a number of applications.

After studying a large number of research paper, the optimum value w, c_1 and c_2 are set-up for the experiment.

In that particular experiment the following parameters of optimization are selected after various trials:

(a) Maximum number of iterations: 50;

(b) Inertia weight factor (w): 0.65;

(c) Acceleration coefficients: c1 = 1.65 and c2 = 1.75.

5.2.1. Development the Optimum performance criteria based on single objective optimization technique

Table 5.18 Optimum value of Top diameter and corresponding process parameters

TD (mm)	Sawing Angle (deg)	Power Setting (watt)	Duty Cycle (%)	Pulse Frequency (kHz)	Scanning Speed (mm/sec)
0.5653	0.1	34.941	80	59.925	0.2

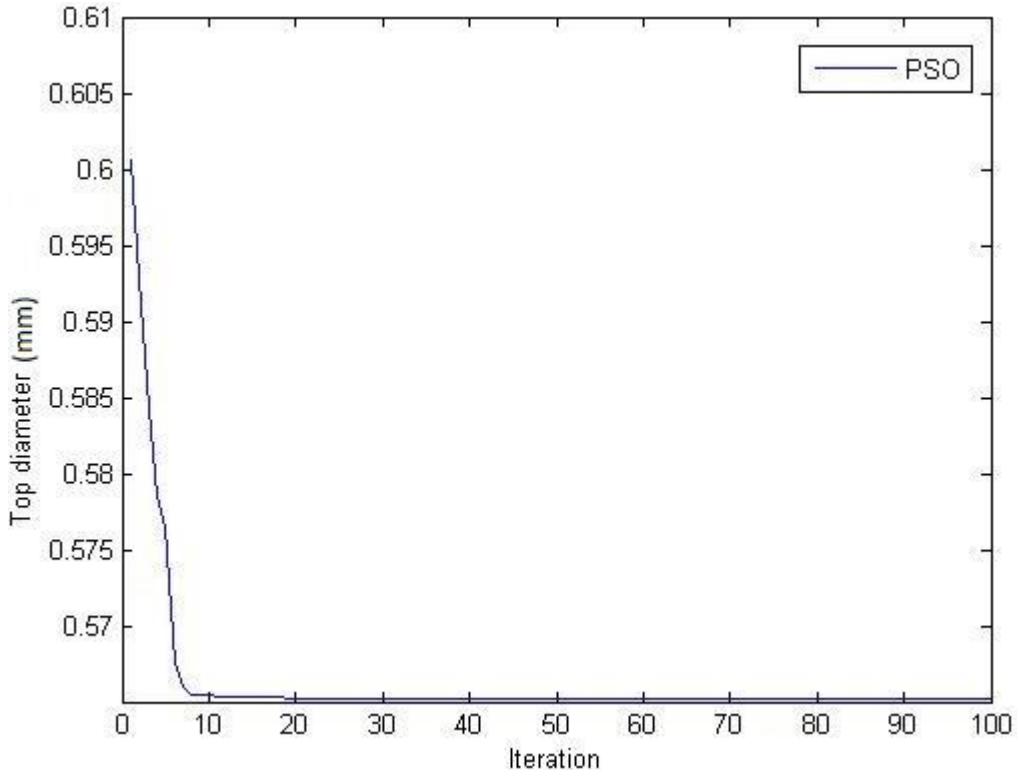

Fig. 5.23 Iteration plot for TD

The result of conformation test for top diameter is shown in the table 5.19

Table 5.19. Confirmation Test for Top Diameter

Responses	Actual Value	Predicted Value	% Error
Top Diameter	0.5721	0.5653	1.1 %

Table 5.20 Optimum value of bottom diameter and corresponding process parameters

BD (mm)	Sawing Angle (deg)	Power Setting (watt)	Duty Cycle	Pulse Frequency (kHz)	Scanning Speed (mm/sec)
0.5209	0.1	40.2235	80	54.029	0.24904

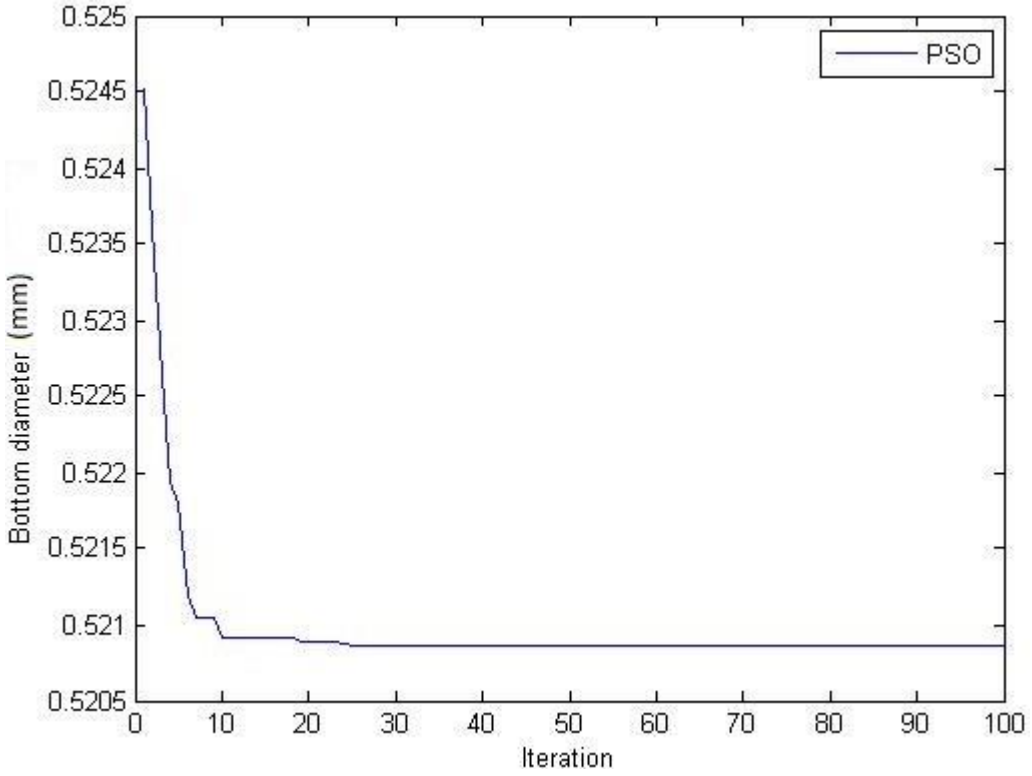

Fig. 5.24 Iteration plot for BD

The result of conformation test for bottom diameter is shown in the table 5.21

Table 5.21. Confirmation Test for Bottom Diameter

Responses	Actual Value	Predicted Value	% Error
Bottom Diameter	0.5342	0.5209	2.48 %

Table 5.22 Optimum value of bottom diameter and corresponding process parameters

Circularity	Sawing Angle (deg.)	Power Setting (watt)	Duty Cycle (%)	Pulse Frequency (kHz)	Scanning Speed (mm/sec)
0.9855	0.1	37.5	92	50	0.1205

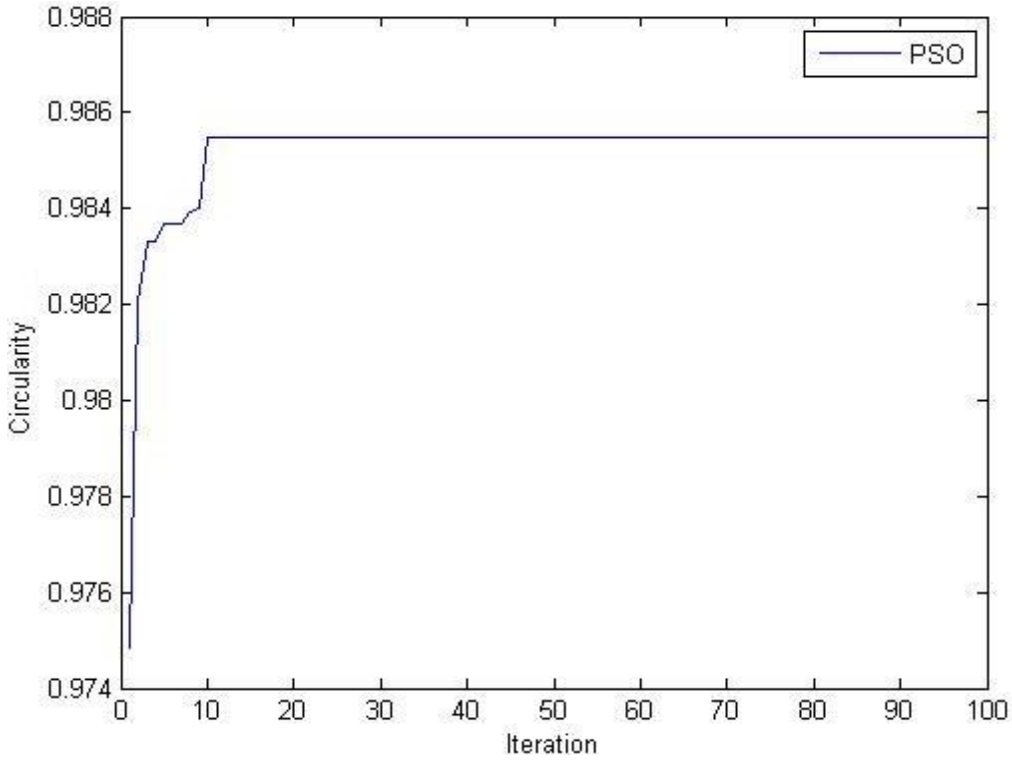

Fig. 5.25 Iteration plot for Circularity

The result of conformation test for circularity is shown in the table 5.23

Table 5.23. Confirmation Test for Circularity

Responses	Actual Value	Predicted Value	% Error
Circularity	0.9855	0.9812	0.436 %

5.2.1. Development the Optimum performance criteria based on multi objective optimization technique

For the multi objective optimization, a new performance criteria (Z) is assumed as the representative of all the performance criteria (Z, Z_2, Z_3). According to the value of the new performance criteria, the optimum process parameters are developed. After developing the optimum process parameters, the optimum performance criteria is also found by putting those values into the regression equations.

The formulation of the new performance criteria (Z) is shown bellow

$$Z = \pm \frac{w1\ Z1}{Z1o} \pm \frac{w2\ Z2}{Z2o} \pm \frac{w3\ Z3}{Z3o}$$

Where, w1, w2 and w3 = weight given to the performance criteria Z1, Z2 and Z3

Z1o, Z2o and Z3o = Optimum value of the performance criteria from the single objective optimization.

The " $\pm$ " sign is used for maximizing and minimizing problems. “+” sign is used for minimization problems and “-” sign is used for maximization problems.

The optimize values are listed below as Table 5.24.

Table 5.24. Optimization value of process parameters and responses

TD (mm)	BD (mm)	Circularity	Sawing Angle (deg.)	Power Setting (watt)	Duty Cycle (%)	Pulse Frequency (kHz)	Scanning Speed (mm/sec)
0.5778	0.5329	0.9612	0.1	38.146	80	53.5115	0.2

The result of conformation test for multi objective is shown in the table 5.25

Table 5.25. Confirmation Test for the Multi Objective Optimization Responses

Responses	Actual Value	Predicted Value	% Error
Top Diameter	0.5908	0.5778	2.2 %
Bottom Diameter	0.5463	0.5329	2.4 %
Circularity	0.9503	0.9612	1.1 %

The percentage of errors for top diameter, bottom diameter and circularity are 2.2, 2.4 and 1.1 % respectively in multi objective optimization. It is observed that developed PSO artificial intelligence tool predict the top diameter, bottom diameter and circularity much more satisfactorily than RSM model prediction.

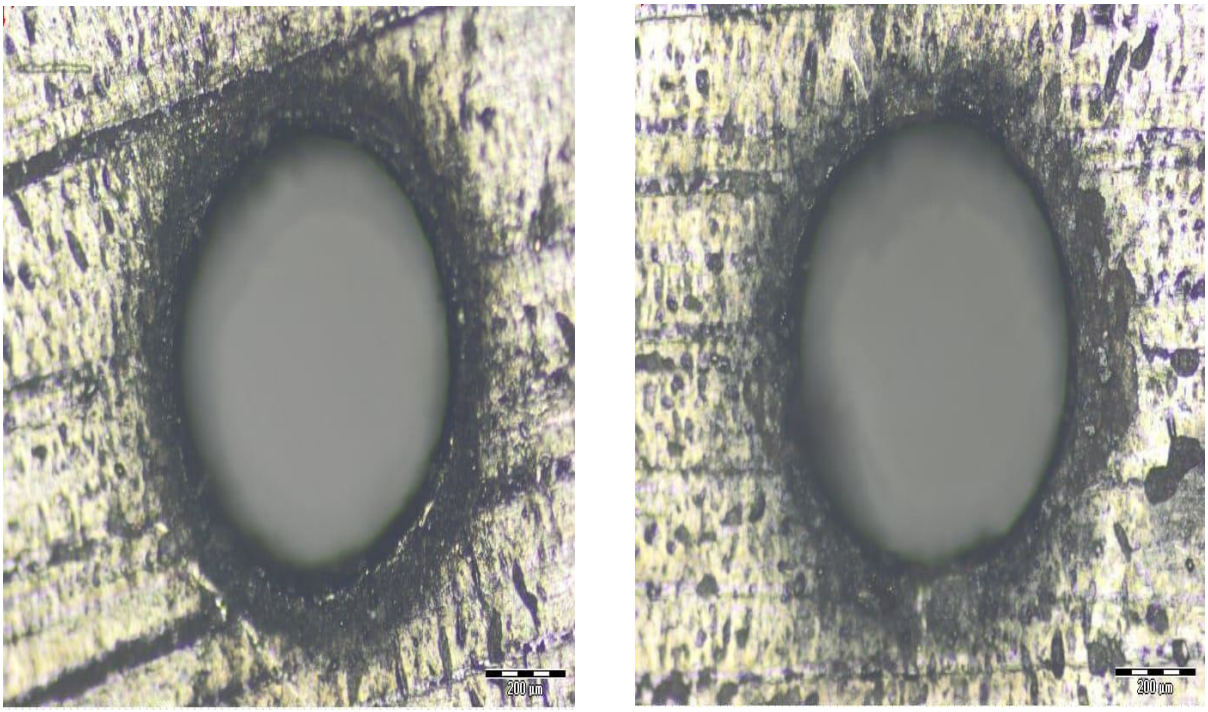

Fig. 5.26 Microscopic view of Top diameter

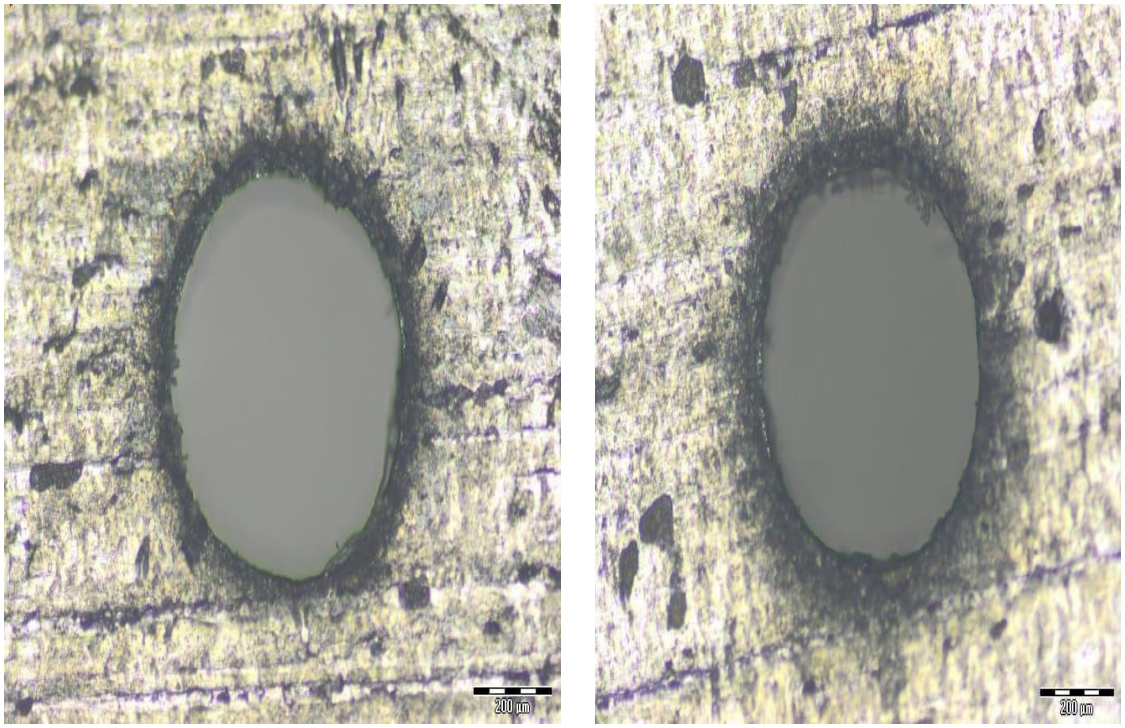

Fig. 5.27 Microscopic view of Bottom diameter

Chapter 6:

6. GENERAL CONCLUSIONS

In present era LBM is a great non-conventional machining process for cutting as well as drilling of metallic and non-metallic materials. At first RSM based experimental investigations and analysis on LBM has been performed to determine the mathematical models and the relation between the process parameters. RSM explains that how much a process parameter is significant on the performance characteristic. Further experiment is done with Particle Swarm Optimization algorithm taking three most significant parameters. Within the constraints of the experimental set up LBM and based on the experimental investigations and analysis, the following conclusions can be drawn:

(i) Using low power (50 watt) fiber laser setup the micro-drilling operation can be performed successfully on Monel K-500.

(ii) The mathematical models for TD, BD & circularity have been developed successfully with the help of RSM approach to express the relationship between various process parameters i.e. sawing angle, power setting, duty cycle, pulse frequency and scanning speed above machining criteria.

(iii) From the ANOVA table of RSM model it has been concluded that Sawing Angle, Power Setting, Duty Cycle, Pulse Frequency and Scanning Speed has a significant influences on the Top Diameter, Bottom Diameter and Circularity.

(iv) The relationship between the process parameters and performance criteria have been developed successfully on surface plot of RSM model.

(v) For achieving minimum TD, The optimal parametric condition for trepan drilling Monel K-500 is obtained as sawing angle 0.10 degree, power setting 36.1364 watt, duty cycle 80 %, pulse frequency 60.7071 kHz and scanning speed 0.02 mm/sec. The optimum condition for minimum BD is obtain as sawing angle 0.1727 degree, power setting 37.9545 watt, duty cycle 84.9697 pulse

frequency 54.6465 kHz and scanning speed 0.3939 mm/sec. And for maximum circularity the sawing angle 0.1722 degree, power setting 34.2159 watt, duty cycle 82.7014 pulse frequency 50.0752 kHz and scanning speed 0.2574 mm/sec.

(vi) Based on the RSM models multi-objective optimization has been performed to determine the optimum value of LTD process parameters and responses. The minimum value of Top Diameter obtained was 0.5890 mm, the minimum Bottom Diameter was 0.5314 mm and the maximum circularity was 0.9544.

(vii) The average percentage of prediction errors for TD, BD and Circularity are 5.47, 4.49 and 3.37 respectively. It is observed that developed RSM model predict the Top Diameter, Bottom Diameter and circularity satisfactorily.

(viii) Based on the PSO algorithm, multi-objective optimization has been performed to determine the optimum value of LTD process parameters and responses. The minimum value of Top Diameter obtained was 0.5778 mm, the minimum Bottom Diameter was 0.5329 and the maximum circularity was 0.9612.

(ix) The average percentage of prediction errors for TD, BD and Circularity are 5.21, 3.14 and 3.06 respectively. It is observed that developed PSO algorithm predict the Top Diameter, Bottom Diameter and circularity satisfactorily.

(x) Based on the comparison between RSM model optimization and PSO artificial intelligence tool, it can be concluded that the PSO gives more accurate optimum results than the RSM model optimization.

6.1 Future Scope of Experiment

Future scope of research includes the following important considerations

1. Effect of different process parameters on HAZ and hole taper can be investigated.
2. Micro-trepan drilling operation on other thick material sheet, using low power laser beam can be carried out.
3. Instead of air other types of assisting gas jet (i.e. N_2, O_2 or other inert gases) can be used to perform the cutting operation

References

[1] Davim, J. P. & Jackson, M. J. (Eds.). (2013). Nano and micromachining. John Wiley & Sons, Vol. 15, pp 115-173.

[2] Mishra, S., & Yadava, V. (2015). Laser beam micromachining (LBMM)–a review. Optics and lasers in engineering, Vol. 73, pp.89-122.

[3] Veiga, C., Davim, J. P., & Loureiro, A. J. R. (2012). Properties and applications of titanium alloys brief review, Rev. Adv. Mater. Sci., Vol. 32, No. 3, pp 133-148.

[4] Jain, V.K.(2010). Introduction to micromachining, Narosa Publishing House Pvt. Ltd., Vol. 12, pp 1-40

[5] Mishra P.K. (2013). Nonconventional Machining, Narosa Publishing House, Vol. 10,PP-147-159

[6] http://nptel.ac.in/courses/112105127/pdf/LM-40.pdf (accessed on 20/09/2017)

[7] Bruck Ed. G. (1988). aser Material Processing, proc. ICA EO'88 USA, Vol. 11, pp 45-122

[8] https://www.orc.soton.ac.uk/how-fibre-lasers-work (accessed on 15/11/2017)

[9] https://www.ipgphotonics.com/en/applications/materials-processing/cutting (accessed on 12/08/2017)

[10] https://www.google.com/search?q=application+of+laser+beam+machining&rlz=1C1AVNE_enIN756IN756&sxsrf=qwu&source=lnms&tbm=isch&sa=X&ved=0ahUKEwjm9sC_4LziAhVWU30KH BIABcQ_AUIDigB&biw=1366&bih=657

[11] Gel H.H.(1989). Laser in Manufacturing, Proc. 6th Int. Conf., Birmingham; ISBN 3-540-51241-1, pp 121-144

[12] Baumeister, M., Dickmann, K., & Hoult, T. (2006). Fiber laser micro-cutting of stainless steel sheets, Applied Physics A, Vol. 85, No. 2, pp121-124.

[13] Kuar, A. S., Doloi, B., & Bhattacharyya, B. (2006). Modelling and analysis of pulsed Nd:

YAG laser machining characteristics during micro-drilling of zirconia (ZrO2). International Journal of Machine Tools and Manufacture, Vol. 46, No. 12, pp 1301-1310.

[14] Ghosal, A., & Manna, A. (2013). Response surface method based optimization of ytterbium fiber laser parameter during machining of Al/Al2O3-MMC. Optics & Laser Technology,Vol 46, pp 67-76.

[15] Kleine, K. F., Whitney, B., & Watkins, K. G. (2002, October). Use of fiber lasers for micro cutting applications in the medical device industry. In Proceedings of ICALEO pp. 1-10.

[16] Nikumb, S., Chen, Q., Li, C., Reshef, H., Zheng, H. Y., Qiu, H., & Low, D. (2005). Precision glass machining, drilling and profile cutting by short pulse lasers. Thin Solid Films, Vol.477, No. 2, pp216-221.

[17] Corcoran., A., Sexton., Scaman., L., Pyan., L., Byrne., G., "The laser drilling of multi-layer aerospace material systems", Journal of Materials Processing Technology Volume 123, Issue 1, 10 April 2002, Pages 100-106

[18] Yalukova, O. and Sarady, I. (2005). Investigations of interaction mechanisms in laser drilling of thermoplastic and thermoset polymers using different wavelengths, Composites Science and Technology, Vol. 66, No. 10, pp 1289-1296.

[19] Zhu, X., Naumov, A. Y., Villeneuve, D. M., & Corkum, P. B. (1999). Influence of laser parameters and material properties on micro drilling with femtosecond laser pulses. Applied Physics A, Vol.69, No. 1, pp 367-371.

[20] Biswas, R., Kuar, A. S., Sarkar, S., & Mitra, S. (2010). A parametric study of pulsed Nd: YAG laser micro-drilling of gamma-titanium aluminide. Optics & Laser Technology, Vol.42, No.1, pp 23-31.

[21] Matsuoka, Y., Kizuka, Y., & Inoue, T. (2006). The characteristics of laser micro drilling using a Bessel beam. Applied Physics A, Vol. 84, No.4, pp 423-430.

[22] Jackson, M. J., & O'Neill, W. (2003). Laser micro-drilling of tool steel using Nd: YAG lasers. Journal of Materials Processing Technology, Vol.142, No. 2, pp 517-525.

[23] Huang, H., Yang, L. M., & Liu, J. (2014). Micro-hole drilling and cutting using femtosecond fiber laser. Optical Engineering, Vol. 53 No. (5), 051513.

[24] Kumar Sanjay., Dubey., Avanish Kumar., Pandey., Arun Kumar., "Computer-Aided Genetic Algorithm Based Multi-Objective Optimization of Laser Trepan Drilling", Journal of PRECISION ENGINEERING AND MANUFACTURING Vol. 14, No. 7, pp. 1119-1125.

[25] Chien., Wen-Tung., Hou., Shiann-Chin., "Investigating the recast layer formed during the laser trepan drilling of Inconel 718 using the Taguchi method", Int J Adv Manuf Technol (2007) 33: 308–316.

[26] Goyal., Rupesh., Dubey., Avanish Kumar., "Quality Improvement by Parameter Optimization in Laser Trepan Drilling of Superalloy Sheet", Journal of Materials and Manufacturing Processes, 29: 1410–1416, 2014

[27] Okasha., M.M., Mativenga., Driver., N., Li., L., "Sequential laser and mechanical micro-drilling of Ni superalloy for aerospace application", Manufacturing Technology 59 (2010) 199–202

[28] Knowles, M. R. H., Rutterford, G., Karnakis, D., & Ferguson, A. (2007). Micro-machining of metals, ceramics and polymers using nanosecond lasers. The International Journal of Advanced Manufacturing Technology, Vol. 33, No.-2, pp 95-102.

[29] Baumeister, M., Dickmann, K., & Hoult, T. (2006). Fiber laser micro-cutting of stainless steel sheets, Applied Physics A, Vol. 85, No. 2, pp121-124.

[30] Yung, K. C., Zhu, H. H., & Yue, T. M. (2005). Theoretical and experimental study on the kerf profile of the laser micro-cutting NiTi shape memory alloy using 355 nm Nd: YAG. Smart materials and structures, Vol.14, No. 2, pp 332-337.

[31] Meng, H., Liao, J., Zhou, Y., & Zhang, Q. (2009). Laser micro-processing of cardiovascular stent with fibre laser cutting system, Optics & Laser Technology, Vol. 41,No. 3, 300-302.

[32] Kleine, K. F., Whitney, B., & Watkins, K. G. (2002, October). Use of fiber lasers for micro cutting applications in the medical device industry. In Proceedings of ICALEO pp. 1-10.

[33] Mauclair, C., Pietroy, D., Di Maio, Y., Baubeau, E., Colombier, J. P., Stoian, R., & Pigeon, F. (2015). Ultrafast laser micro-cutting of stainless steel and PZT using a modulated line of multiple foci formed by spatial beam shaping. Optics and Lasers in Engineering, Vol.67, pp 212-217.

[34] Biswas, R., Kuar, A. S., & Mitra, S. (2008). Influence of machining parameters on surface roughness in Nd: YAG laser micro-cutting of alumina-aluminium interpenetrating phase composite. International Journal of Surface Science and Engineering, Vol. 2, No. 3, pp 252-264

[35] Erika, G.L., Alexis, M.T., Juansethi, I.M., Hector R, S. And Ciro A, R. (2016). Fiber laser micro-cutting of AISI 316L stainless steel tubes- influence of pulse energy and spot overlap on back wall dross, Procedia CIRP, Vol.49 ,pp222 – 226

[36] Erika, G.L., Alexis, M.T., Juansethi, I.M., Hector R, S. And Ciro A, R. (2016). Fiber laser micro-cutting of AISI 316L stainless steel tubes- influence of pulse energy and spot overlap on back wall dross, Procedia CIRP, Vol.49 ,pp222 – 226

[37] Chien., Wen-Tung., and Hou., Shiann-Chin., "Investigating the recast layer formed during the laser trepan drilling of Inconel 718 using the Taguchi method", Int J Adv Manuf Technol (2007) 33: 308–316

[38] Ancona., A., Roser., F., Rademaker., K., Limpert., J., Nolte., S., and Tünnermann., A., "High speed laser drilling of metals using a high repetition rate, high average power ultrafast fiber CPA system", Osa publishing optics express volume 16 issue 12 pp. 8958-8968 (2008)

[39] https://patentimages.storage.googleapis.com/4c/cd/cc/7e43673c639f64/US5837964.pdf

[40] Goyal., Rupesh., Dubey., Avanish Kumar., "Modeling and optimization of geometrical characteristics in laser trepan drilling of titanium alloy", journal of mechanical science and technology(march 2016) Volume 30 pp 1281–1293

[41] Ghoreishi., M., Law., D., K., Y., and Li., L., "Comparative statistical analysis of hole taper and circularity in laser percussion drilling", International journal of Machine Tool and Manufacturing, volume 42, issue 9 July 2002, Pages 985-995

[42] NG., G., L., K.., Li., L., "The effect of laser peak power and pulse width on the hole geometry repeatability in laser percussion drilling", optics and laser technology, volume 33, issue 6 September 2001, Pages 393-402